# The Effects of Stress on *In Vivo* Hippocampal CA1 Synaptic Dynamics and Hippocampal Learning and Memory

Ghabiba Weston

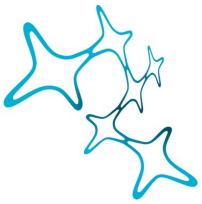

Graduate School of
Systemic Neurosciences
LMU Munich


Dissertation der
Graduate School of Systemic Neurosciences der
Ludwig-Maximilians-Universität München

18 July, 2019

Supervisor: Dr Alessio Attardo
Second Reviewer: Professor Tobias Bonheoffer
External Reviewer: Professor Yi Zuo

Date of Submission: 18 July 2019
Date of Defense: 13 November 2019

# Abstract

Chronic stress is associated with impairments in learning and memory, as well as changes in dendritic structure and synaptic connections of the hippocampus, a brain region key for spatial and episodic learning and memory. However, the cellular- and circuit- level mechanisms by which stress-induced structural synaptic changes impair learning and memory are not yet clear. Structural changes have historically been studied mostly by *ex vivo* preparations, due to the necessity to sacrifice the subjects to quantify structural changes. This approach however, is limited in its temporal resolution and lacks the ability to study the dynamic response to stress within the same subjects. This is important because responses to stress and learning and memory are intrinsically dynamic processes and individuals may differ in their baseline dynamics based on a host of uncontrollable factors.

In order to overcome these drawbacks, I employed deep brain 2-photon *in vivo* time lapse optical imaging to longitudinally study the dorsal hippocampal CA1 region in live mice. I used a transgenic mouse model where a green fluorescent protein targeted to the cytoplasm sparsely labels a subset of excitatory neurons (Thy1-GFPm line). This enabled me to visualize the structure and the spines – protrusions on the dendrites where most of the excitatory synapses of excitatory neurons occur – of CA1 pyramidal neuron's basal dendrites, further allowing me to track structural synaptic changes upon multi-modal stress (MMS). MMS involves exposure of mice to multiple simultaneous stressors.

In this work, I tracked synaptic dynamics over two weeks during baseline and acute and repeated MMS by deep brain 2-photon *in vivo* time lapse optical imaging of groups of Thy1-GFPm mice. This enabled me to investigate – for the first time *in vivo* – stress-induced changes in CA1 synaptic dynamics.

With this approach I was able to determine that MMS results in disruption of homeostatic structural plasticity. In addition I found that MMS strongly alters dynamics of immature synapses by decreasing their survival. Conversely, recovery increased the survival of spines born after stress, demonstrating higher survival rates in comparison to internally controlled baseline survival.

In addition, I observed that stress increased the distance between newly formed spines and decreased the distance between lost spines, supporting spatially modulated alterations.

Finally, I investigated the extent to which acute MMS and recovery and repeated MMS impair CA1 dependent learning and recall by using the Morris Water Maze (MWM) spatial learning paradigm and observed an impairment in learning in both stress groups.

Understanding how stress impacts the dynamics of synapses is important to elucidate the basic mechanisms by which stress impairs learning and memory and it will be important for the development of therapeutic interventions both in terms of time scales and targets.

To my boys, Reyan and Kahlil Weston.

# TABLE OF CONTENTS

# List of Figures

# List of Tables

**Table** **Page**

# List of Abbreviations

ACTH - adenocorticotropic hormone
AMPAR - $\alpha$-amino-3-hydroxy-5-methyl-4-isoxazolepropionic acid receptor
B1 - baseline day 1, imaging day 1
B2 - baseline day 2, imaging day 2
B4 - baseline day 4, imaging day 4
B7 - baseline day 7, imaging day 7
BST - bed nucleus of the stria terminalis
CA1 - cornu ammonis 1
CA2 - cornu ammonis 2
CA3 - cornu ammonis 3
CRFR1 - corticotropin releasing factor receptor type 1
CRH - corticotropin-releasing hormone
CSDS - chronic social defeat stress
CUS - chronic unpredictable stress
dCA1 - dorsal cornu ammonis 1
DG - dentate gyrus
DNN - distance to nearest neighbour
DREADD - Designer Receptors Exclusively Activated by Designer Drugs
FC - fear conditioning
GABA - gamma-aminobutyric acid
GFP - green fluorescent protein
GR - glucocorticoid receptors
GR-KO - glucocorticoid receptor knock out
GUI - graphical user interface
HPA - hypothalamic-pituitary-adrenal
i.p. - intraperitoneal
KO - knock out
L5 - Layer 5
L.Sept - lateral septum
LTD - long term depression
LTP - long term potentiation

MIP - maximum intensity projection
MMS - multimodal stress
MR - mineralocorticoid receptors
MWM - Morris water maze
NB - newborn
NMDAR - N-methyl-D-aspartate receptor
NRT - nucleus reunions of the thalamus
OLM - oriens lacunosum-moleculare
PBS - phosphate buffered solution
PFC - prefrontal cortex
PTSD - post traumatic stress disorder
PV - parvalbumin
PVN - paraventricular nucleus
R1 - recovery day 1, imaging day 9
R3 - recovery day 3, imaging day 11
R6 - recovery day 6, imaging day 14
S1 - stress day 1, imaging day 8
S2 - stress day 2, imaging day 9
S4 - stress day 4, imaging day 11
S7 - stress day 7, imaging day 14
SOM - somatostatin
TAM - tamoxifen
VBA - Visual Basic for Applications
WT - wild type

CHAPTER 1

# INTRODUCTION

In this section I will introduce concepts and review literature relevant to this work. In particular, I will introduce the hippocampus and its role in learning in memory in relation to plasticity and behaviour. I will also review the effects of acute and chronic stress on plasticity and behaviour within the framework of hippocampal function.

## 1.1 Hippocampal role in learning and memory

The hippocampus is a medial temporal lobe structure that plays a pivotal role in the encoding and retrieval of spatial and declarative memories (Scoville and Milner (1957); O'Keefe and Dostrovsky (1971); O'Keefe and Nadel (1978); Morris et al. (1982, 1986); Squire and Zola-Morgan (1991); Moser et al. (1998); Eichenbaum (2000)). It is one of the most intensively studied regions of the brain since its' biophysical role in memory formation became apparent in 1957 with the report of an epileptic patient, H.M., who was no longer able to form declarative memories after his temporal lobes had been surgically removed. Since then, the discovery of numerous cell types and their roles in memory formation and spatial navigation have been elucidated and intra-regional variability in plasticity and response mechanisms have begun to be unraveled. The hippocampus comprises a number of sub-regions, including the cornu ammonis 1 (CA1), cornu ammonis 2 (CA2), cornu ammonis 3 (CA3), dentate gyrus (DG) and ventral subiculum (Swanson and Cowan (1977)).

The entorhinal cortex (EC) sends projections to the DG and to apical dendrites of the CA3 and CA1. The CA3 receives further inputs from the DG via mossy fibre (MF) afferents, as well as being highly recurrently connected (Figure 1.1a). The CA1 additionally receives afferents from the CA3 via the schaffer collateral (SC) pathway and sends projections to the lateral septum, subiculum and back to the EC. The CA1 also receives inhibitory inputs from oriens lacunosum-moleculare

(OLM) and bi-stratified cells which are primarily driven by CA3, EC and thalamic inputs (Figure 1.1a, b).

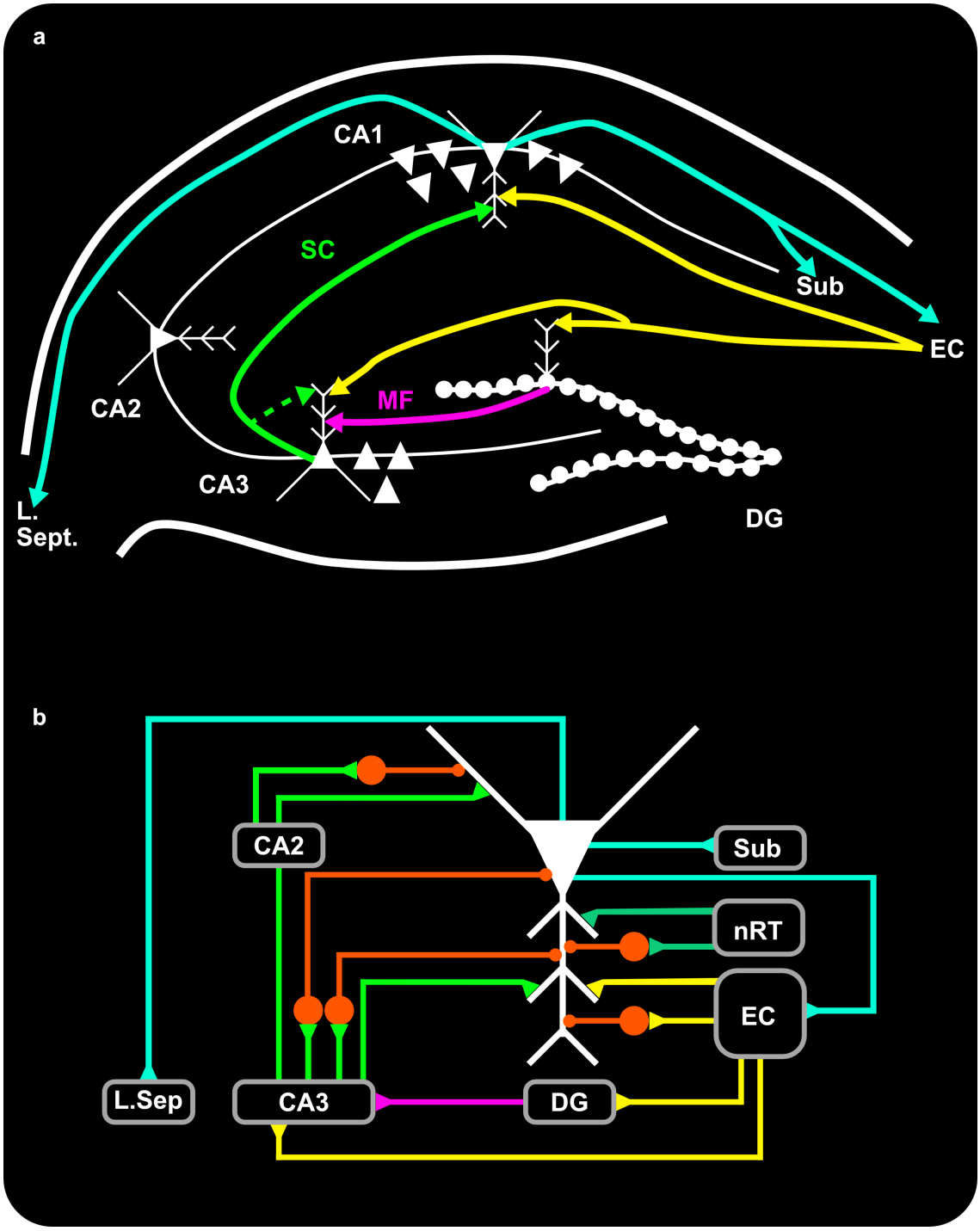


**Figure 1.1:** Murine hippocampal formation. (a) Hippocampal regions and pathways. The EC sends projections to the DG, CA3 and CA1. Mossy fibres project from the DG to apical dendrites of the CA3. CA3 projects recurrently to apical CA3 dendrites and to the apical dendrites of the CA1 via the Schaffer collateral pathway. CA1 projects to the EC, Subiculum and Lateral Septum. (b) Detailed afferents and efferents of CA1 pyramidal cells. Orange circles, inhibition; Triangles, excitation. EC, entorhinal cortex; DG, dentate gyrus; CA, cornu ammonus; Sub, subiculum; L.Sept., lateral septum.: NRT, nucleus reunions of the thalamus; MF, mossy fibres; SC, schaffer collaterals.

### 1.1.1 Synaptic dynamics

Pyramidal cells of the hippocampus typically display extensive dendritic branching and dendritic branches of CA1 pyramidal cells are densely enumerated with dendritic spines. Dendritic spines are biochemical compartments which are generally accepted to be proxies for excitatory synapses (Chen et al. (2012b)). They have been shown to be highly dynamic in nature and in particular, to change their formation and elimination rates, size and type in relation to experiences such as learning and stress. Up until recent years, a large body of work focused on 'snapshot' observations of changes in spine densities, mostly due to limitations in accessing *in vivo* dynamics.
Technological advances enabling live imaging of spines have been instrumental in forming a more comprehensive understanding of the temporal dynamics of both structure and function. 2-photon microscopy, a technique which makes use of fluorophore excitation using 2 photons of infrared light, is currently one of the few methods which enable tracking of such dynamics in sub-cortical structures.
*In vivo* studies implementing 2-photon imaging in the cortex have shown that the greater part of a population of spines tends to be persistent over time (up to years) whereas a subset of the population are more dynamic in nature (changing over days) (Grutzendler et al. (2002)). Learning has been shown to increase stabilisation but not spine density, supporting the role of equilibrium between persistent and newborn spines in learning related plasticity (Keck et al. (2008); Yang et al. (2009)). Spine formation and stabilisation have also been demonstrated to correlate with motor learning, with the fraction of new spines predicting long term performance (Xu et al. (2009); Yang et al. (2009)). Recent years and the invent of technologies which enable longitudinal *in vivo* studies have thus greatly aided the progress of studying these elements, yet still much remains to be understood in relation to their functional significance.
As mentioned, pyramidal neurons in the CA1 integrate excitatory synaptic input, primarily onto dendritic spines, from the upstream CA3 and EC. Spine dynamics therefore play an integral role in circuit changes within this network. Yet despite the instrumental role of the hippocampus in memory processing, *in vivo* studies of synaptic plasticity have predominantly been conducted in cortical structures.
In the hippocampus, longitudinal tracking of spine dynamics in the dorsal CA1 (dCA1) has demonstrated a striking difference to cortical dynamics (Attardo et al. (2015)). A single population of spines was predicted to survive 1-2 weeks, effecting full turnover in up to 6 weeks, thus implying complete elimination of the corresponding pattern of synaptic connectivity in this time. In addition, spine loss in the CA1 was seen to increase with N-methyl-D-aspartate receptor (NMDAR) blockade, opposite to its effect in the cortex. Ultimately, spine turnover was consistent with and supportive of the known transience of hippocampal memory. Pfeiffer et al. (2018) imaged hippocampal synapses at higher resolution using 2-photon stimulated emission depletion microscopy (STED) and measured a  40% spine turnover within 4 days. Acker et al. (2019) used computational modeling to demonstrate that new synapses can be integrated into memories by

Hebbian plasticity during replay of pre-synaptic activity patterns.
It should be noted that window implantation over the CA1 has been shown to increase micro- and astro-gliosis, resolved over a few weeks. No behavioural differences in contextual fear conditioning (FC) and open field tests were observed in comparison to unimplanted controls (Gu et al. (2014)). Taken together, there is ample evidence to support spines as biochemical domains which play a pivotal role in pathway signaling, the disruption of which results in changes in connectivity strength. Such elemental understanding needs to be extended to circuit level mechanisms to bridge the gap between structural and functional synaptic plasticity and the eventual effects on behaviour under conditions such as stress.

### 1.1.2 Synaptic clustering

Numerous studies provide evidence to support the storage of memories as discrete spatiotemporal patterns in the mammalian brain (Kastellakis et al. (2015); De Roo et al. (2008b)). Although there have been some advances in understanding memory encoding at a cellular level, little has been demonstrated on a synaptic level. The link between synaptic connections and memory formation was first proposed by Ramon y Cajal and later formed the foundation of Hebbian learning (Cajal (1893); Hebb (1949)). Hebb's theory postulates that synapses between neurons are strengthened with highly correlated activation of neighbouring synapses, forming the underlying process enabling learning and memory. Synaptic clustering has been shown, both computationally and electrophysiologically, to play a functional role in the computational efficacy of neuronal networks by enabling nonlinear summation of synaptic inputs, prompting the study of dendrites as computational elements (Kastellakis et al. (2015)). Spatial organisation further determines the effect of spread of proteins and kinases which are limited in their extent of travel. Thus far, evidence of the involvement of synaptic clustering in memory encoding have been identified in cortical structures such as the retrosplenial cortex (Frank et al. (2018)), visual cortex (Gökçe et al. (2016)) and motor cortex (Fu et al. (2012)). Fu et al. (2012) have shown that a third of newborn spines born during a motor learning task appear in clusters and mostly as paired neighbours. Clustering of synaptic connectivity between hippocampal CA3 and CA1 has also been observed (Druckmann et al. (2014)).

### 1.1.3 Engrams

An engram is defined as a physical memory trace in the brain (Josselyn et al. (2015); Dudai (2004); Thompson (1976); Tonegawa et al. (2015)). It has been shown that cells tagged as active during an event are reactivated during retrieval (Liu et al. (2012)). Silencing engram cells has been demonstrated to suppress memory retrieval whereas activating these cells outside of their original encoding context has been demonstrated to induce retrieval of an artificial memory (Liu et al. (2012)).
Zhang et al. (2018) demonstrated that mice susceptible to chronic social defeat (CSDS) stress

showed higher reactivation of CA1 engram cells labeled during defeat compared to control and resilient mice. Designer Receptors Exclusively Activated by Designer Drugs (DREADD) reactivation of these cells resulted in increased social avoidance behaviour. Increased hippocampal activity is a well known characteristic of patients and animal models of depression and the results reported here may be a downstream effect of this feature. Interestingly, in another study involving stress-induced depression (Ramirez et al. (2015)), it was shown that optogenetic reactivation of positive association engrams were able to acutely suppress depression like behaviour brought about by stress. Chronic reactivation of these same engram cells was additionally found to extend anti-depressant like behaviour beyond the duration of stimulation.
When studying structural plasticity and its potential alterations in relation to stress or learning, it is important to consider the role these changes may play in neuronal function. Engram activation and manipulation studies such as those mentioned bear significance in their support of rewiring of synaptic connections.

## 1.2 Stress

Stress has long been a phenomenon which most would claim to understand, but find difficult to define. Kim and Diamond (2002) propose a 3 part definition for stress which attempts to encompass the reaction of both animals and people. By their definition, a situation is perceived as stressful if

1. it causes heightened excitability or arousal
2. it is perceived as aversive
3. its magnitude of effect is dependent on the degree of controllability the individual has over it.

Aversive environmental changes which may be perceived as a potential threat initiate the release of glucocorticoids in the hypothalamic-pituitary-adrenal (HPA) axis cascade. This is a necessary response for refocusing energy distribution in situations where rapid adaptation for survival is critical. To support this process, a number of limbic-neuroendocrine circuits are synchronously activated resulting in alterations in physiological synaptic traits, mechanistic regulation of stress response circuits and ultimately, behavioural outcome.

### 1.2.1 HPA axis response

The HPA-axis response (Figure 1.2) is a neuroendocrine cascade of events initiated by the perception of a threat to the organism. The response is characterised by the release of corticotropin-releasing hormone (CRH) from the paraventricular nucleus (PVN) of the hypothalamus. These

bind to CRH-receptors in the anterior pituitary gland, resulting in the release of adenocorticotropic hormone (ACTH). ACTH in turn binds to receptors in the adrenal cortex, stimulating the release of glucocorticoids (cortisol in humans and corticosterone in rodents). Glucocorticoids are circulated throughout the body causing multiple changes at the periphery as well as crossing the blood-brain barrier where they bind to mineralocorticoid (MR) and glucocorticoid (GR) receptors. Homeostasis is re-established by negative feedback based on circulating glucocorticoid levels.

This protective response mechanism does however, become counter-productive with prolonged elevation and circulation of glucocorticoids in the system, as in the case of chronic stress. Dysregulation of the HPA-axis response or a mismatch between environmental input and physiological response, increases the likelihood of development of stress-related pathologies such as depression. The effects of glucocorticoids on cellular plasticity in the brain are dependent on a number of factors, such as the brain region, MR and GR expression in these regions, the organisms' history of stress and the duration of stress exposure (Myers et al. (2014)).

The hippocampus, as well as being critical to memory formation, is also highly sensitive to stress due to the presence of high concentrations of corticosterone receptors. There is ample evidence supporting stress impairment of mammalian hippocampal learning and memory (Sapolsky (1992); Oitzl and De Kloet (1992); Kirschbaum et al. (1996); Dominique et al. (1998); de Kloet et al. (1999); Diamond et al. (1999); McEwen and Sapolsky (1995); McEwen (2000); Roozendaal (2002); Donley et al. (2005)). Hippocampal atrophy for instance, is present in patients who suffer from post-traumatic stress disorder, depression and Cushing's disease (in which patients have an excess production and circulation of glucocorticoids). In both cases this is associated with disruptions in the recall of declarative memories (Uddo et al. (1993); Bremner et al. (1997, 2000); Starkman et al. (1992); Sapolsky (2000); McEwen and Sapolsky (1995); Kim and Yoon (1998); McEwen (2000)).

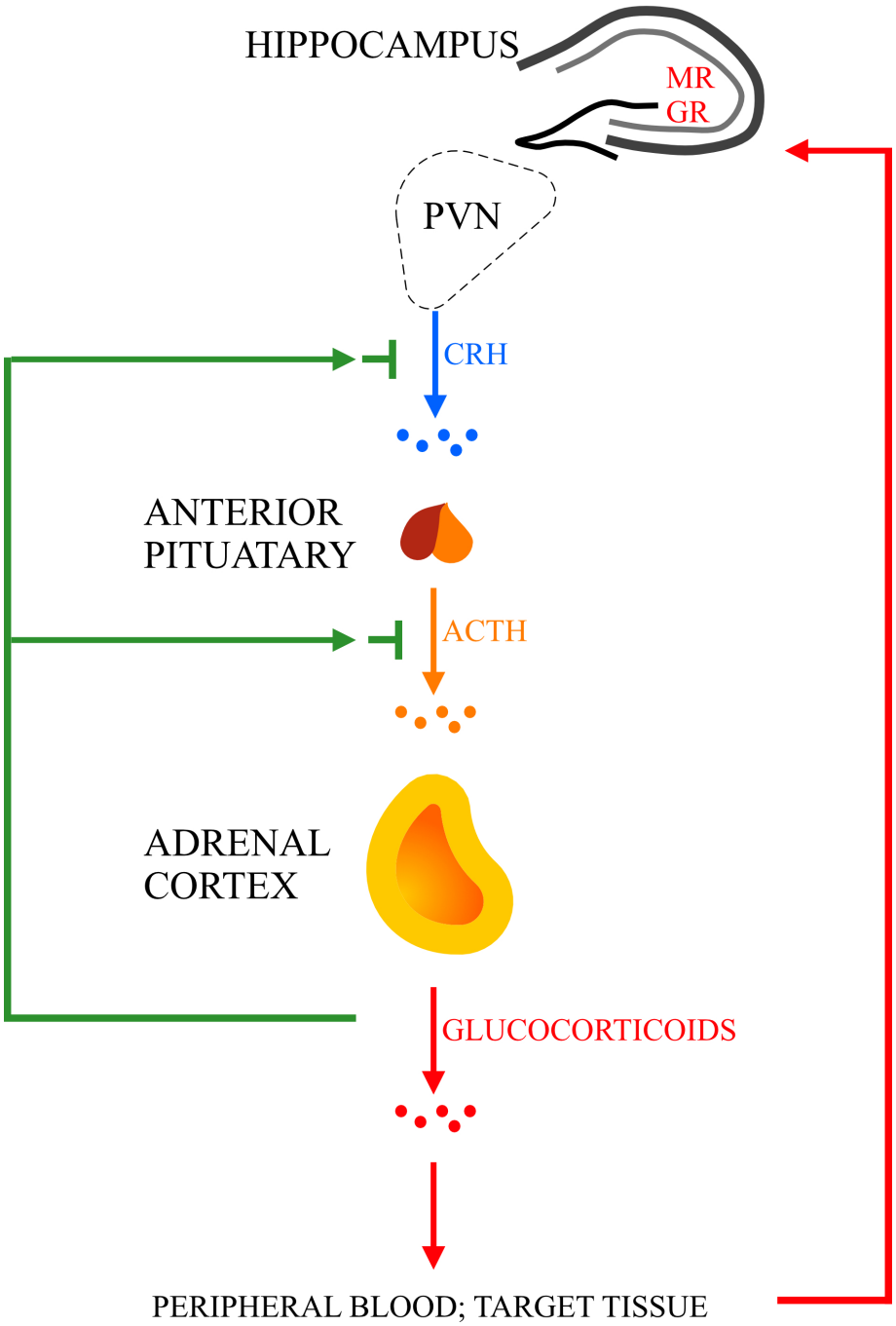


**Figure 1.2:** HPA axis response. The HPA axis response involves the release of CRH from the PVN of the hypothalamus. This stimulates the release of ACTH from the anterior pituitary and subsequently the release of glucocorticoids (corticosterone in rodents) from the adrenal cortex. These circulate peripherally and cross the blood brain barrier to bind to MRs and GRs in the various brain regions, such as the hippocampus. Circulating levels of glucocorticoids are controlled by negative feedback mechanisms (green arrows) which, under normal conditions, allow for the re-establishment of homeostasis.

## 1.3 Stress effects on neuronal plasticity

The mammalian brain is a remarkable structure, able to respond to the environment by modifying connections in a rapid and region specific manner, often via numerous mechanisms of receptor activation. With stress exposure, the first response to glucocorticoid increase occurs at the level of MR receptor activation. MRs have been found to mediate the non-genomic actions of glucocorticoids at both a pre- and post-synaptic level (Joëls et al. (2008); Olijslagers et al. (2008); Pasricha et al. (2011)). MR activation causes a concert of physiological changes which act to increase neuronal excitability. These actions involve increases in the likelihood of glutamate release, inhibition of potassium conductance and increases in the trafficking of glutamate receptors (Karst and Joëls (2005); Groc et al. (2008); Olijslagers et al. (2008)).

MRs and GRs are both abundantly expressed in hippocampal regions. Hippocampal lesions result in reduced feedback and hence extended HPA axis response. MRs appear to play a key role in reduced feedback of this system as MR antagonists have been shown to increase HPA axis output.

The delayed response to glucocorticoid increase occurs at the level of GR receptor activation. With the presumable aim of re-establishing baseline hippocampal activity post-stress and maintaining information pertaining to the stressful encounter, GR activation results in delayed suppression of neuronal excitability (by increased influx and decreased efflux of calcium and increased calcium-dependent potassium current) and impairs long term potentiation (LTP), (described in more detail in section 1.3.1) as a result of lateral diffusion of glutamate receptors (Joels and De Kloet (1989); Karst et al. (1994); Pavlides et al. (1996); Chameau et al. (2007); Bhargava et al. (2002); Groc et al. (2008)). Adverse effects of stress on the hippocampus appear to be primarily mediated by low affinity GRs where high occupancy with corticosteroids occurs with increased stress (Conrad et al. (1999); Oitzl et al. (2001)). The binding of corticosterone to GRs in the rat hippocampus has been demonstrated to adversely affect neuronal metabolism, survival, physiological activity and morphology (Sapolsky (1992); McEwen and Sapolsky (1995); Kim and Yoon (1998); McEwen (2000)).

MRs and GRs are not the only receptors involved in stress responses. NMDARs are pivotal in their role of mediating the influx of $Ca^{2+}$ ions in synaptic plasticity and mechanisms of memory formation (Bliss and Collingridge (1993); Bear and Malenka (1994); Martin et al. (2000); Martin and Morris (2002); Malenka and Bear (2004); Whitlock et al. (2006)).

In addition to direct modulation via MRs and GRs in the CA1, upstream modulation of network processing (Hartner and Schrader (2018)) may further contribute to the concert of changes observed with stress exposure.

Stress-induced disruption of homeostasis in various brain regions can undoubtedly lead to signaling dysfunction between connected regions, such has been demonstrated in the prefrontal cortex (PFC) (Cerqueira et al. (2007)) and thalamus (Quan et al. (2011)) where reduced LTP in relation to hippocampal afferents was observed.

It should be noted that the ventral hippocampus differs largely in its response to glucocorticoids when compared to the dorsal hippocampus. These discrepancies will not be detailed here since our concern is primarily with dorsal hippocampal physiology.

### 1.3.1 Long Term Potentiation and Long Term Depression

LTP is largely considered to form the basis of a physiological model of memory (McGaugh (2000)). It can be described as a lasting increase in synaptic strength which is brought about by a high-frequency stimulation of excitatory afferents (Malenka and Bear (2004)).

A suppression of LTP in the hippocampal CA1 pyramidal cell layer in association with stress was first demonstrated by Foy et al. (1987) in the rat hippocampus. Stress was induced by inescapable restraint and tail shock, the latter of which was repeated every minute for the 30 minutes of restraint before the preparation of hippocampal slices. The DG in the rat hippocampus has also been shown to demonstrate a reduction in LTP with acute restraint and simultaneous repeated tail shock (Shors and Dryver (1994)). In a similar experiment on mice, this suppression of LTP has been shown to last for at least 24h in hippocampal CA1 after stress (Garcia et al. (1997)).

Interestingly, when the aspect of control over a stressor was introduced, the stress effect on LTP was dampened, providing evidence that the uncontrollable psychological dimension of stress contributes largely to suppression of LTP (Shors et al. (1989); Kim and Diamond (2002)).

In an effort to dissect the mechanisms of memory consolidation, Saito et al. (2016) reported enhanced synaptic strength and subsequent synapse formation in slice with 3 LTP inductions, believed to be akin to *in vivo* mechanisms of memory consolidation by repeated exposure. This was further examined by acute exposure of slice tissue to glucocorticoids which resulted in a suppression of this effect. Glucocorticoid exposure decreased spine dynamics previously observed to occur prior to an increase in synapse formation. This was aimed as a model of acute stress effects.

Chronic stress has been demonstrated to impair LTP in dorsal hippocampal CA1 and DG when corticosterone is at basal levels. Further application of corticosterone in this situation did not further impair LTP in these regions (Alfarez and Krugers (2003)). Evidence suggests that these modifications in LTP are mediated by GRs, since blocking GRs in the last 4 days of 21 days of chronic unpredictable stress has been shown to eliminate the effects of chronic stress on LTP (Krugers et al. (2006)). Impairment of synaptic plasticity in animals which have a history of chronic stress may also be due to GR-dependent increases in calcium influx into CA1 neurons at baseline corticosterone levels Karst and Joëls (2007)).

Interestingly, Matsuzaki et al. (2004) used glutamate uncaging in single spines to demonstrate selective and fast spine enlargement, an effect which persisted in small spines. Single spine stimulation did not result in the formation of new spines suggesting that LTP induction in multiple synapses may be required for formation. Their work demonstrated that individual

spines can operate under Hebbian mechanisms and suggested that spines may act as units of memory, where large spines, which were resistant to LTP, would be crucial to long term memory storage. Applications of this technique to stress remain to be explored, but hold attractive possibilities for targeting specific populations of spines *in vivo*.

Long term depression (LTD) is considered the physiological opposite of LTP and can be described as a lasting decrease in synaptic strength which could be brought about by, for instance, extended low frequency stimulation (Collingridge et al. (2010)). The induction of acute stress and the administration of corticosterone have been demonstrated to enhance the induction of LTD in hippocampal CA1 (Xu et al. (1997)). These alterations in LTP and LTD support the notion that stress may induce *metaplasticity* (a form of plasticity which drives subsequent synaptic plasticity), in such a way as to preferentially favour depression over potentiation (Abraham and Bear (1996); Kim and Yoon (1998)).

The effects on LTP and LTD have been demonstrated to be reversible after single stressors and intermittent alternating stressors, indicating that the dynamics of hippocampal plasticity is impacted by how the subject perceives its' environment.

In the context of emotional memories and recall impairment, Diamond et al. (2005) hypothesized depotentiation, LTD and LTP to be solely initiated with concurrent arousing experiences and memory related hippocampal and amygdala activation which may be motivated by competition over synaptic resources.

### 1.3.2 Morphology

Changes in hippocampal morphology due to stress are well-documented. In particular, stress has been shown to alter dendritic morphology in the CA3 (Christian et al. (2011); Sousa et al. (2000)), decrease spine density in a region-specific manner (Murmu et al. (2006); Radley et al. (2005); Martínez-Téllez et al. (2009)), as as well as impede neurogenesis in the adult brain (Mirescu et al. (2004); Snyder et al. (2011)), all of which may influence learning and memory processes. Multiple pharmacological interventions have proven effective in preventing the atrophic product of chronic stress, signifying the contribution of numerous systems to stress-induced atrophy (Brown et al. (1999); Kim and Diamond (2002)).

#### 1.3.2.1 Effect of stress on dendritic morphology

Dendritic retraction in apical CA3 dendrites has been observed after chronic stress exposure (McEwen (2000)), but has been found to be reversible. Some studies have also reported retraction of CA1 apical dendrites with chronic unpredictable stress (CUS) exposure (Sousa et al. (2000)) and chronic immobilisation stress (Christian et al. (2011)) without altering the number of apical dendritic segments. Christian et al. (2011) demonstrated dependency of apical CA1 dendritic retraction on upstream CA3 NMDAR activation.

An *ex vivo* study of the effects of chronic mild stress on structural morphology of hippocampal interneurons reported a reduction in dendritic complexity of interneurons in the CA1 but not the CA3 after chronic mild stress exposure(Gilabert-Juan et al. (2017)).

Dendritic retraction has most often been observed to occur at terminal dendrites which presumably led to the eventual reduction in dendritic complexity observed in some studies (Magariños et al. (1996, 1997); Watanabe et al. (1992); Magarin and McEwen (1995)). Corticosterone and NMDARs were shown to be key players in this atrophic effect (Magarin and McEwen (1995)).

#### 1.3.2.2 Effect of stress on synaptic structure and clustering

Evidence of structural plasticity changes in the dCA1 is severely lacking in literature. Mostly *ex vivo* characterisations of spine changes have been investigated thus far. A decrease in spine density was observed in apical dendrites of CA1 pyramidal cells when rats were exposed to 1 month of CUS (Sousa et al. (2000)). Inaccessibility and high spine density in basal regions are both strong contributing factors to the difficulties of detecting potential effects of stress in this region.

Confounding results on the changes in spine density with stress exposure are however, abundant in the literature. Observations of no change (Sunanda et al. (1995)), increases (Magariños et al. (1996)) and reversible decreases (Sandi et al. (2003); Stewart et al. (2005)) in spine density in the CA3 have been reported. In the CA1, increased post synaptic density size with CRS exposure has been reported (Donohue et al. (2006)). The numerous differences in observations may be due to differences in types of stress, duration of exposure, measurement techniques and experimental design. Whatever the case, it is clear that an establishment of baseline conditions prior to exposure would greatly aid in understanding stress effects in an internally controlled manner.

However, the recognition of stress as an instigator of dynamic processes in the brain has not been ignored. Studies (although few) have attempted to determine these dynamic effects in the cortex (Chen et al. (2018); Moda-Sava et al. (2019)).

Moda-Sava et al. (2019) investigated *in vivo* PFC synaptic dynamics with chronic corticosterone administration, reporting a decrease in spine gain and opposing increase in clustered spine loss after 21 days. Ketamine treatment was found to restore both spine gain as well as coordinated multicellular ensemble activity. Further, spinogenesis was not necessary for the induction of anti-depressant effects, but was found to be necessary for long term preservation thereof.

Layer 5 (L5) pyramidal neurons in the barrel cortex experienced a clustered and continued spine loss on apical dendrites with exposure to repeated restraint stress (Chen et al. (2018)). Stress was additionally shown to decrease parvalbumin (PV) expressing interneuron excitability. Interestingly, by pharmacogenetically activating PV interneurons of stressed mice, stress-induced alterations in structural dynamics of L5 pyramidal neurons was reversed, as was the effect on behaviour. Equally striking was the fact that mice raised in an enriched environment demonstrated resilience to stress induced structural plasticity and PV excitability in this brain region. This

study beautifully demonstrates the multiple levels of complexity which are involved with stress response and further highlights the importance of baseline conditions as a contributing factor.

These cortical studies are interesting in their approach to *in vivo* structural changes as they are the only known longitudinal investigations into synaptic stress response.

### 1.3.3 Multi-modal stress

Stress effects on plasticity have thus far demonstrated a complex dependency on type, duration and timing in relation to learning and age. The dorsal hippocampus has been shown to play a role in integrating sensory signals of events into memory (Fanselow and Dong (2010); Moser and Moser (1998)). Short stress exposures in the range of seconds to minutes have been shown to enhance learning and longer exposures have in general been shown to impede learning, but little has been shown in the way of simultaneous stress exposures. Maras et al. (2014) addressed the question of complexity of stress and its effects on structure and hippocampal dependent behaviour. To this aim, they developed a multimodal stress (MMS) paradigm which involved exposure to multiple concurrent stressors including restraint, jostling, loud noise, bright light and awareness of peer discomfort. Translationally, MMS serves as a post traumatic stress disorder (PTSD) model and also attempts to recapitulate the reality of stress, since rarely are stress exposures confined to one mode.

Mice exposed to MMS for 1h, 2h, and 5h displayed impairments in hippocampal dependent novel object recognition memory and decreased spine density in dCA1 (although whether changes occur in both basal and apical dendrites was not specified). MMS strengthened connectivity between hippocampal-amygdala (important in the perception of fear and anxiety) and hippocampal-BST (bed nucleus of the stria terminalis - afferent to hypothalamic neurons which are stress sensitive) circuits. Importantly, exposure to individual stressors did not recapitulate the effects of MMS.

Chen et al. (2016) demonstrated the requirement of synergistic actions of corticosterone and CRH in mediating hippocampal dependent memory impairment when released in response to MMS. RhoA, a regulating protein of actin in spines was shown to be deactivated by corticosterone and degraded by CRH, providing an underlying mechanism for spine elimination and a structural correlate to memory impairment.

## 1.4 Behaviour

Acute stress has been shown to enhance learning of emotionally salient experiences (de Kloet et al. (1999); Smeets et al. (2009)). At a receptor level, MRs play a role in the acquisition of fear memories as well as in strategy selection during novel spatial orientation tasks (Oitzl and De Kloet (1992); Oitzl et al. (1994); Khaksari et al. (2007)). GRs mediate the consolidation of contextual information pertaining to fear memory and spatial memory tasks (Oitzl and De Kloet (1992); Pugh et al. (1997); Sandi et al.; Donley et al. (2005); Chen et al. (2012a)).

Glucocorticoid levels related to acute stress contribute to the inhibition of memory retrieval in already learned spatial and contextual tasks, including the MWM and the radial arm maze, novel object recognition and contextual FC (Dominique et al. (1998); Roozendaal (2002)).

Impairment of novel object location after acute stress exposure has been shown to be accompanied by actin remodeling proteins and elevated levels of NMDA receptor sub-units (Aguayo et al. (2018)). In this study, apical level 2 dendrites of the CA1 displayed an increased density of immature spines after 6h of recovery and elevated levels of $\alpha$-amino-3-hydroxy-5-methyl-4-isoxazolepropionic acid receptor (AMPAR) sub-units. All changes were reversible after 24h of recovery.

Chronic stress and chronic exposure to glucocorticoids (administered in doses reflective of a natural physiological stress response) are associated with disruptions in spatial reference memory (Luine et al. (1993); Diamond et al. (1999, 1996)). The complexity of the effects of stress and glucocorticoids on hippocampal processing is further demonstrated by the selectivity of these effects on specific functionality. Chronic stress for instance, enhances hippocampal dependent excitatory trace eye blink conditioning as well as hippocampal-independent delay eye blink conditioning and in a fear learning task, it enhances hippocampal dependent contextual FC, but does not affect hippocampal-independent tone FC (Shors et al. (1992); Pugh et al. (1997); Beylin and Shors (1998); Sandi et al. (2001)).

The retention of emotionally salient information which is relevant for adaptation and survival appears to be prioritized over less critical memory processes. Glucocorticoid levels and time windows of action appear to facilitate the selection of such processes (Myers et al. (2014)). One might give some regard to the notion that stress improves hippocampus-dependent learning and memory tasks corresponding to fear whilst impairing spatially-related computations obtained outside of the FC context (Sandi et al. (2001); Kim and Diamond (2002)).

### 1.4.1 Morris Water Maze

The Morris Water Maze (MWM) (Morris (1981)) is often used as a means of determining rodent ability to spatially navigate. The task is hippocampal dependent and both learning and recall have been shown to be affected by stress.
In one study, rats subjected to 1 month of CUS showed no impairment in 12 days of spatial learning of a MWM task when compared to unstressed controls, but stressed and stressed-recovered rats had significantly longer swim distances during later trial blocks of learning, which was not observed in an unstressed, corticosterone administered or corticosterone administered-recovered group (Sousa et al. (2000)). Another study however, contradicted this finding by demonstrating an improvement in MWM learning as well as an adoption of more direct strategies after rats were subjected to 10 days of CUS (Gouirand and Matuszewich (2005)).
Interestingly, when acute stress induced LTD was blocked, rats were impaired in reversal platform learning, suggesting a role of LTD in adaptive learning (Dong et al. (2013)).

Originally, the test was designed with rats as the subjects. Today, it is employed with mice of various strains and genetic backgrounds and many variations in numbers of trials and days of training exist. Important factors to consider when using this test with mice are water temperature, maze size and sufficient inter-trial interval to allow subjects to rest before commencement of the next trial. In mice, MWM performance has been shown to vary between strains (Francis et al. (1995)), thus emphasizing the importance of comparison between animals of the same genetic background and maintaining consistency between experimental groups.

CHAPTER 2

# AIMS AND JUSTIFICATION OF STUDY

Although much has been discovered about the mechanisms of stress and their impacts on various aspects of physiology and behaviour, it is imperative to address the dynamic aspect of these effects. The evidence for CA1 involvement in stress is clear, but typical measurements of dendritic spine density and retraction have failed to yield measureable differences. In order to gain a deeper insight into *in vivo* structural dynamics at the level of individual response, one must employ tools which enable the study of the same organism under multiple conditions. This level of internal control is essential for detecting both small changes as well as highly dynamic changes which may maintain overall densities and thus be undetectable in *ex vivo* characterisations.
Therefore, in this study I aim to

1. address these factors by implementing *in vivo* chronic 2-photon imaging of dorsal hippocampal CA1 synaptic dynamics during baseline and stress periods. Repeated imaging of the same dendrites at different time intervals allows for the comparison of an individuals synaptic dynamics as well as enabling individual dendritic spines to be tracked - we are able to tell the duration of a spines' survival, when it was born and when it disappears within the imaged time frame. This provides a powerful means of separating populations of spines into persistent or newborn populations.

2. determine potential effects of stress on clustered birth and loss of excitatory synapses.

3. determine the effects of stress on spatial learning and memory by use of the MWM.

4. determine potential differential effects of acute stress and recovery and repeated stress exposure, both in terms of plasticity as well as behaviour.

These advantages, none of which can be achieved with *ex vivo* characterisation, allow for the first time the study of CA1 basal dendrites and their synaptic dynamics during stress.

CHAPTER 3

# MATERIALS AND METHODS

This section details the methods used for induction of stress, surgical preparation, 2-photon optical time lapse imaging, image processing and measurement of hippocampal-dependent learning and memory.
All experimental procedures were approved by the Government of Upper Bavaria (licence 2016_ROB-55.2Vet-2532.Vet_02-16-48).

## 3.1 Animals

A total of 43 mice were used for experiments. 13 heterozygous Thy1GFPm male mice were used for imaging experiments. 30 C57BL/6N male mice were used for MWM experiments. Mice were 3 to 6 months of age at the time of experiments. All mice were sourced from the animal facility of the Max Planck Institute of Biochemistry, Martinsried, Germany. Mice were transferred to holding rooms at the Max Planck Institute of Psychiatry at least 2 weeks prior to the start of experiments to provide an adjustment and habituation period to the new environment. Mice were group housed in individually ventilated cages under a 12h dark/light cycle. Food and water were provided *ad libitum*.

### 3.1.1 Use of transgenic mice

The use of Thy1GFPm mice was first described by Feng et al. (2000). These mice express cytoplasmic enhanced green fluorescent protein (GFP) in a sparse, random subset of pyramidal neurons and under the control of the Thy1 promoter. For this work, homozygous Thy1GFPm mice were crossed with C57BL/6N mice in order to obtain heterozygous Thy1GFPm experimental animals.

## 3.2 Drugs

Vetalgin: 200mg/kg administered subcutaneously as an analgesic. Used in chronic preparation for *in vivo* 2-photon time lapse imaging.
Meloxicam: 1mg/kg administered subcutaneously as an anti-inflammatory for surgical and post-operative care.
Isofluorane: 3% in 1L/min $O_2$ for induction of anaesthesia. 1.5-2% in 1L/min $O_2$ to maintain anaesthesia during surgery and 2-photon imaging.

## 3.3 Imaging cannula preparation

Custom designed cannulas of inner diameter 2.5mm and outer diameter 3.0mm, were machined from stainless steel (Figure 3.1). One end tapered into a rim which was designed to sit flush with the skull upon implantation and hence increase the stability of the cannula insertion. Cannulas were 1.6mm long below the rim in order to ensure implantation securely above hippocampal CA1. Machined cannulas and 4mm diameter glass coverslips (custom made, Engelbrecht Medizin and Labortechnik) were rinsed in 100% acetone and allowed to dry for approximately 5 minutes. Coverslips were between 0.13-0.17mm thick.
The rim-free end of the cannula was then dipped into a thin layer of UV-curing optical adhesive (Thorlabs), ensuring that only the bottom surface of the cannula was coated. In the case of adhesive forming a film over the open centre, the film was broken with a blunt needle.
The clean and dry glass coverslip was placed under a stereoscope (Zeiss Stemi 305) and the cannula was placed onto the centre of the coverslip, adhesive side down. Care was taken to ensure that the adhesive formed a ring at the interface of the coverslip without spreading to the centre of the coverslip. If adhesive spread to the centre, the cannula was removed and placed onto a clean coverslip so as to avoid obstructing the imaging field of view with any material other than the glass.
A UV-curing LED light (Thorlabs, 365 nm) was used to cure the optical adhesive by exposing the adhesive for 1 minute to 365nm with equal illumination from all angles. This was achieved by rotating the light source at 10 second intervals for the 1 minute of exposure. The adhesive was then left to harden overnight.
Since the glass coverslip was of 4mm diameter and the cannula of 3mm outer diameter, excess glass needed to be filed away. This was achieved by clamping the rimmed end of the cannula with a hemostat and, working under the stereoscope (Zeiss Stemi 305), filing the glass with a dental drill angled at 45 degrees to the cannula until the glass was flush with the edge. Glass and stainless steel debris were removed gently with compressed air from the dental drill and the cannulas were rinsed in phosphate buffered solution (PBS) 1x and allowed to dry before being used for surgical implantation.

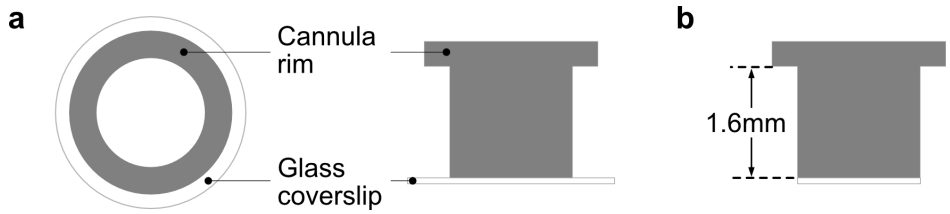


**Figure 3.1:** Preparation and design of imaging cannula. (a) LEFT: top view of cannula placed onto 4mm diameter glass coverslip. RIGHT: side view of glued cannula and coverslip, cannula rim is indicated. Excess glass remains until UV curing optical adhesive has been cured and hardened. (b) Excess glass is filed away. Cannula ready for implantation is 1.6mm deep plus 0.13-0.17mm of coverslip.

## 3.4 Chronic preparation for *in vivo* 2-photon time-lapse imaging

Male heterozygous Thy1GFPm 2-3 month old mice were implanted with a chronic imaging window. The following description details the surgical implantation procedure (Ulivi et al. (2019)):

Mice were weighed and analgesic (200mg/kg Vetalgin, MSD Animal Health, Unterschleißheim, Germany) and anti-inflammatory (1mg/kg Meloxicam, Boehringer Ingelheim, Vetmedica, Rohrdorf, Germany) drugs were administered sub-cutaneously in accordance with the approved protocol. Anaesthesia was given at 3% isoflurane and 1L/min $O_2$. Mice were then transferred to a heating blanket and secured to a stereotactic apparatus by means of a nose cone and ear bars. The flow of isoflurane was adjusted to 2% and a toe-pinch reflex test was done. Eye ointment (Bepanthan, Bayer Vital, Leverkusen, Germany) was applied. Fur was removed from the scalp and the exposed skin was subsequently removed to expose bregma, lambda, the parietal bones and the posterior half of the frontal bones. Xylocaine was applied to the skull and the periosteum was removed. A 0.5mm micro-drill bit was used to make a small craniotomy 1.5mm left of the sagittal suture and 2mm rostral to the coronal suture. A 0.86mm stainless steel bone screw was fixed into the exposed column. Quick adhesive cement was applied to the clean, dry skull and allowed to dry for 1 minute. A 3mm trephine drill bit was used to make a craniotomy over the right hippocampus, 1.5mm right of the sagittal suture and 2mm rostral to the lambdoid suture (Figure 3.2a). The meninges were carefully removed with fine forceps. The size of the craniotomy was checked by positioning a 3mm outer diameter cannula over the craniotomy. Further bone was removed along the perimeter of the craniotomy if the cannula was too big. Cortical matter was ablated with vacuum attached to a blunt tip 0.9mm diameter cannula until the final of the three layers of the *corpus callosum* was exposed (Figure 3.2b). The exposed matter was rinsed with saline and any bleeding resolved. The cannula was positioned into the 3mm hole and gently pushed down until flush with the third layer of the *corpus callosum*. The skull was dried and quick adhesive cement was applied to the skull and around the outer rim of the cannula. The adhesive

was allowed to dry for 1 minute. A custom head plate (Figure 3.2c) was fixed to a stereotaxic arm and positioned against the dry skull. Dental acrylic was applied over the exposed skull, making sure to cover also the skull screw and exposed skin. The acrylic was left to harden for 20 minutes. A removable adhesive film was applied over the head plate to avoid debris entering the cannula. Mice were weighed and Meloxicam (1mg/kg) was administered for a further 2 days. Daily monitoring continued for 9 days post-surgery.

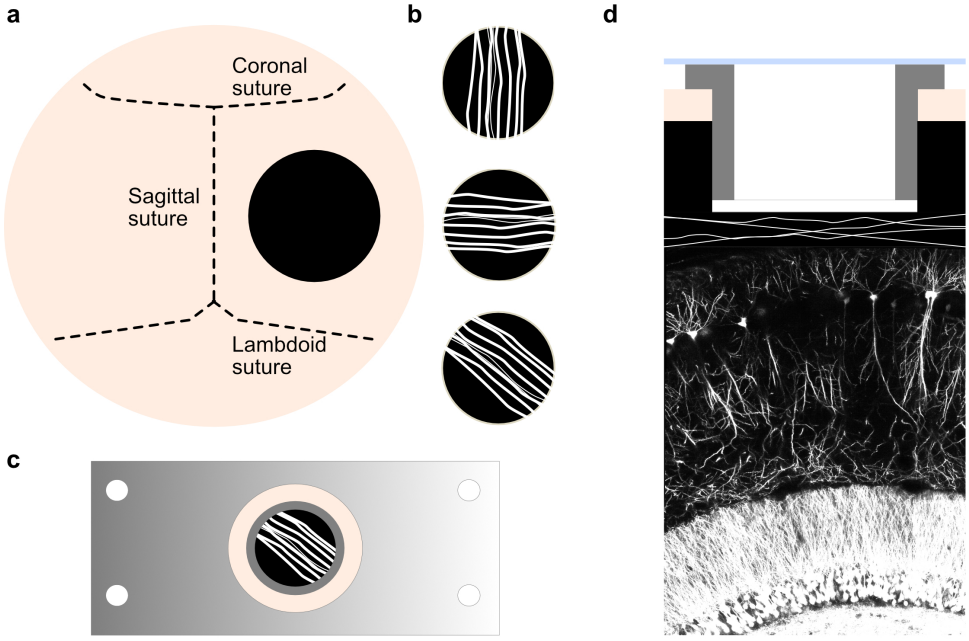


**Figure 3.2:** Surgical implantation of imaging cannula. (a) a 3mm diameter craniotomy was made over the right hippocampus, 1.5mm right of the sagittal suture and 2mm rostral to the lambdoid suture. (b) three layers and orientations of *corpus callosum* fibres. The first two layers (top and middle schemes) were removed and the final oblique fibres (bottom scheme) were left in tact. (c) custom designed head plates were fixed to the skull with dental acrylic such that the imaging cannula was in the centre of and perpendicular to the head plate. (d) cross sectional schematic view of implanted cannula. The cannula rim was sealed with removable adhesive film; the bottom surface of the rim was flush with the skull; the glass coverslip is shown on top of the last layer of *corpus callosum* fibres, directly above dCA1.

## 3.5 2-photon Imaging

### 3.5.1 Fundamentals of 2-photon microscopy

I will briefly introduce the theory of 2-photon laser scanning microscopy, the use of which forms a critical aspect of *in vivo* experiments conducted in this thesis.
The principal of 2-photon excitation was first described in doctoral work by Göppert-Mayer (1931) and its first demonstrated use in biology occurred 60 years later in pioneering work by Denk et al. (1990).

The phenomenon of 2-photon excitation derives from the simultaneous (within $10^{-18}$seconds) absorption of two photons in one quantum event. Each of the photons contributes half of the energy required to excite a fluorophore. Upon excitation, a fluorescence photon is emitted at higher energy than each of the photons used for excitation. Given that the energy of a photon is inversely proportional to its wavelength, the excitation photons require a wavelength about two times that required for 1 photon excitation. Figure 3.3a illustrates a Jablonski energy diagram to describe this concept.

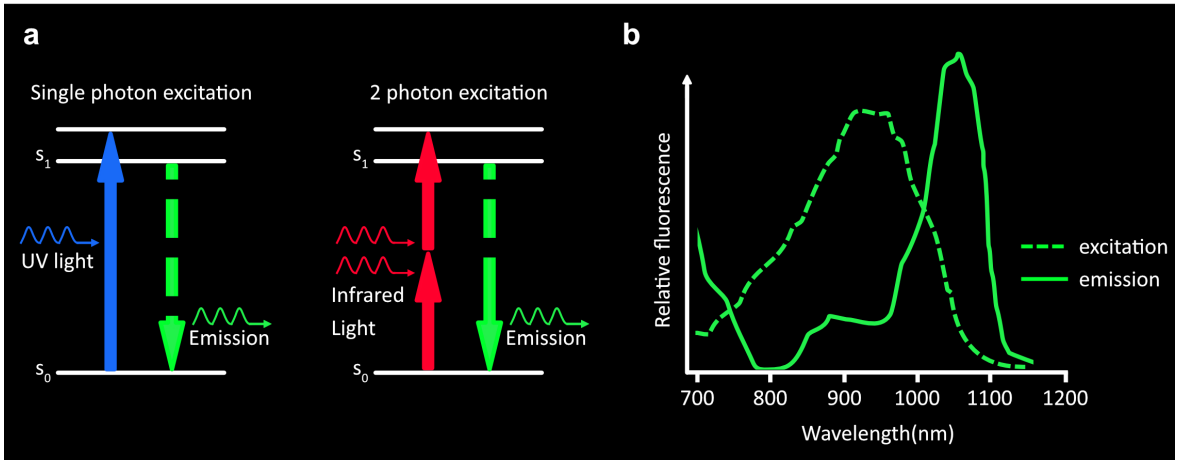


**Figure 3.3:** 2-photon excitation and emission. (a) Jablonksi energy diagram illustrating the concept of 2-photon excitation in relation to single photon excitation. (b) 2-photon excitation and emission spectra for GFP. $s_0$, ground state; $s_1$, excited state.

Since simultaneous absorption is required with 2-photon excitation, fluorescence emission varies quadratically with excitation intensity. To circumvent the low probability of a simultaneous event, high excitation photon density is required - around 1 million times the density required for the same number of 1 photon absorptions. This is achieved with the use of pulsed lasers (with pulse width in the order of 100 femotoseconds at 80MHz to achieve the required excitation photon density and flux), where the peak pulse power is sufficient to generate 2-photon excitation. The required density of excitation photons is passed through an objective lens and concentrated at

the focal point, thus restricting excitation to the focal volume and minimising out of focus signal, ultimately providing a strong advantage over single photon techniques. Lasers are tunable to a range of wavelengths. Emission signal is passed back through the objective lens and through a set of dichroic filters to be detected by photo multiplying tubes (PMTs).
One advantage of 2-photon excitation has already been mentioned and that is the controlled focus volume of excitation. Additionally, less scattering occurs with longer wavelengths allowing for superior results in thicker specimens and the use of low energy photons have a lower probability to damage tissue outside of the focal point.
However, as with any system, 2-photon microscopy has its disadvantages. Smaller objects in thin tissue are better obtained with confocal imaging. 2-photon use in this case would increase photobleaching in the focal plane.

### 3.5.2 *In vivo* application of 2-photon imaging to determine structural dynamics in dCA1

After 2-3 weeks of recovery time, the potential for 2-photon repeated imaging was assessed. Only mice which demonstrated a stable preparation and allowed for use of a suitable laser power (5-25mW at the sample) were selected for further imaging. These mice were imaged with a femtosecond pulsed Ti:Sapphire laser tuned to 920nm to excite GFP. Laser power was adjusted to achieve 5-25mW at the sample. Mice were anaesthetized at 3% isoflurane and 1L/min $O_2$ and anaesthesia was maintained at 1.7% isoflurane and 1L/min $O_2$ for a maximum of 2hours per imaging session. A pre-imaging session was used to determine suitable imaging parameters. Images were processed according to the protocol outlined in section 3.6. Imaging parameters were subsequently adjusted accordingly for experiment imaging based on the outcome of the pre-imaged, post-processed data. To ensure fair comparison across imaging time points, parameters were adjusted throughout the experiment to maintain raw images of the same resolution throughout.

## 3.6 Image Processing

The raw images obtained from 2-photon *in vivo* imaging of dorsal hippocampal CA1 are noisy and prone to misalignment due to motion artefacts and drift. In order to address these issues and obtain images optimal for identifying spines clearly, I developed a fully automated image processing pipeline.
I sought to minimise any resulting moderate to severe aberrations in the images which occur due to both motion artefacts in live animals and varying degrees of stability in the surgical preparation. To decrease acquisition time and hence the potential to capture these artefacts, I

1. employed the use of a resonant galvanometer (30 frames per second at 512x512) for faster acquisition times (compared to galvanometer raster scanning 1.65 frames per second at

512x512).

2. modified the acquisition software (Prairie View, Bruker) to obtain successive repetitions of image slices as opposed to the original software which acquires each z-stack before acquiring the next repetition of the same z. The modification increased the speed of acquisition because the z motor is slower than those for xy motion.

Using this method of acquisition, I then established the optimal number of image stack repetitions to acquire within a reasonable time whilst still being enough to produce a clear averaged resultant image. Four repetitions were found to be ideal and were used throughout all imaging experiments. The four repetitions of each image stack then underwent a series of post-processing steps as outlined below and further represented schematically in Figure 3.4.

1. Align each stack repetition through z using ImageJ plugin, StackReg. This is necessary for the deconvolution step 2 below in which the deconvolution of each slice is dependent on the signal in adjacent slices.

2. Deconvolve each stack using commercial software, Autoquant X3 (Media Cybernetics) to remove signal captured due to out of focus light.

3. Align each slice with its respective repetitions using custom scripted implementation of ImageJ StackReg plugin.

4. Calculate the difference between each slice and every other repetition in custom Matlab script.

5. Remove the repetition with the biggest difference. This removes the largest motion artefacts as no single artefacts were found to span multiple images.

6. Average the remaining 3 slices using custom ImageJ script.

7. Align the resultant stack through z using ImageJ StackReg plugin.

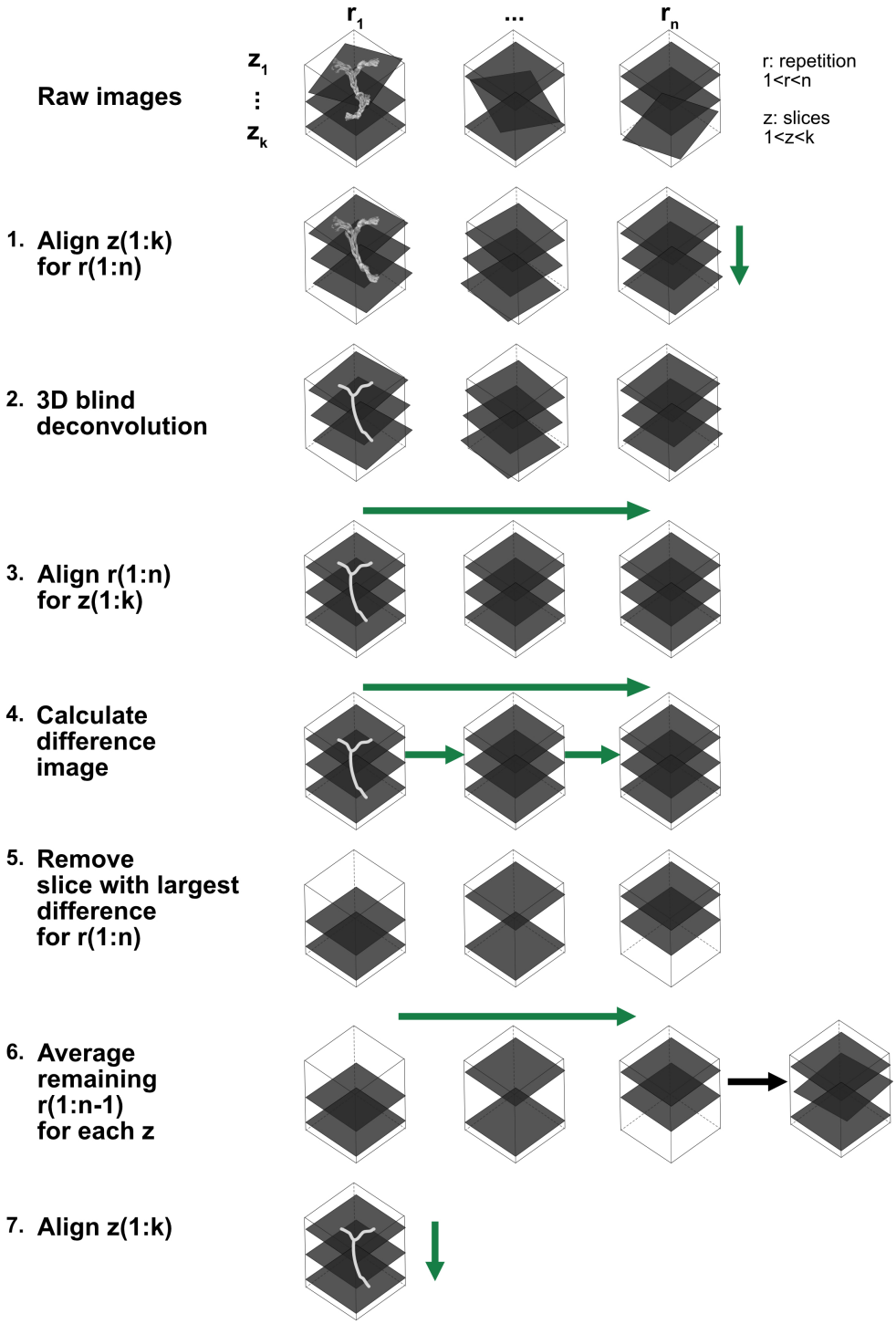


**Figure 3.4:** Automated post-processing of raw 2-photon images acquired *in vivo*. I wrote a custom script to acquire raw images with the 2-photon Prairie View software such that each slice repetition was acquired before acquiring the next z-slice. Shown here are the fully automated post-processing steps, taking images from their raw acquisition state to a countable form. Each raw image stack was aligned through z and 3D deconvolved. Slice repetitions were aligned and the image with the largest difference to the others excluded. Remaining slice repetitions were averaged and the resultant stack aligned through z and output for counting.

I programmed the post-processing pipeline in Matlab, Autoquant and ImageJ. A graphical user interface (GUI) allowed users to input imaging parameters (Figure 3.5a). For convenience, common parameters were implemented and could be adjusted via a secondary GUI (Figure 3.5b), allowing for quick input times and minimal user interaction. User interaction time was cut to less than 1 minute and processing could run unassisted. Compared to weeks of manual processing time which would ordinarily be required to achieve the same processed images, this proved a useful tool for implementation not only for processing of data produced for this thesis, but also for general implementation in the lab. Figure 3.6 illustrates the difference between raw and processed images in a maximum intensity projection (MIP) of an image stack (z step = 1µm, k = 16 slices).

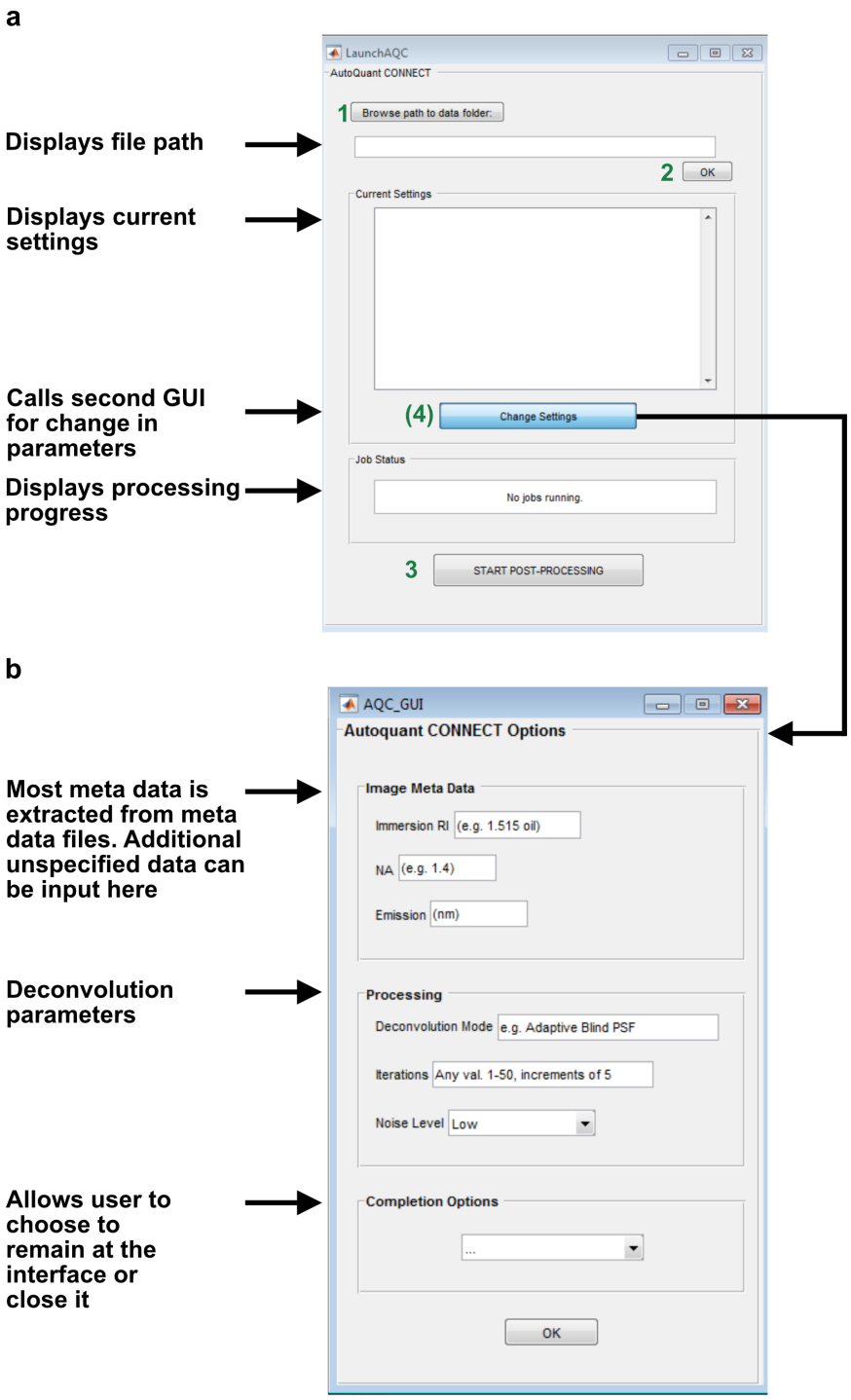


**Figure 3.5:** GUI's for implementing post-processing. (a) Primary GUI allows user to (1) navigate to directory where data is stored, (2) upon clicking 'OK', default parameters are loaded into the 'Current Settings' area, (3) if these are the desired settings, clicking 'Start Processing' begins the post-processing steps as described in Figure 3.4. (4) The imaging parameters remain fairly standard within the lab. However, the GUI allows for added flexibility of changing parameters such as those indicated in 'b'. (b) Secondary GUI which can be called from the primary GUI in 'a'. Allows for imaging parameters to be adjusted as required. The interfaces were designed for minimal intervention to enable users to save as much time as possible.

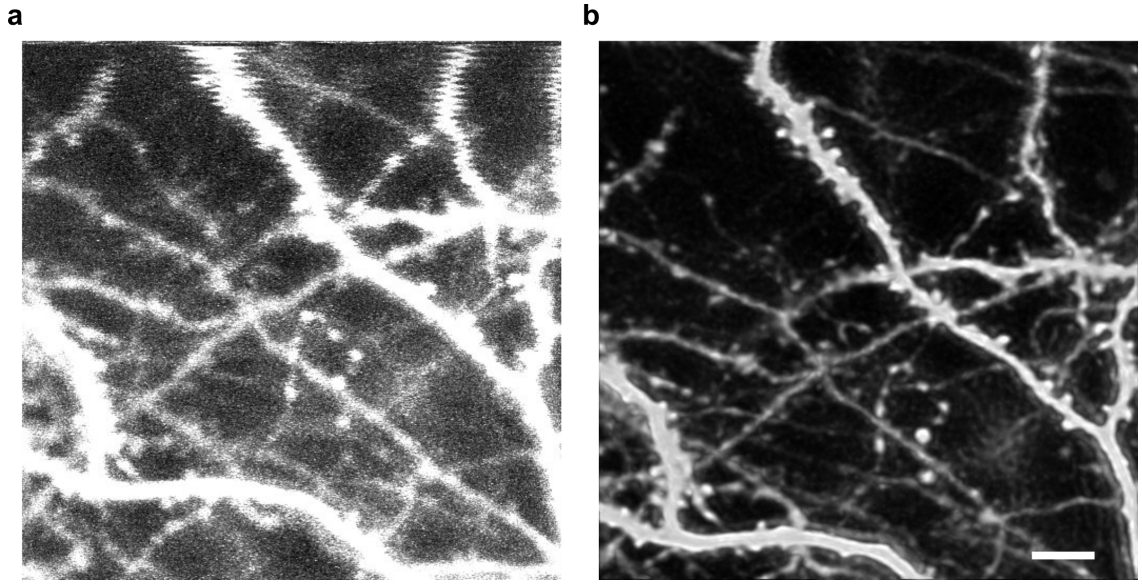


**Figure 3.6:** MIPs of raw and post-processed data. (a) Representative MIP of raw data acquired with a resonant scanner and custom script in Prairie View software. (b) MIP of the same data in 'a' post processed with the steps shown in Figure 3.4. Aberrations were removed and spines made more easily visible for counting. Scale bar, 2.5µm.

## 3.7 Spine counting and quantification

After data was post processed using the pipeline described in section 3.6, spines were counted using a custom GUI, iCount, previously written in MATLAB (Figure 3.7) by a collaborator, Ju Lu and further edited by me. iCount enables the spines to be tracked over all time points whilst keeping the same unique spine identification (ID) at each time point. In addition, each dendrite and its' cell are given ID's which are also maintained through each time point. Time points were pseudo-randomised such that the user was blind to the time point being counted, but time points were presented in succession. Given that structural changes can be more pronounced over time, presenting the data to count successively afforded the user the advantage of making more informed decisions about spine gain, loss or same ID.
Pixel size and z-step were input into the GUI to determine length and location data.
Spine ID's, locations and presence and dendrite ID's and lengths were output from iCount for further analysis.

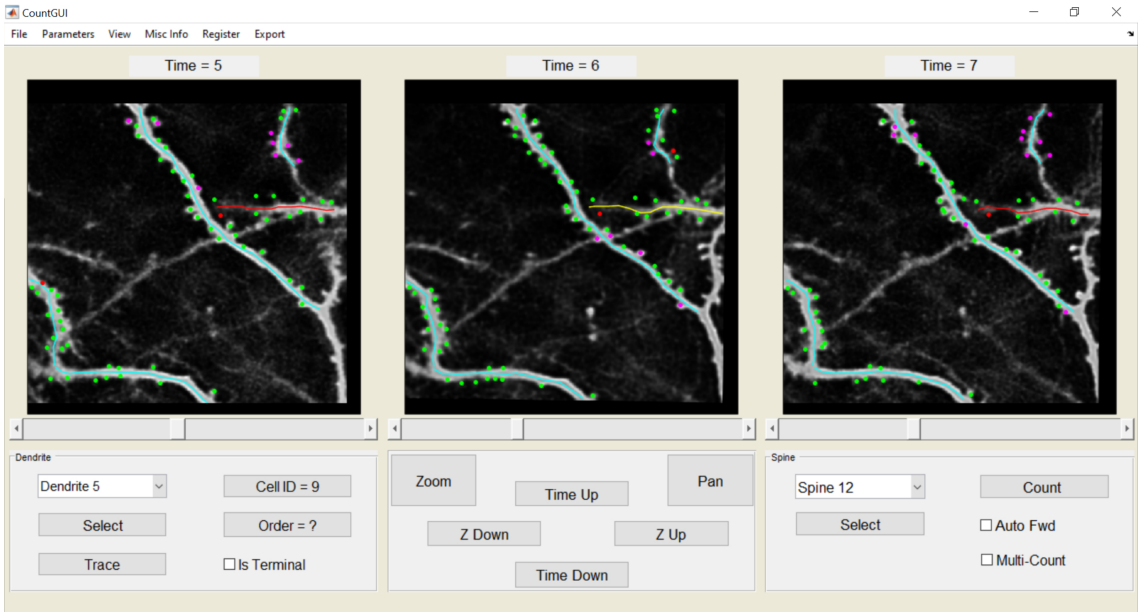


**Figure 3.7:** Representative images counted in iCount, a MATLAB GUI for longitudinal spine tracking.

## 3.8 Clustering analysis

3D spine locations were projected to a linearised dendrite and this location data extracted from iCount to determine proximity of spines in relation to one another. Distances between new spines, new and persistent spines, lost spines, lost and newborn spines and lost and persistent spines (Figure 3.8) were calculated with custom Visual Basic for Applications (VBA) code.

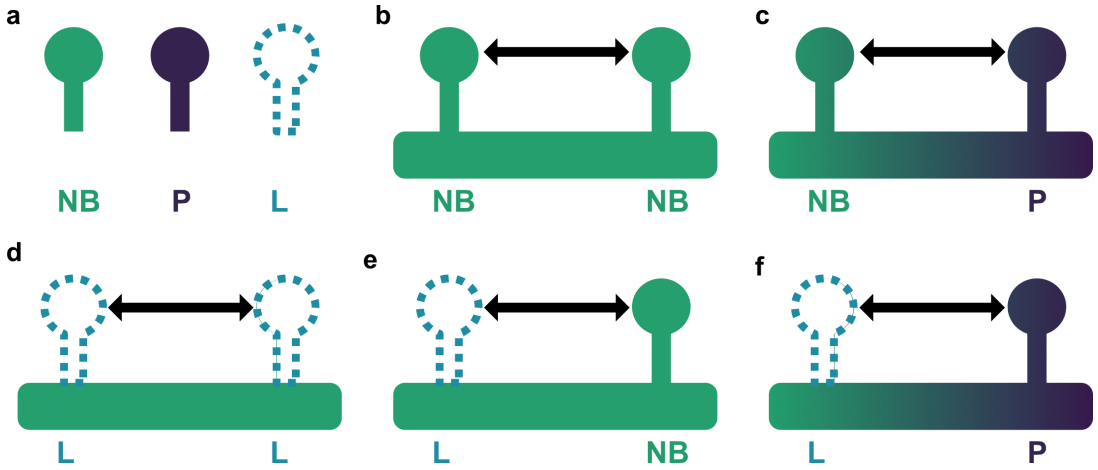


**Figure 3.8:** Types of spine pairs for which nearest neighbours were calculated. (a) Key for schematic spine type. NB, newborn; P, persistent; L, lost. Distances were calculated between (b) new spines (c) new and persistent spines (c) lost spines (d) lost and new spines (e) lost and persistent spines.

## 3.9 Perfusion

After the end of imaging experiments, intra-cardial perfusions were performed on Thy1GFPm mice using heparin in saline for 10 minutes, followed by fixation with 4% PFA in PBS 1x for 10 minutes. Perfused brains were extracted and post-fixed in 4% PFA in PBS 1x overnight with gentle mixing. Brains were then transferred to 30% sucrose in PBS 1x and left to sink for 2 days before slicing.

## 3.10 Histology

Dorsal hippocampal CA1 was collected from perfused brains by 40µm coronal sectioning using a vibratome. Slices were stained with DAPI 1:5000 in PBS 1x for 10 minutes at room temperature with gentle shaking. Samples were washed once more in PBS 1x before being mounted on slides with a hard set anti-fade mounting medium, Vectashield (Vector Laboratories, Burlingame, CA, USA). The slices were used to verify correct implantation position above dorsal hippocampal CA1.

## 3.11 Stress models

Two stress models were used in the course of this work, namely restraint stress and MMS.

### 3.11.1 Restraint stress

Repeated restraint stress was used in a pilot experiment described in section 4.3.3. Briefly, each mouse was placed in a 50ml falcon tube which contained ventilation holes. The tail was free to move via a hole in the falcon tube lid. Restraint lasted for a period of 2h and was repeated for 5 days at different times of the day between 8:00 and 14:00.

### 3.11.2 Multi-modal stress

I further employed MMS as first described by Chen et al. (2016). Briefly, the paradigm involves exposure to multiple simultaneous stressors. This included placing the mice into restraint tubes and onto a shaker under bright light whilst loud rat noises were played for two consecutive hours. Additionally, restrainers were placed adjacently on the shaker so the mice had additional awareness of peer discomfort. The use of rat calls deviated from the original protocol which employed the use of rap music.
I designed restrainers (Figure 3.9) to minimise forces on the head plate of implanted mice and to allow for easy access to the tail for blood collection. These consisted of 2 parts: one open ended tube and a ball bearing which was fitted on the open end. Restraint tubes were custom 3D printed to include a groove on the side allowing for access to the tail so that mice did not have to be removed from restraint for tail blood collection. Support rims on the sides of the restrainers were

included for the bearing housing to rest on and removed additional force from any weight of the bearings. Head plates fit into the inner rim of the bearings with a close running fit.

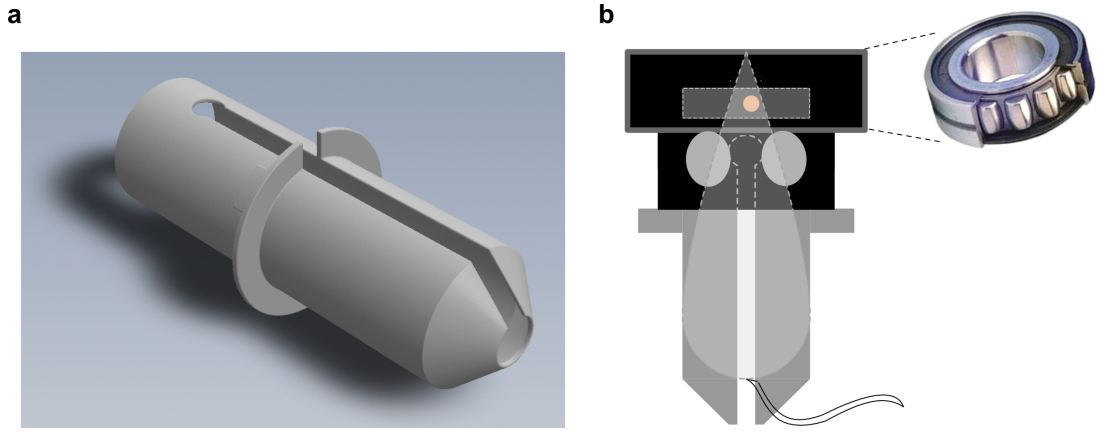


**Figure 3.9:** Custom designed restrainers for implanted mice exposed to MMS. (a) 3D printed restraint tube including groove for tail blood collection and outer rims to support bearing housing. (b) schematic of restraint with mouse placed into 3D printed restrainer, head plate fixed into inner rim of ball bearing, ball bearing resting on support housing of 3D printed restraint tube and free access to the tail for blood collection. Insert: cross section of ball bearings with loose running fit to reduce torque on head plates when mice struggled.

Two stress groups were tested, one in which the mice were stressed for 2hours once and a second group in which the mice were stressed for 2 hours at different times of the day for 7 consecutive days, except for those coupled with learning, where stress was performed in the morning and ended 1h before the start of a Morris Water Maze learning trial.
Circulating corticosterone levels were determined by collection of trunk blood (Figure 4.2) into labeled 1.5ml EDTA-coated microcentrifuge tubes (Kabe Labortechnik, Germany). Two samples per animal per time point of interest were taken, one at 30 minutes after the start of stress and the other at 90 minutes after the start of stress. Blood collection was always between 08:00 and 14:00 to account for dependency of corticosterone levels on circadian rhythm. Samples were stored on ice for up to 1h before being centrifuged at 8000rpm for 15 minutes. Plasma samples were plated and stored at -20 °C for up to two weeks before corticosterone levels were determined by radioimmune assay (MP Biomedicals Inc., sensitivity 6.25ng/ml)

## 3.12 Morris Water Maze

The MWM, first described by Morris (1981), was developed as a measure of hippocampal spatial learning and memory recall in rodents.

The MWM used in these experiments comprised a 150cm circular tank filled with clear water. A transparent acrylic platform was placed into the tank and remained hidden 1.3cm below the surface of the water. For analysis purposes the maze was divided into 4 quadrants (not visible to

the mice). Spatial cues were placed on the walls and the room itself contained other stable cues such as overhead lights and the positions of recording apparatus. Many variations of the task exist, here I used a 7 day learning trial. Groups of 10 mice performed 4 trials per day, where each trial corresponded to a different entry point into the maze (NE, NW, SE, SW), corresponding to the 4 quadrants. Entry points were randomised every day so mice could not learn a pattern of entry over days. In this way they were forced to navigate via spatial cues (allocentrically) rather than egocentrically. The water temperature was kept between 23-24°C. Swim time was limited to 90 seconds. If mice had not located the platform within this time, they were guided to it. All mice (those who located the platform as well as those which had to be guided) were to remain on the platform for a total of 30 seconds. Inter-trial intervals were 10-15 minutes. Cues were placed on the walls to aid spatial orientation. Mice were tested for platform location memory on the 8th day. For the memory probe, the platform was removed from the maze and mice placed in at one location and allowed to swim for 60 seconds, during which time their time spent in each quadrant and number of virtual platform crosses was measured.

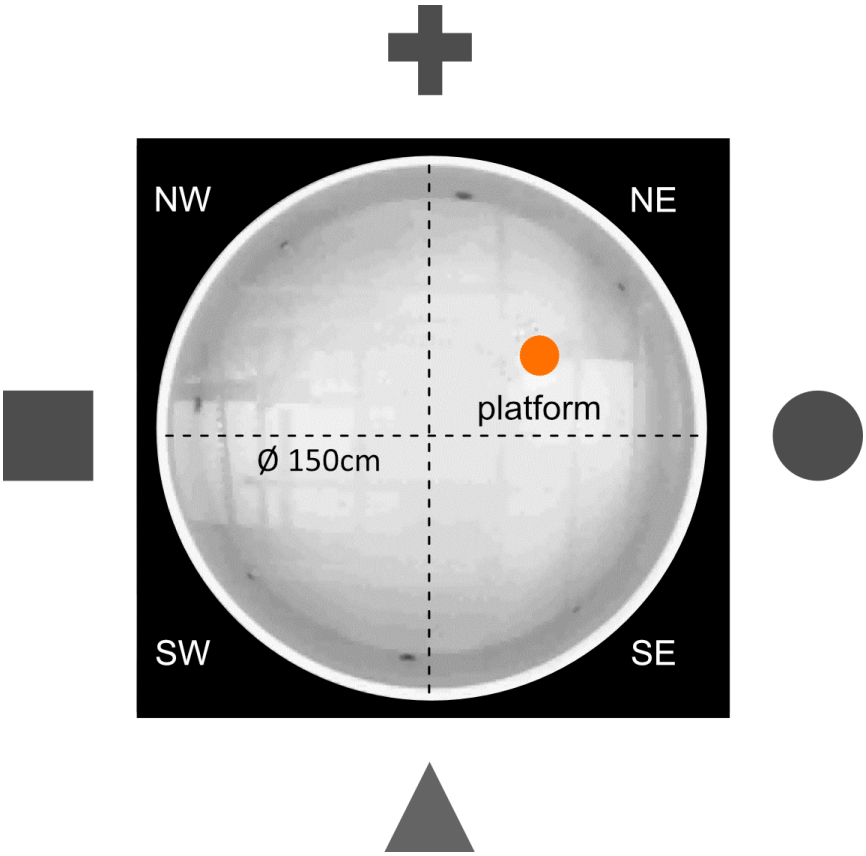


**Figure 3.10:** Morris water maze set up. Quadrants are indicated with dashed lines. Symbols are indicative of visual queues used for spatial learning. Platform is indicated by the orange circle.

Garthe et al. (2009) developed a classification algorithm for swimming strategies employed

by mice in the MWM. Strategies were classified according to the time mice spent in zones defined by proximity to the platform and walls of the maze (Figure 3.11). The algorithm measured the average distance of the swim path in relation to its centroid and goal location and a goal corridor whose bisecting line spanned from starting point to goal location. Based on these measures, strategies progressed from thigmotaxis (in which mice swim in the closer wall zone) to direct swimming in the following order:

1. Thigmotaxis
2. Random search
3. Scanning
4. Chaining
5. Directed search
6. Focal search
7. Direct swimming
8. Perseverance (when platform reversal is used in the MWM)

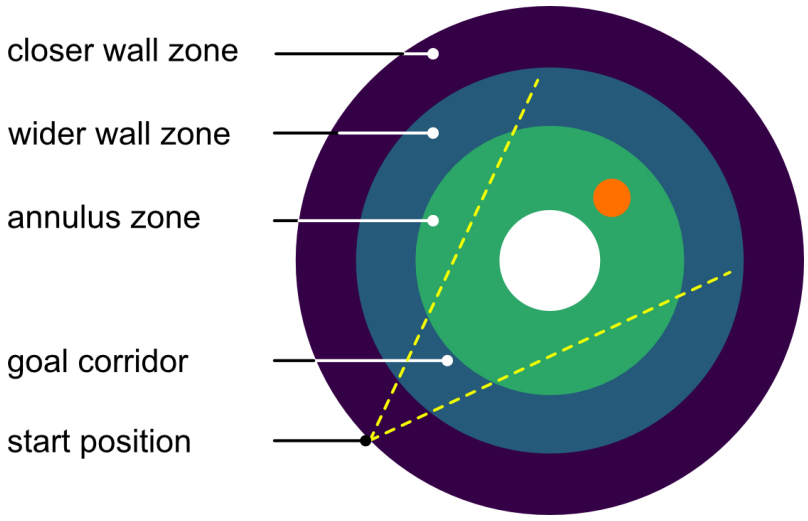


**Figure 3.11:** Swim strategies as established by Garthe et al. (2009) were classified according to the time spent in the closer wall zone, wider wall zone, annulus zone and goal corridor.

I extracted location data from ANY-maze (behavioural tracking software) and used it to perform swim strategy classification. I modified the original analysis to adjust for assignment errors in which mice swam directly to the platform but did so along the wall of the maze in under the average time it took control mice on the last training day. These cases were

originally incorrectly assigned as thigmotaxis and, with the implemented correction, subsequently reclassified as direct swimming.
Target quadrant times and platform crossing data were extracted from ANY-maze. Tracking errors were corrected by post hoc retracking of acquired videos.

### 3.12.1 Statistical analysis

Data was checked to understand whether it fit with the assumptions underlying the statistical tests. For example is it normally distributed (for t-tests) or does it have equal variances (for ANOVA).
If these held true, statistical significance was assessed by paired t-tests, unpaired t-test or analysis of variance (ANOVA) as appropriate. Sidak's multiple comparisons test was used as a post hoc analysis to ANOVA to test for differences between unpaired groups.
If criteria did not hold true, p-values were calculated using the Mann-Whitney test for 2 independent samples or Kruskall Wallis ANOVA on ranks for 3 or more independent samples. To test for significance between paired samples, Wilcoxon signed rank test for 2 paired samples or Friedman test for paired samples of 3 or more was used. Dunn's multiple comparisons test was used as a post hoc analysis to ANOVA and Friedman tests as a non-parametric test for differences between pairs.
Data was considered significant if $p < 0.05$.

CHAPTER 4

# RESULTS

This chapter details the results obtained during my doctoral thesis. The first section details structural synaptic dynamics. The second component comprises spine clustering analysis, established for the first time in hippocampal CA1. The final part of this chapter comprises spatial learning determined by the MWM learning paradigm. Figure 4.1 presents a schematic overview of the main aspects of the study.

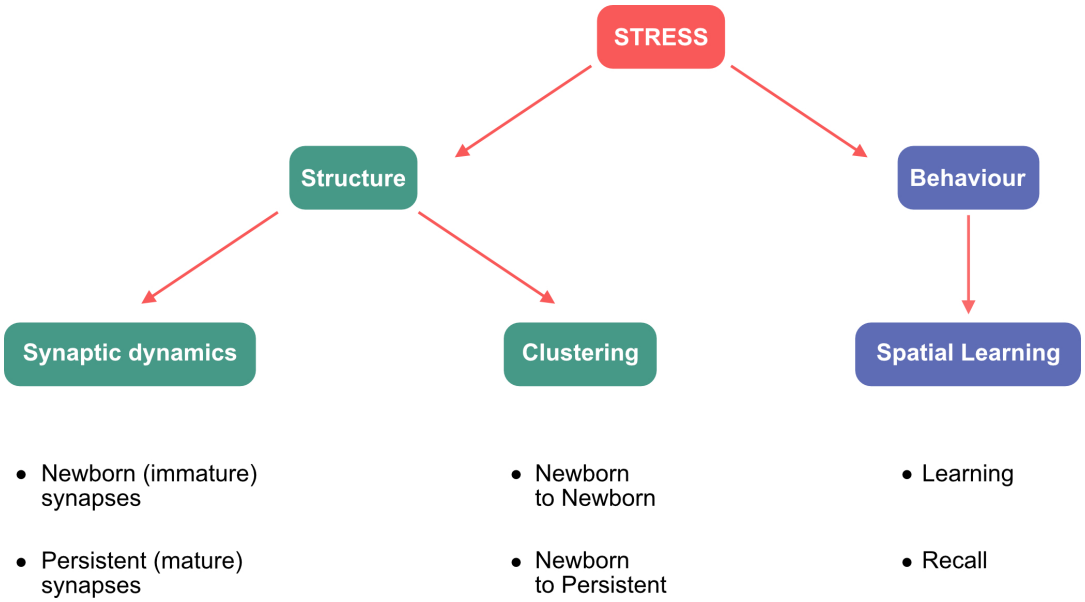


**Figure 4.1:** Overview of main aspects of the study. On a mechanistic level, structural synaptic plasticity was evaluated, in terms of both synaptic and clustering dynamics. On a behavioural level, spatial learning and memory were assessed.

## 4.1 Structural Plasticity

In order to study potential dynamic changes due to stress, I used 2-photon microscopy in two cohorts of mice. One cohort was stressed acutely by MMS and allowed to recover (Figure 4.2a). The other was stressed repeatedly (Figure 4.2b). Both groups were imaged for a 2 week period on days 1, 2, 4, 7, 8, 9, 11 and 14.

### 4.1.1 Acute MMS and 2-photon imaging

Thy1GFPm mice (Figure 4.2a) were implanted with imaging cannulas over the right hippocampus. After 2-3 weeks of recovery, the *in vivo* imaging potential of each mouse was determined by checking fluorescence and image stability with 2-photon imaging as described in section 3.5. The imageable mice (n = 5) were selected for continuation of the experiment and multiple dendritic regions were selected from each mouse for repeated imaging. Imaged mice were randomly assigned to groups and imaged in a different order for every imaging day. The experiment comprised 1 week of baseline imaging in which mice were imaged on days 1, 2, 4 and 7. Baseline corticosterone levels were measured by collecting tail blood on the first day of baseline (as described in section 3.11.2) and performing a radioimmune assay. On day 8 of the experiment, mice were subjected to 2h of MMS. Blood was collected at 30 and 90 minutes after the start of stress. 1h after the end of stress, mice were imaged to determine any change in dynamics after stress in comparison to the equivalent baseline period. Mice were imaged again during a recovery period of 6 days. Recovery imaging was done on days 9, 11 and 14. Blood was collected at day 14 for determination of corticosterone levels after 6 days of recovery. Stress and recovery imaging days were chosen to match the time periods of baseline imaging. This design enabled complete internal control of stress effects on dorsal hippocampal CA1 synaptic dynamics.

### 4.1.2 Repeated MMS and 2-photon imaging

This experiment followed the same design as in section 4.1.1 with the exception that mice were stressed with 2h of MMS repeatedly for 7 consecutive days (Figure 4.2b, n = 8 stressed, n = 4 imaged). Additionally, mice were randomly assigned to groups and stress was done in multiple rounds by rotating and shuffling groups to ensure that the start of imaging was always between 20 minutes and 2 hours after the start of stress.

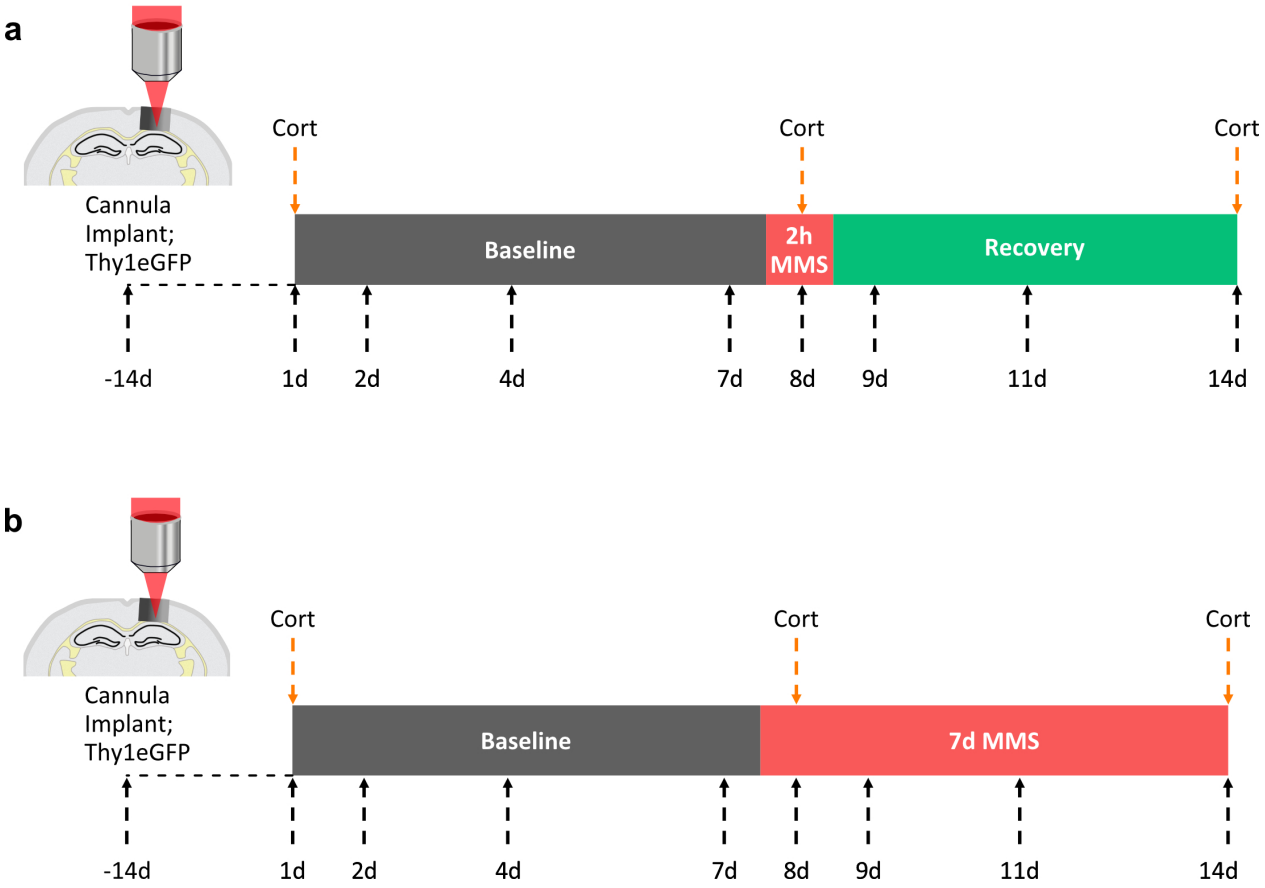


**Figure 4.2:** 2-photon imaging experiments and timeline. Heterozygous Thy1GFPm mice were implanted with an imaging cannula 2-3 weeks prior to imaging. Mice were imaged for a baseline period of 7 days on days 1, 2, 4 and 7. Subsequent to the baseline period, mice were stressed (a) once for 2h on Day 8 of the experiment and in a separate group (b) were stressed repeatedly for 2h/day for 7 days and imaged on days 8, 9, 11 and 14 at intervals corresponding to the baseline imaging periods. Blood was collected by a tail cut on days 1, 8 and 14. Two samples were collected per time point, at 30' and 90' after the start of stress. Cort, corticosterone; orange arrows, blood collection; black arrows, imaging days.

The two imaging experiments as described in sections 4.1.1 and 4.1.2 (Figure 4.2) enable a comparison between acute stress followed by recovery and repeated stress dynamics within the same time frame. The results of these two experiments will be presented in parallel.

Implementing a cranial window to track the same dendritic and synaptic structures longitudinally (Figure 4.3) affords the advantage of observing the birth and death of spines. It is largely accepted that spines which are newly born play a role in the acquisition of new memories (Xu et al. (2009); Yang et al. (2009); Fu et al. (2012); Rogerson et al. (2014)). Here we distinguish between two populations of spines:

1. newborn spines: a spine is considered newborn at a time point if it did not exist at the

previous time point.

2. persistent spines: a spine is considered persistent at a time point if it existed at the previous time point.

Since these definitions require knowledge of the previous time point, we cannot distinguish between the populations of spines on the first imaging day (baseline day 1). In this work, a non-specific population of spines is simply termed 'all' spines.

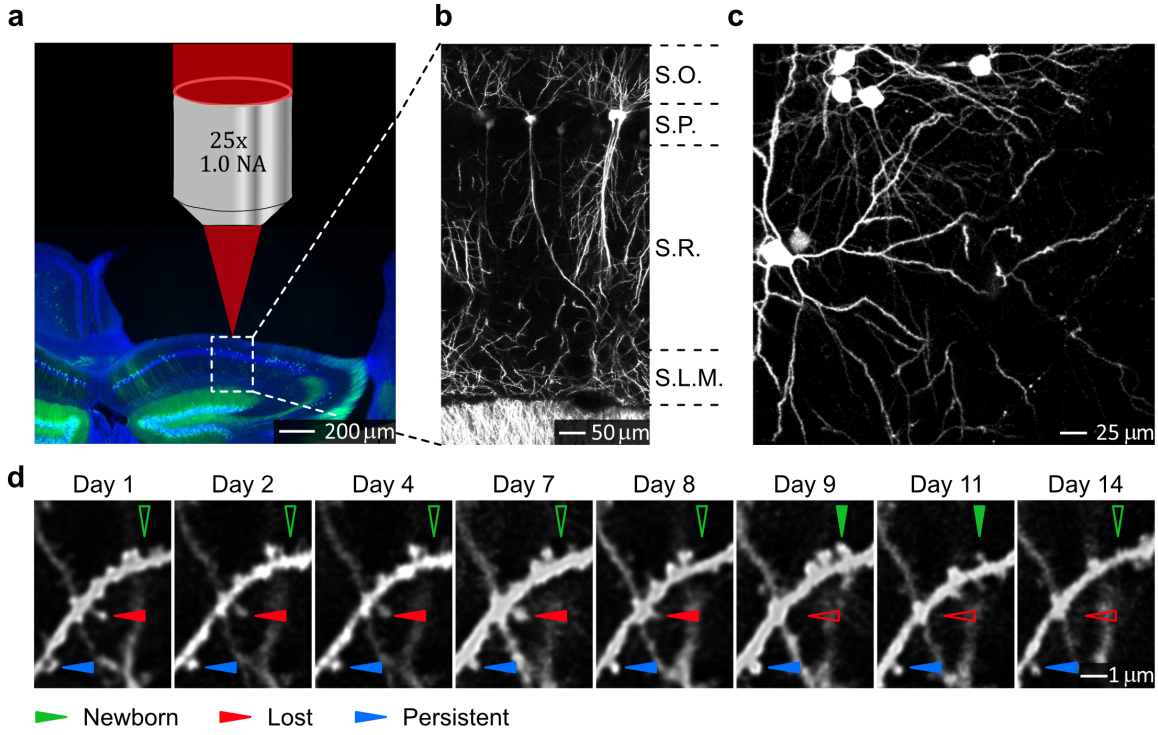


**Figure 4.3:** Repeated *in vivo* 2-photon optical imaging of dorsal hippocampal CA1. (a) GFP positive pyramidal cells in the dCA1 are excited by 920nm light. Scale bar, 200µm. (b) Distribution of CA1 pyramidal cell across hippocampal layers. All dendrites imaged were taken from the basal dendrites of pyramidal cells. These cells span the S.O., stratum oriens, S.P., stratum pyramidale, S.R., stratum radiatum, S.L.M., stratum lacunosum moleculare. Scale bar, 50µm. (c) Maximum intensity projection of an overview region acquired *in vivo*. Scale bar, 25µm. (d) Time series of dendritic spine tracking. The series shows the same dendrite imaged across the 2 week experimental period. Spines can be seen being born (green), being lost (red) and persisting through all time points (blue). Scale bar, 1µm.

### 4.1.3 Spine Density

Most studies have reported no measureable change in spine density of basal dendrites of dCA1. Since basal dCA1 dendrites are densely populated with spines, decreases in density between groups can be difficult to detect. Our results (Figure 4.4) demonstrate no decrease in density of all spines, both after an acute (Figure 4.4a, NS; 1-way ANOVA Dunn's multiple comparisons),

as well as with repeated (Figure4.4c, NS; 1-way ANOVA Dunn's multiple comparisons) MMS exposure.

Interestingly however, when we consider the population of newborn spines, we show for the first time a significant reduction in the density of newborn spines after stress exposure (Figure 4.4b, day 8, ****p < 0.0001, day 14, *p = 0.0484; 1-way ANOVA, Dunn's multiple comparisons test and Figure 4.4d, day 8, *p = 0.0256, day 9, ***p = 0.0002 and day 11, **p = 0.0018; 1-way ANOVA, Dunn's multiple comparisons test). This decrease in density occurs in a matter of hours after the conclusion of stress, as demonstrated on days 8 of both the acutely and repeatedly stressed mice. Further, mice which were stressed acutely recovered their newborn spine density to baseline levels already by the first day of recovery (day 9, baseline density compared to day 9 NS, p > 0.9999, 1-way ANOVA, Dunn's multiple comparisons test), whereas mice stressed repeatedly continued to demonstrate a decrease in newborn spine density following up to 4 days of repeated stress exposure (Figure 4.4d, days 8, 9 and 11).

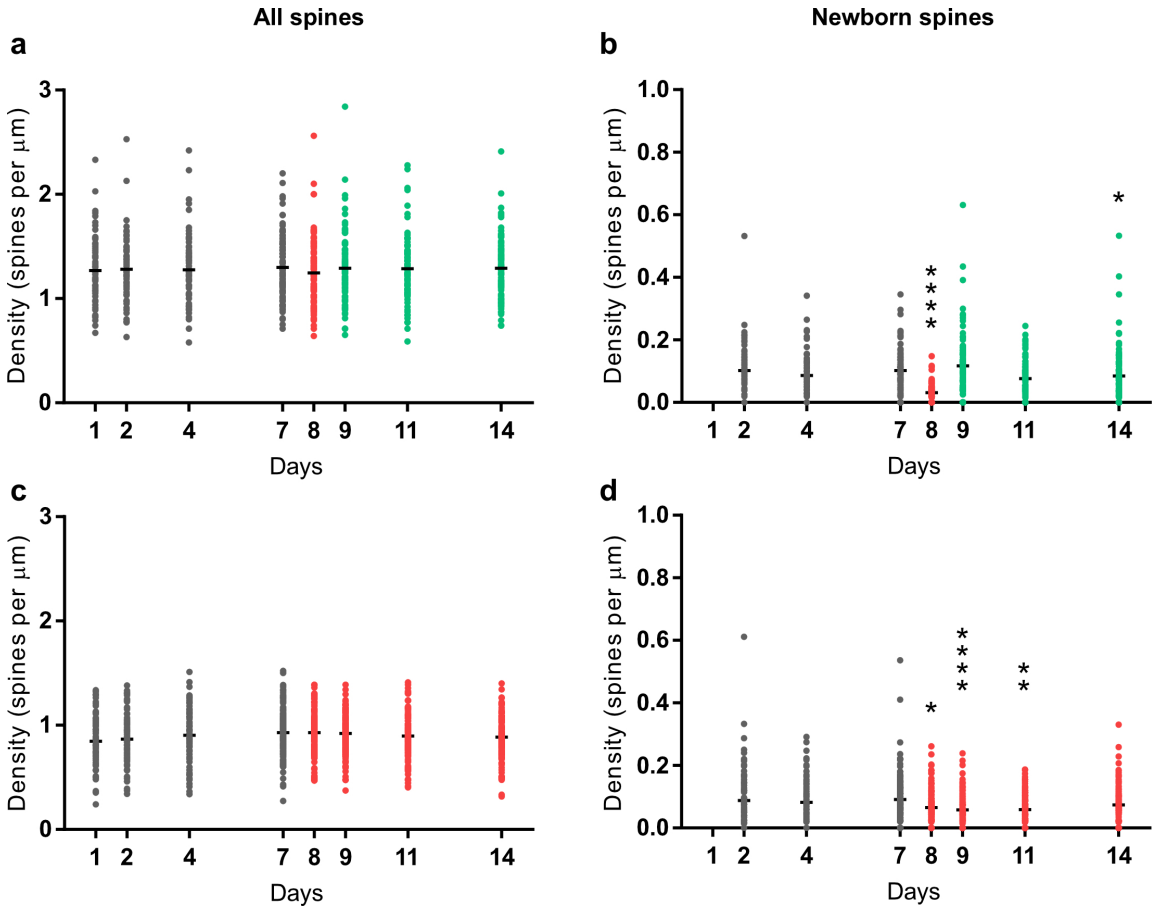


**Figure 4.4:** Effect of acute and repeated MMS on all and newborn spine densities. TOP: Acute 2h MMS treated mice, density of (a) all spines on each imaging day during baseline, stress and recovery. Pooled densities from days 1, 2, 4 and 7 compared to each day 1 NS $p > 0.9999$; 2 NS $p > 0.9999$; 4 NS $p > 0.9999$; 7 NS $p > 0.9999$, 1-way ANOVA, Dunn's multiple comparisons test. Pooled data from days 1, 2, 4 and 7 compared to stress day 8 NS $p = 0.8209$; and recovery days 9 NS $p > 0.9999$; 11 NS $p > 0.9999$; and 14 NS $p > 0.9999$, 1-way ANOVA, Dunn's multiple comparisons test. (b) newborn spines on each imaging day during baseline, stress and recovery. Pooled densities from days 2, 4 and 7 compared to each day 2 NS $p > 0.9999$; 4 NS $p > 0.4297$; 7 NS $p > 0.9999$, 1-way ANOVA, Dunn's multiple comparisons test. Pooled days 2, 4, 7, compared to stress day 8 ****$p < 0.0001$ and recovery days 9 NS $p > 0.9999$; 11 NS $p > 0.0563$ and 14 *$p = 0.0484$, 1-way ANOVA, Dunn's multiple comparisons test. BOTTOM: Repeated 2h MMS treated mice, density of (c) all spines on each imaging day during baseline and throughout stress. Pooled densities from days 1, 2, 4 and 7 compared to each day 1 NS $p = 0.2277$; 2 NS $p > 0.9999$; 4 NS $p > 0.9999$; 7 NS $p = 0.2350$; 1-way ANOVA, Dunn's multiple comparisons test. Pooled data from days 1, 2, 4 and 7 compared to stress days 8 NS $p = 0.1488$; 9 NS $p = 0.2811$; 11 NS $p > 0.9999$; and 14 NS $p > 0.9999$; 1-way ANOVA, Dunn's multiple comparisons test. (d) newborn spines on each imaging day during baseline and throughout stress. Pooled densities from days 2, 4 and 7 compared to each day 2 NS $p > 0.9999$; 4 NS $p > 0.9999$; 7 NS $p > 0.9999$, 1-way ANOVA, Dunn's multiple comparisons test. Pooled days 2, 4, 7, compared to stress days 8 *$p = 0.0256$, 9 ***$p = 0.0002$, 11 **$p = 0.0018$ and 14 NS $p = 0.8867$, 1-way ANOVA, Dunn's multiple comparisons test. Acute MMS, n = 88 dendrites from 5 mice; Repeated MMS, n = 124 dendrites from 4 mice. Data represented as individual points and mean. Grey, baseline; red, stress; green, recovery.

### 4.1.4 Spine gain and loss

After one exposure of 2h MMS, a reduction in spine gain was observed when compared to the same 24h interval at baseline (Figure 4.5a, ****p < 0.0001; 1-way ANOVA, Dunn's multiple comparisons test). One day of recovery resulted in no difference in spine gain over a 24h period when compared to baseline (Figure 4.5a). Spine gain was not significantly different during recovery compared to the same baseline interval for 48h (Figure 4.5b) but was slightly decreased compared to baseline over a period of 72h (Figure 4.5c, *p = 0.0182; Wilcoxon matched pair signed rank test).

In mice exposed to repeated stress, the reduction in spine gain was again significant after the first stress exposure, as expected (Figure 4.5d, ***p = 0.0001; 1-way ANOVA, Dunn's multiple comparisons test). This reduction in gain continued with 2 stress exposures (Figure 4.5d, ****p < 0.0001; 1-way ANOVA, Dunn's multiple comparisons test) which was not the case with the first day of recovery in acutely stressed mice, and furthermore was still evident after 4 repeated stress exposures (Figure 4.5e, **p = 0.0022; Wilcoxon matched pair signed rank test). After 7 days of MMS however, spine gain was no longer significantly different in comparison to baseline (Figure 4.5f).

After one exposure of 2h MMS, no change in loss was observed when compared to the same 24h interval at baseline (Figure 4.5a). This was true also for the 24h (Figure 4.5a, green bar), 48h (Figure 4.5b) and 72h (Figure 4.5c) intervals which comprised the stress recovery period.

Mice stressed repeatedly, again showed an expected non-significant difference in loss over 24h when compared to baseline (Figure 4.5d), hence confirming the result as seen in the acutely stressed cohort. Interestingly however, an increase in loss was observed over a 48h interval, corresponding to 4 stress exposures (Figure 4.5e, **p = 0.0024; Wilcoxon matched pair signed rank test). This remained significant after 7 stress exposures (Figure 4.5f, *p = 0.0166; Wilcoxon matched pair signed rank test).

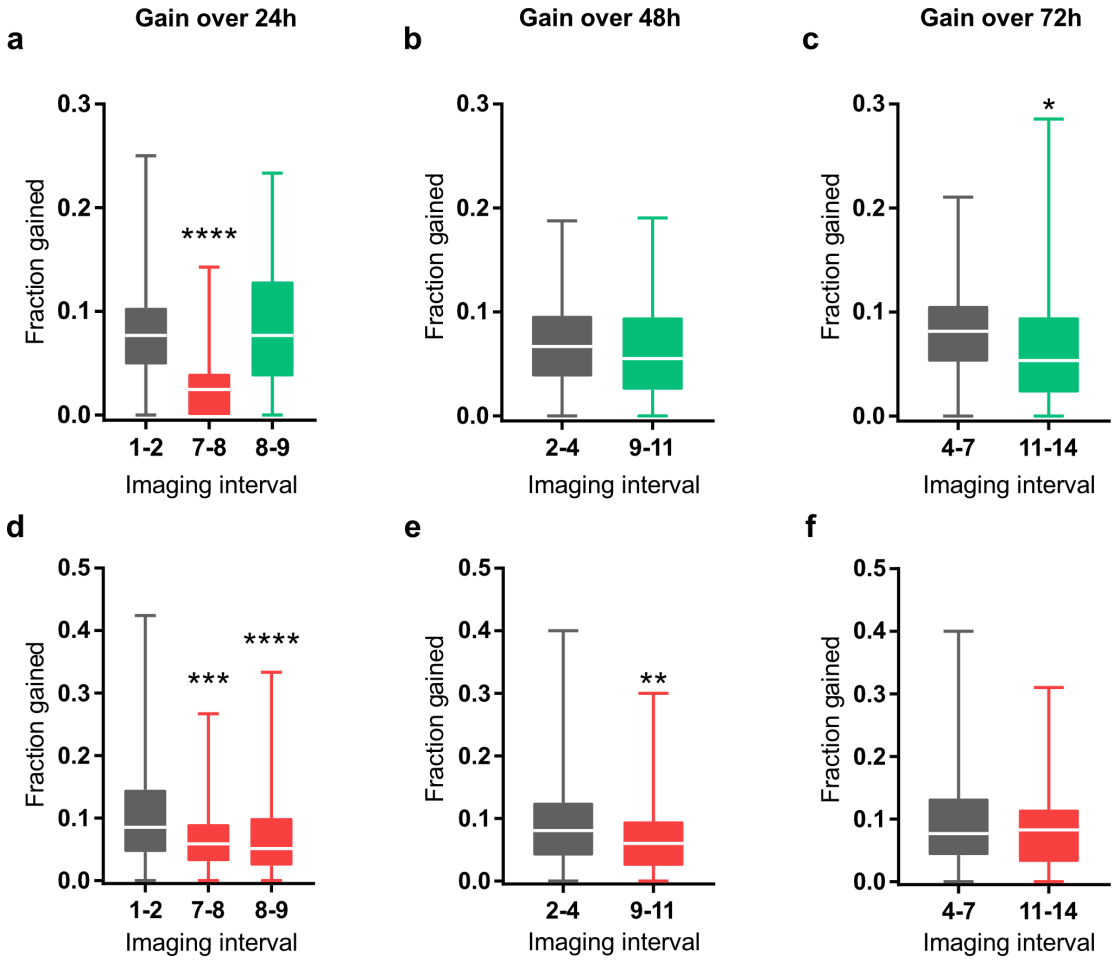


**Figure 4.5:** Effect of acute and repeated MMS on spine gain. TOP: Acute 2h MMS treated mice (a) Gain of spines over a 24h period. Gain over days 1-2 compared to days 7-8 ****$p < 0.0001$ and days 8-9 NS $p > 0.9999$, 1-way ANOVA, Dunn's multiple comparisons test. (b) Gain of spines over a 48h period. Days 2-4 compared to days 9-11 NS $p = 0.3483$, Wilcoxon matched pairs signed rank test (c) Gain of spines over a 72h period. *$p = 0.0182$; Wilcoxon matched pairs signed rank test. BOTTOM: Repeated 2h MMS treated mice (d) Gain of spines over a 24h period. Gain over days 1-2 compared to days 7-8 ***$p = 0.0001$ and days 8-9 ****$p < 0.0001$; 1-way ANOVA, Dunn's multiple comparisons test. (e) Gain of spines over a 48h period. **$p = 0.0022$; Wilcoxon matched pairs signed rank test. (f) Gain of spines over a 72h period. Days 4-7 compared to days 11-14 NS $p = 0.7466$, Wilcoxon matched pairs signed rank test. Acute MMS, n = 88 dendrites, 5 mice; Repeated MMS, n = 124 dendrites, 4 mice. Data represented as min to max and average. Grey, baseline; red, stress; green, recovery.

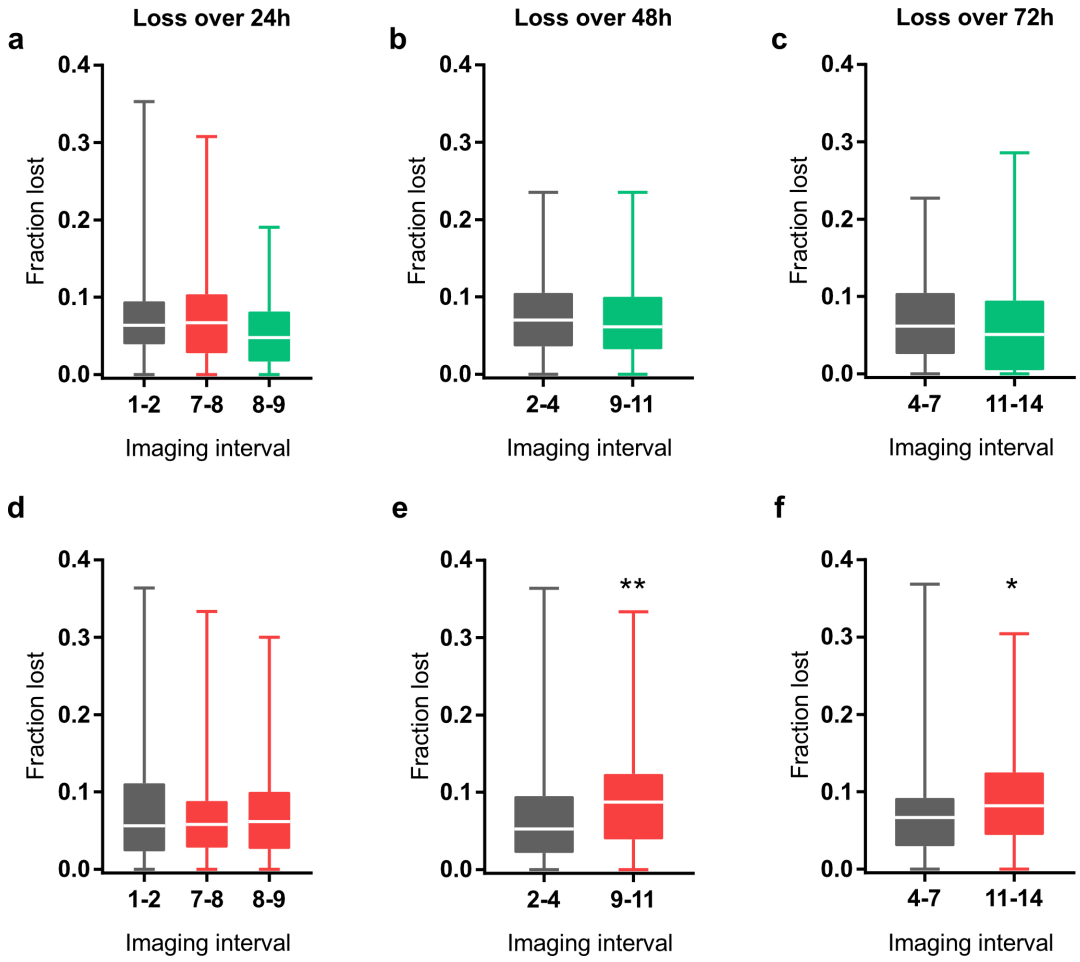


**Figure 4.6:** Effect of acute and repeated MMS on spine loss. TOP: Acute 2h MMS treated mice (a) Loss of spines over a 24h period. Days 1-2 compared to days 7-8 NS p > 0.9999 and days 8-9 NS p = 0.3263, 1-way ANOVA, Dunn's multiple comparisons test. (b) Loss of spines over a 48h period. Days 2-4 compared to days 9-11 NS p = 0.8860m Wilcoxon matched pairs signed rank test. (c) Loss of spines over a 72h period. Days 4-7 compared to days 11-14 NS p = 0.2665, Wilcoxon matched pairs signed rank test. BOTTOM: Repeated 2h MMS treated mice (d) Loss of spines over a 24h period. Days 1-2 compared to days 7-8 NS p = 0.7144 and days 8-9 NS p > 0.9999, 1-way ANOVA, Dunn's multiple comparisons test. (e) Loss of spines over a 48h period. **p = 0.0024, Wilcoxon matched pairs signed rank test.(f) Loss of spines over a 72h period. *p = 0.0166; Wilcoxon matched pair signed rank test. n = 88 dendrites, 5 mice; Repeated MMS, n = 124 dendrites, 4 mice. Data represented as min to max and average. Grey, baseline; red, stress; green, recovery.

### 4.1.5 Spine survival

In addition to observing the appearance and disappearance of spines, *in vivo* 2-photon imaging allows one to track the survival of spines within the time frame of the experiment. A disruption in structural dynamics was already seen with stress-induced alterations in spine gain and loss and I sought to determine whether the spine populations of interest (all spines, newborn spines and persistent spines) survived differently.

Both acute and repeated stress exposure were found to significantly affect the surviving fraction of all spines over a period of seven days in comparison to baseline (Figure 4.7a, ***p = 0.0007; 2-way ANOVA and Figure 4.7e, **p = 0.0092; 2-way ANOVA). The survival of persistent spines was only affected by repeated stress exposure (Figure 4.7b, NS and Figure 4.7f, ***p = 0.0008; 2-way ANOVA) and was shown to decrease. Newborn spines born after acute 2h MMS exposure had a higher surviving fraction during the subsequent recovery period (Figure 4.7c, ***p = 0.0009; 2-way ANOVA), whereas those born after a single 2h MMS and then re-exposed to stress for the rest of the week demonstrated a decrease in survival Figure 4.7g, ****p < 0.0001; 2-way ANOVA). In the acutely stressed cohort, newborn spines born on the first day of recovery did not survive differently to baseline (Figure 4.7d). However, in the repeated stress cohort, newborn spines born on the second day of stress were also shown to have a lower surviving fraction, much the same as those born after the first stress exposure. Moreover, two stress exposures resulted in a steeper decay rate of newborn spines between days 9-11 (Figure 4.7g) indicating that a second exposure strongly influences the population born in the hours after the first stress exposure, or that this population (of day 8) are more vulnerable to homeostatic disruption, or both.

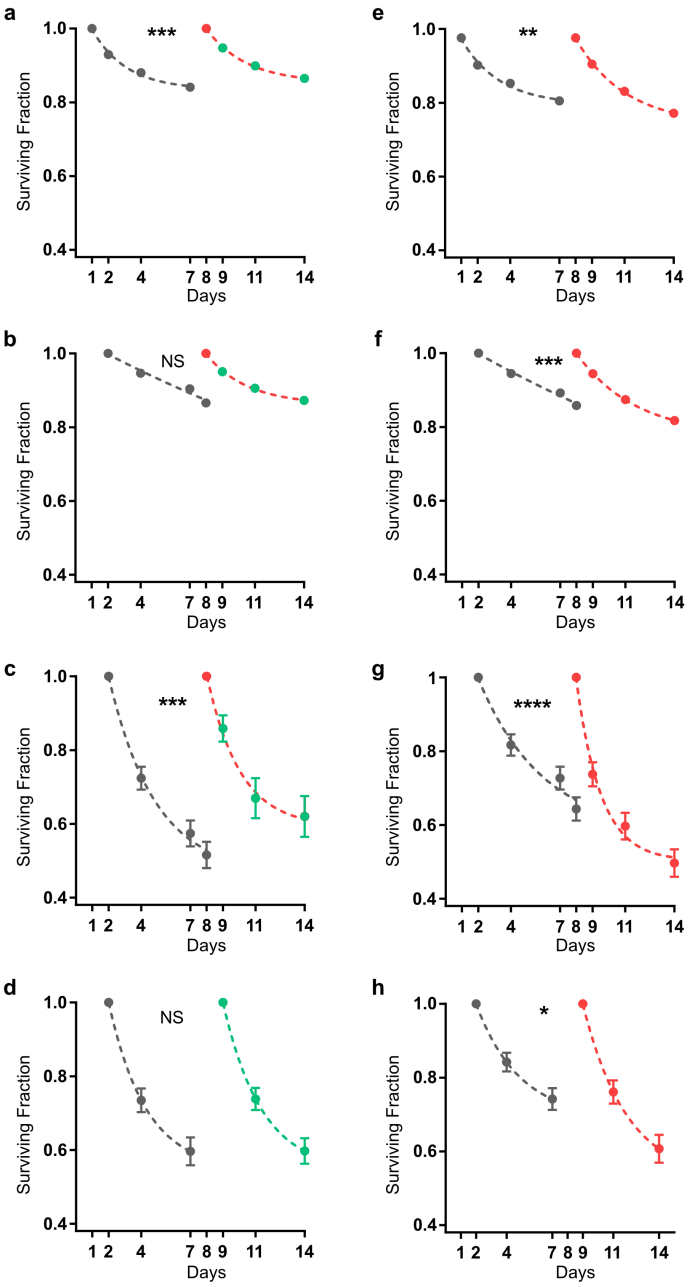


**Figure 4.7:** Effect of acute and repeated MMS on spine survival. LEFT: Acute 2h MMS treated mice. Survival fraction of (a) all spines that existed on day 1 and day 8, ***p = 0.0007; 2-way ANOVA. (b) persistent spines identified on day 2 and day 8 , NS p = 0.4347, 2-way ANOVA. (c) newborn spines identified on day2 and day 8, ***p = 0.0009; 2-way ANOVA. (d) newborn spines identified at day 2 and day 9, NS p = 0.8608, 2-way ANOVA. RIGHT: Repeated 2h MMS treated mice. Survival fraction of (e) all spines that existed on day1 and day 8, **p = 0.0092; 2-way ANOVA. (f) persistent spines identified on day 2 and day 8, ***p = 0.0008; 2-way ANOVA. (g) newborn spines identified on day 2 and day8, ****p < 0.0001; 2-way ANOVA. (h) newborn spines identified at day 2 and day 9, *p = 0.0353; 2-way ANOVA. Acute MMS, 5 mice; Repeated MMS, 4 mice. n dendrites: Tables A.1 and A.2. Data presented as mean ± s.e.m. Grey, baseline; red, stress; green, recovery.

### 4.1.6 Spine clustering

As demonstrated in section (1.1.2), clustering has been studied extensively in the cortex. It is important to note however, that spine density in the cortex is lower than in the hippocampus, essentially meaning that spines are generally much further apart. In the cortex therefore, thresholds for clustering are meaningful based on the extent of protein travel. Since hippocampal CA1 has a far denser spine population, I have instead leveraged on the advantage of the internal baseline control for each animal to compare the distribution of distances between spines before and after stress, thus importantly emanating an unbiased approach and eliminating the need for selecting a threshold. For this reason, the term 'clustering' is used in the context of distances between spines relative to the baseline condition. The following section details the results of the first *in vivo* hippocampal spine clustering analysis.
The following data demonstrates the effects of stress on clustering between

1. newborn spines
2. newborn and persistent spines

#### 4.1.6.1 Clustering between newborn spines per dendrite

Here I conducted a per dendrite analysis of distances to nearest neighbour (DNNs) between newborn (NB) spines by taking the median DNN per dendrite and normalising to newborn spine density.
Density corrected median DNNs were not significantly different after one 2h MMS exposure compared to the same baseline time period (Figure 4.8a, NS p = 0.1731; Wilcoxon matched pairs signed rank test and Figure 4.9a, NS p = 0.0628; Wilcoxon matched pairs signed rank test).
Recovery exposure did not significantly alter DNNs between NB spines compared to baseline ranges (Figure 4.8b-d, B2 compared to R1 NS, p = 0.3286; Wilcoxon matched pairs signed rank test; B4 compared to R3 NS, p = 0.2680; Wilcoxon matched pairs signed rank test and B7 compared to R6 NS, p = 0.2043; Wilcoxon matched pairs signed rank test).
Repeated stress also showed no effect on DNNs between newborn spines (Figure 4.9b-d, B2 compared to S2 NS, p = 0.2162; Wilcoxon matched pairs signed rank test; B4 compared to S4 NS, p = 0.9607; Wilcoxon matched pairs signed rank test and B7 compared to S7 NS, p = 0.5291; Wilcoxon matched pairs signed rank test).

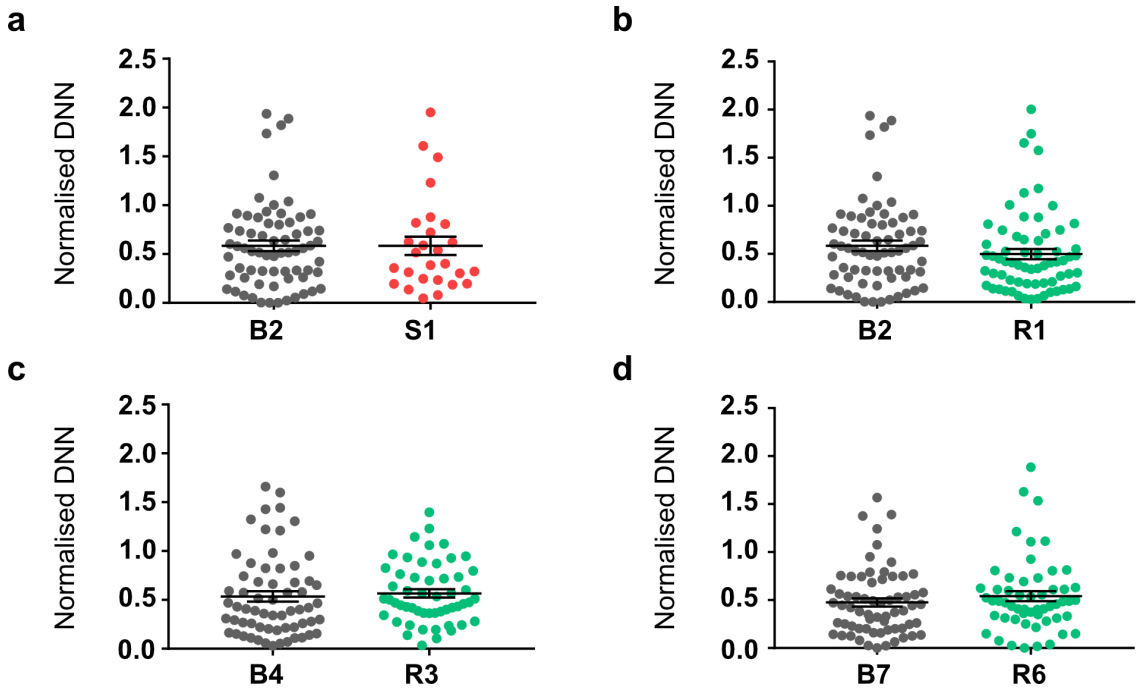


**Figure 4.8:** The effect of acute 2h MMS and recovery on distances between newborn spines per dendrite. Median DNN normalised by newborn spine density per dendrite over a (a) 24 h period, B2 compared to S1, NS p = 0.1731; Wilcoxon matched pairs signed rank test (b) 24h period, B2 compared to R1, NS p = 0.3286; Wilcoxon matched pairs signed rank test (c) 48h period, B4 compared to R3, NS p = 0.2680; Wilcoxon matched pairs signed rank test (d) 72h period, B7 compared to R6, NS p = 0.2043; Wilcoxon matched pairs signed rank test. n = 5 mice; n dendrites: Table A.3. Data presented as mean ± s.e.m. B2, baseline day 2, imaging day 2; B4 baseline day 4, imaging day 4; B7, baseline day 7, imaging day 7; S1, stress day 1, imaging day 8; R1, recovery day 1, imaging day 9; R3, recovery day 3, imaging day 11; R6, recovery day 6, imaging day 14. Grey, baseline; red, stress; green, recovery.

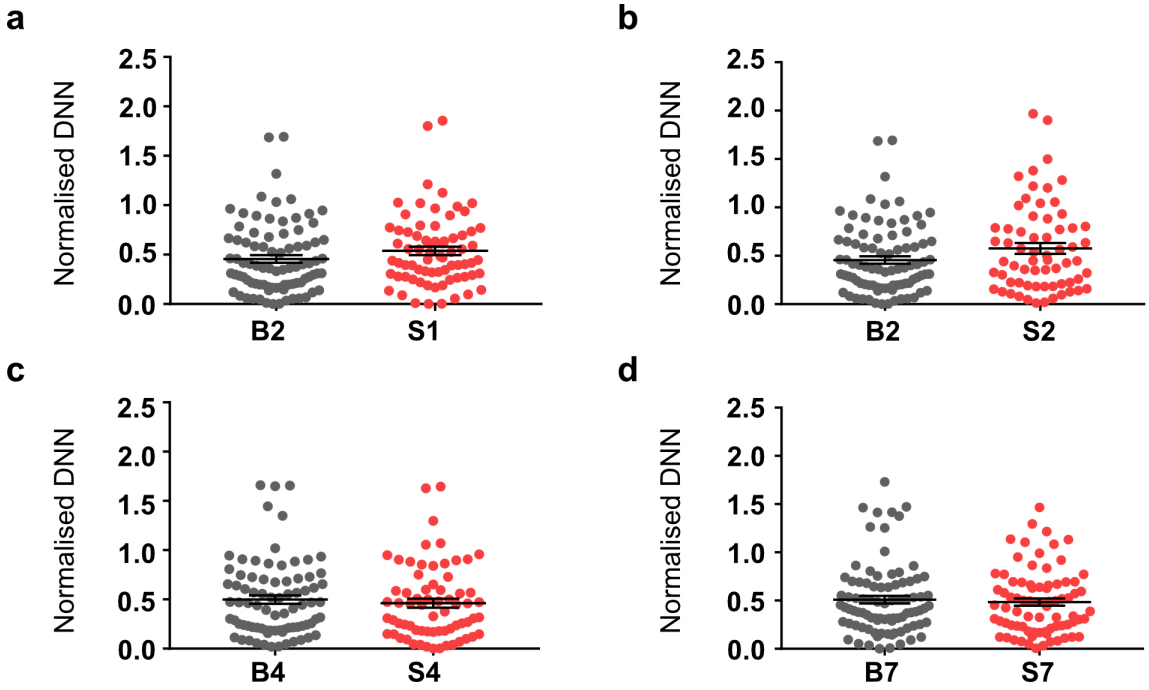


**Figure 4.9:** The effect of repeated 2h MMS on distances between newborn spines per dendrite. Median DNN normalised by newborn spine density per dendrite over a (a) 24 h period, B2 compared to S1, NS p = 0.0628; Wilcoxon matched pairs signed rank test (b) 24h period, B2 compared to S2, NS p = 0.2162; Wilcoxon matched pairs signed rank test (c) 48h period, B4 compared to S4, NS p = 0.9607; Wilcoxon matched pairs signed rank test (d) 72h period, B7 compared to S7, NS p = 0.5291; Wilcoxon matched pairs signed rank test. n = 4 mice; n dendrites: Table A.3. Data presented as mean ± s.e.m. B2, baseline day 2, imaging day 2; B4 baseline day 4, imaging day 4; B7, baseline day 7, imaging day 7; S1, stress day 1, imaging day 8; S2, stress day 2, imaging day 9; S4, stress day 4, imaging day 11; S7, stress day 7, imaging day 14. Grey, baseline; red, stress.

#### 4.1.6.2 Clustering between newborn and persistent spines per dendrite

Here I conducted a per dendrite analysis of DNNs between NB and persistent spines. I again took the median DNN per dendrite, normalised by the density of NB spines of each respective dendrite.
Density corrected median DNNs were smaller after one 2h MMS exposure compared to baseline (Figure 4.10a, ****p < 0.0001; Wilcoxon matched pairs signed rank test; and Figure 4.11a, **p = 0.0049; Wilcoxon matched pairs signed rank test).
Recovery exposure returned DNNs between NB and persistent spines to baseline ranges (Figure 4.10b-d, B2 compared to R1 NS, p = 0.7561; Wilcoxon matched pairs signed rank test; B4 compared to R3 NS, p = 0.8306; Wilcoxon matched pairs signed rank test and B7 compared to R6 NS, p = 0.0900; Wilcoxon matched pairs signed rank test).
Normalised median DNNs measured after 2 (Figure 4.11b, ***p = 0.0001; Wilcoxon matched pairs signed rank test) and 4 (Figure 4.11c, *p = 0.01; Wilcoxon matched pairs signed rank test) stress exposures showed a continued decrease when compared to the same baseline periods.

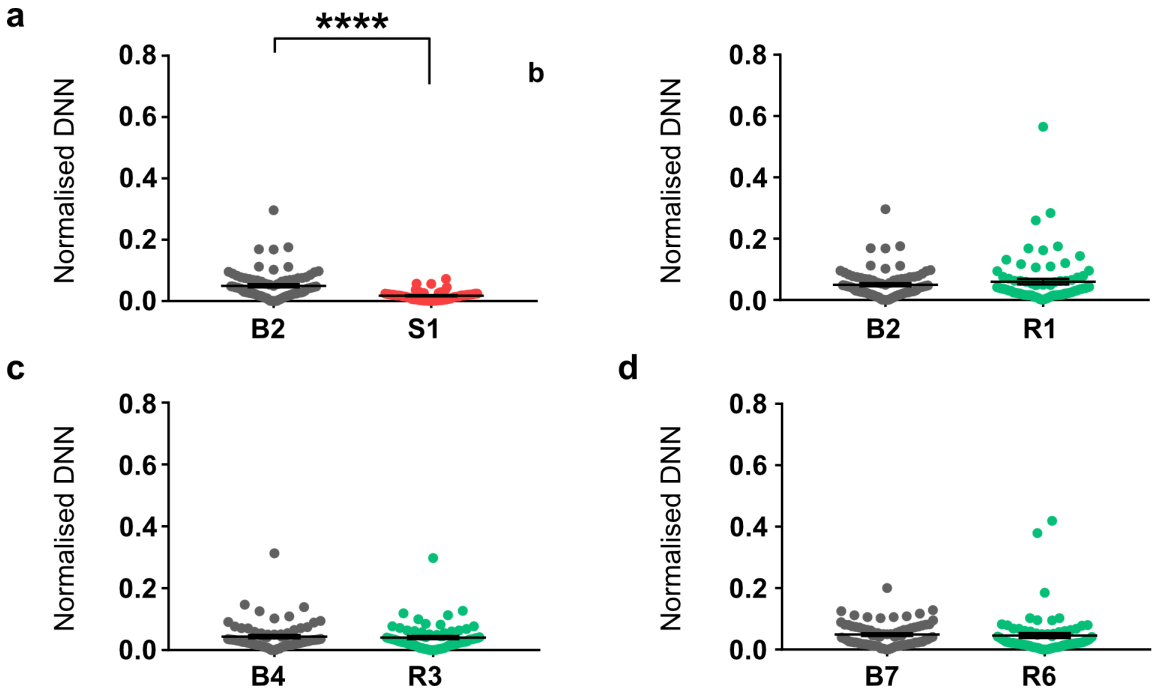


**Figure 4.10:** The effect of acute 2h MMS and recovery on distances between newborn and persistent spines per dendrite. Median DNN normalised by newborn spine density per dendrite over a (a) 24 h period, B2 compared to S1, ****p < 0.0001; Wilcoxon matched pairs signed rank test (b) 24h period, B2 compared to R1, NS p = 0.7561; Wilcoxon matched pairs signed rank test (c) 48h period, B4 compared to R3, NS p = 0.8306; Wilcoxon matched pairs signed rank test (d) 72h period, B7 compared to S7, NS p = 0.0900; Wilcoxon matched pairs signed rank test. n = 5 mice; n dendrites: Table A.4. Data presented as mean ± s.e.m. B2, baseline day 2, imaging day 2; B4 baseline day 4, imaging day 4; B7, baseline day 7, imaging day 7; S1, stress day 1, imaging day 8; R1, recovery day 1, imaging day 9; R3, recovery day 3, imaging day 11; R6, recovery day 6, imaging day 14. Grey, baseline; red, stress; green, recovery.

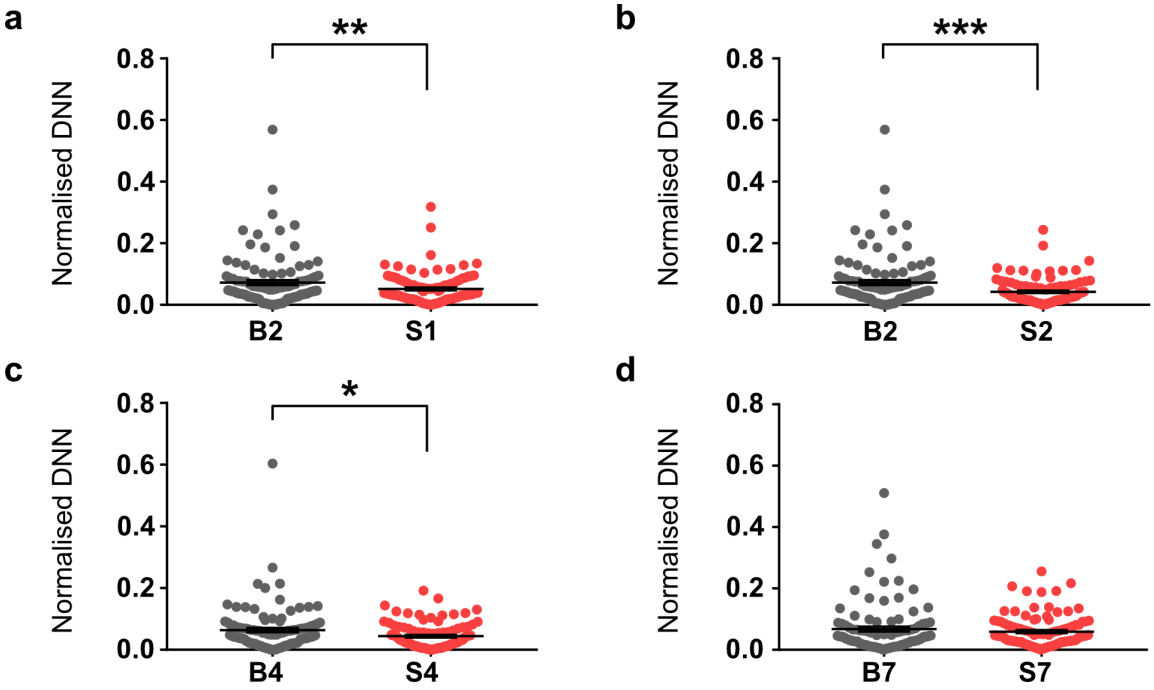


**Figure 4.11:** The effect of repeated 2h MMS on distances between newborn and persistent spines per dendrite. Median DNN normalised by newborn spine density per dendrite over a (a) 24 h period, B2 compared to S1, **p = 0.0049; Wilcoxon matched pairs signed rank test (b) 24h period, B2 compared to S2, ***p = 0.0001; Wilcoxon matched pairs signed rank test (c) 48h period, B4 compared to S4, *p = 0.01; Wilcoxon matched pairs signed rank test (d) 72h period, B7 compared to S7, NS p = 0.4457; Wilcoxon matched pairs signed rank test. n = 4 mice; n dendrites: Table A.4. Data presented as mean ± s.e.m. B2, baseline day 2, imaging day 2; B4 baseline day 4, imaging day 4; B7, baseline day 7, imaging day 7; S1, stress day 1, imaging day 8; S2, stress day 2, imaging day 9; S4, stress day 4, imaging day 11; S7, stress day 7, imaging day 14. Grey, baseline; red, stress.

Just as spines can be gained closer or further apart under varying conditions, I also sought to determine whether the same was true for spine loss - did spines that were lost after stress tend to be lost in closer or further proximity from each other? To perform this analysis I considered the location of a lost spine on its previous time point of existence and checked the closest position of the next lost spine, much the same way as was done for newborn spines, with the exception of the spine location data being taken from the previous time point. I calculated median DNNs per dendrite and normalised the result by lost spine density. The following data demonstrates the effects of stress on clustering between

1. lost spines
2. lost and newborn spines
3. lost and persistent spines

#### 4.1.6.3 Clustering between lost spines per dendrite

Here I aimed to determine whether spine loss was more or less clustered after stress compared to baseline.

Density corrected median DNNs between lost spines were unaffected by one 2h MMS exposure compared to the same baseline period (Figure 4.12a, NS, p = 0.4072; Wilcoxon matched pairs signed rank test and Figure 4.13a, NS, p = 0.7507; Wilcoxon matched pairs signed rank test).

Recovery exposure also showed no effect on distances between lost spines when compared to the same baseline periods (Figure 4.12b-d, B2 compared to R1 NS, p = 0.0946; Wilcoxon matched pairs signed rank test; B4 compared to R3 NS, p = 0.6011; Wilcoxon matched pairs signed rank test and B7 compared to R6 NS, p = 0.0844; Wilcoxon matched pairs signed rank test).

Repeated stress caused neither more nor less clustered spine loss in comparison to baseline (Figure 4.13b-d, B2 compared to S2 NS, p = 0.8231; Wilcoxon matched pairs signed rank test; B4 compared to S4 NS, p = 0.1047; Wilcoxon matched pairs signed rank test and B7 compared to S7 NS, p = 0.8809; Wilcoxon matched pairs signed rank test).

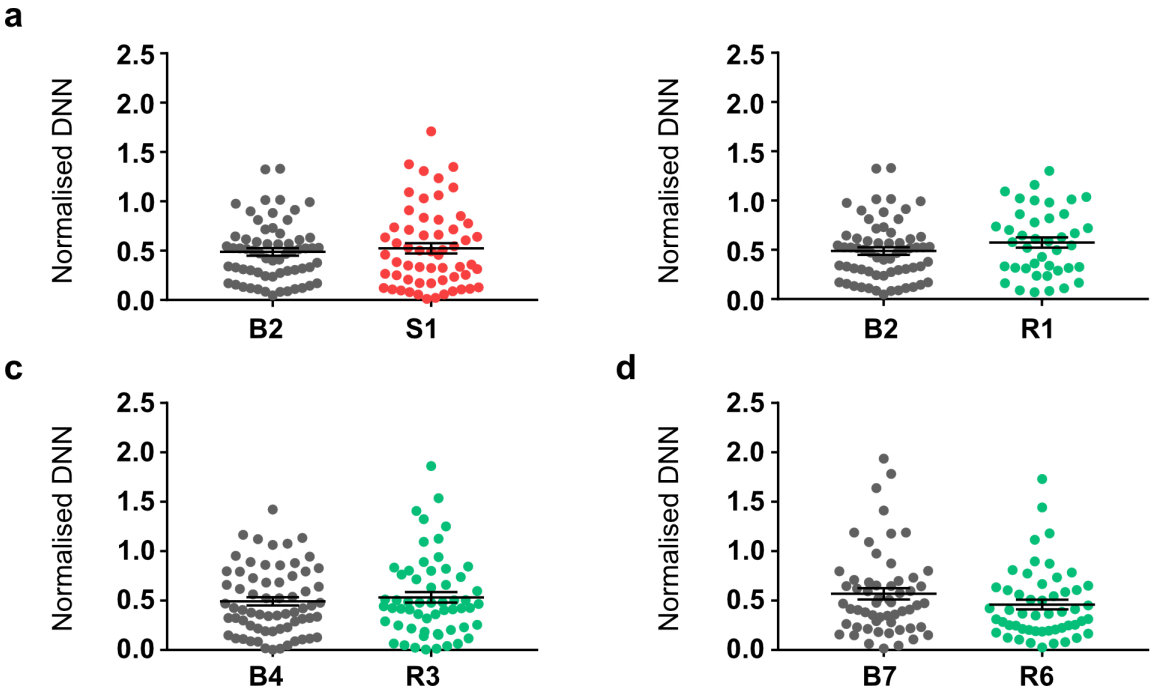


**Figure 4.12:** The effect of acute 2h MMS and recovery on distances between lost spines per dendrite. Median DNN normalised by lost spine density per dendrite over a (a) 24 h period, B2 compared to S1, NS p = 0.4072; Wilcoxon matched pairs signed rank test (b) 24h period, B2 compared to R1, NS p = 0.0946; Wilcoxon matched pairs signed rank test (c) 48h period, B4 compared to R3, NS p = 0.6011; Wilcoxon matched pairs signed rank test (d) 72h period, B7 compared to S7, NS p = 0.0844; Wilcoxon matched pairs signed rank test. n = 5 mice; n dendrites: Table A.5. Data presented as mean ± s.e.m. B2, baseline day 2, imaging day 2; B4 baseline day 4, imaging day 4; B7, baseline day 7, imaging day 7; S1, stress day 1, imaging day 8; R1, recovery day 1, imaging day 9; R3, recovery day 3, imaging day 11; R6, stress day 6, imaging day 14. Grey, baseline; red, stress; green, recovery.

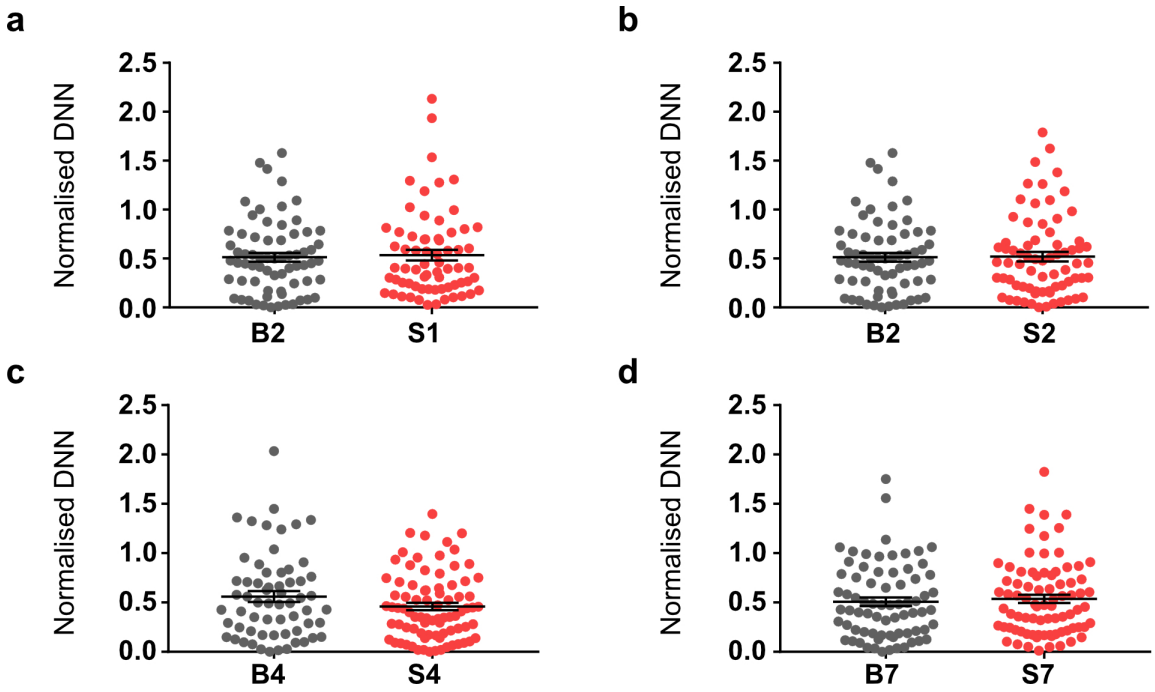


**Figure 4.13:** The effect of repeated 2h MMS on distances between lost spines per dendrite. Median DNN normalised by lost spine density per dendrite over a (a) 24 h period, B2 compared to S1, NS p = 0.7507; Wilcoxon matched pairs signed rank test (b) 24h period, B2 compared to S2, NS p = 0.8231; Wilcoxon matched pairs signed rank test (c) 48h period, B4 compared to S4, NS p = 0.1047; Wilcoxon matched pairs signed rank test (d) 72h period, B7 compared to S7, NS p = 0.8809; Wilcoxon matched pairs signed rank test. n = 4 mice; n dendrites: Table A.5. Data presented as mean ± s.e.m. B2, baseline day 2, imaging day 2; B4 baseline day 4, imaging day 4; B7, baseline day 7, imaging day 7; S1, stress day 1, imaging day 8; S2, stress day 2, imaging day 9; S4, stress day 4, imaging day 11; S7, stress day 7, imaging day 14. Grey, baseline; red, stress.

#### 4.1.6.4 Clustering between lost and newborn spines per dendrite

Here I aimed to determine whether lost spines were more or less clustered to newborn spines after stress compared to baseline.

Density corrected median DNNs between lost and newborn spines were unchanged by one 2h MMS exposure compared to the same baseline period (Figure 4.14a, NS p = 0.0993; Wilcoxon matched pairs signed rank test and Figure 4.15a, NS p = 0.1768; Wilcoxon matched pairs signed rank test).

Recovery exposure showed no effect on distances between lost and newborn spines when compared to the same baseline periods (Figure 4.14b-d, B2 compared to R1 NS, p = 0.3796; Wilcoxon matched pairs signed rank test; B4 compared to R3 NS, p = 0.3396; Wilcoxon matched pairs signed rank test and B7 compared to R6 NS, p = 0.7258; Wilcoxon matched pairs signed rank test).

4 repeated stress exposures increased the distances between lost and newborn spines compared to the same baseline period (Figure 4.15c, B4 compared to S4 *p = 0.0116; Wilcoxon matched pairs signed rank test).

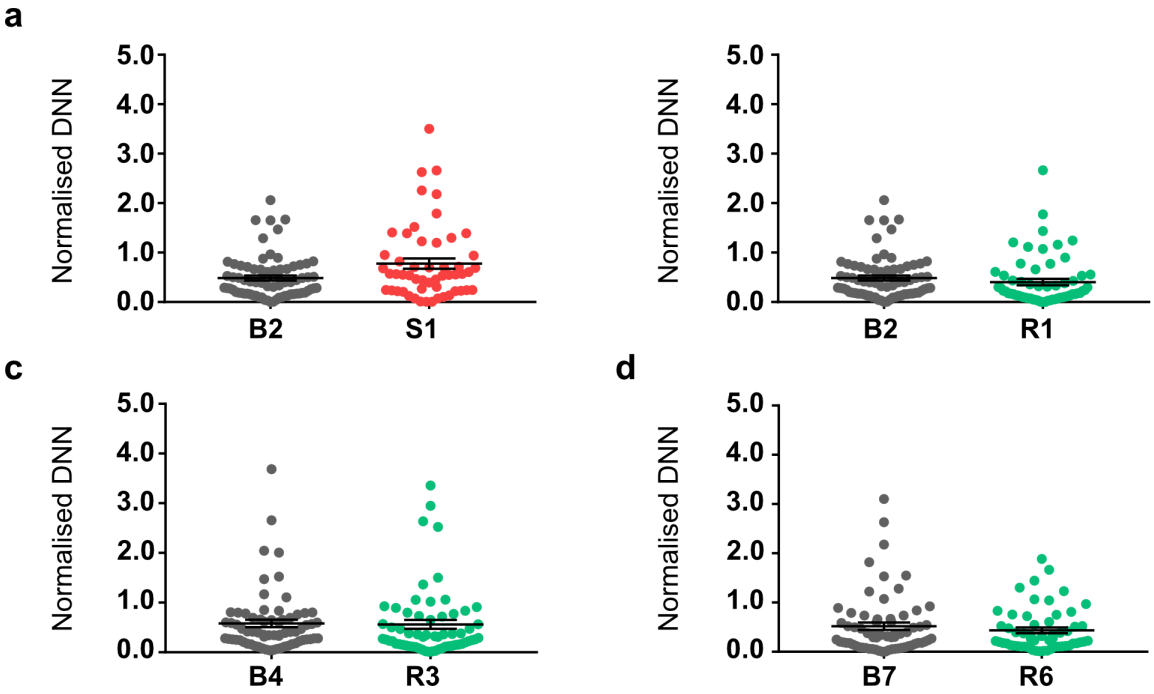


**Figure 4.14:** The effect of acute 2h MMS and recovery on distances between lost and newborn spines per dendrite. Median DNN normalised by lost spine density per dendrite over a (a) 24 h period, B2 compared to S1, NS p = 0.0993; Wilcoxon matched pairs signed rank test (b) 24h period, B2 compared to R1, NS p = 0.3796; Wilcoxon matched pairs signed rank test (c) 48h period, B4 compared to R3, NS p = 0.3396; Wilcoxon matched pairs signed rank test (d) 72h period, B7 compared to S7, NS p = 0.7258; Wilcoxon matched pairs signed rank test. n = 5 mice; n dendrites: Table A.6. Data presented as mean ± s.e.m. B2, baseline day 2, imaging day 2; B4 baseline day 4, imaging day 4; B7, baseline day 7, imaging day 7; S1, stress day 1, imaging day 8; R1, recovery day 1, imaging day 9; R3, recovery day 3, imaging day 11; R6, recovery day 6, imaging day 14. Grey, baseline; red, stress; green, recovery.

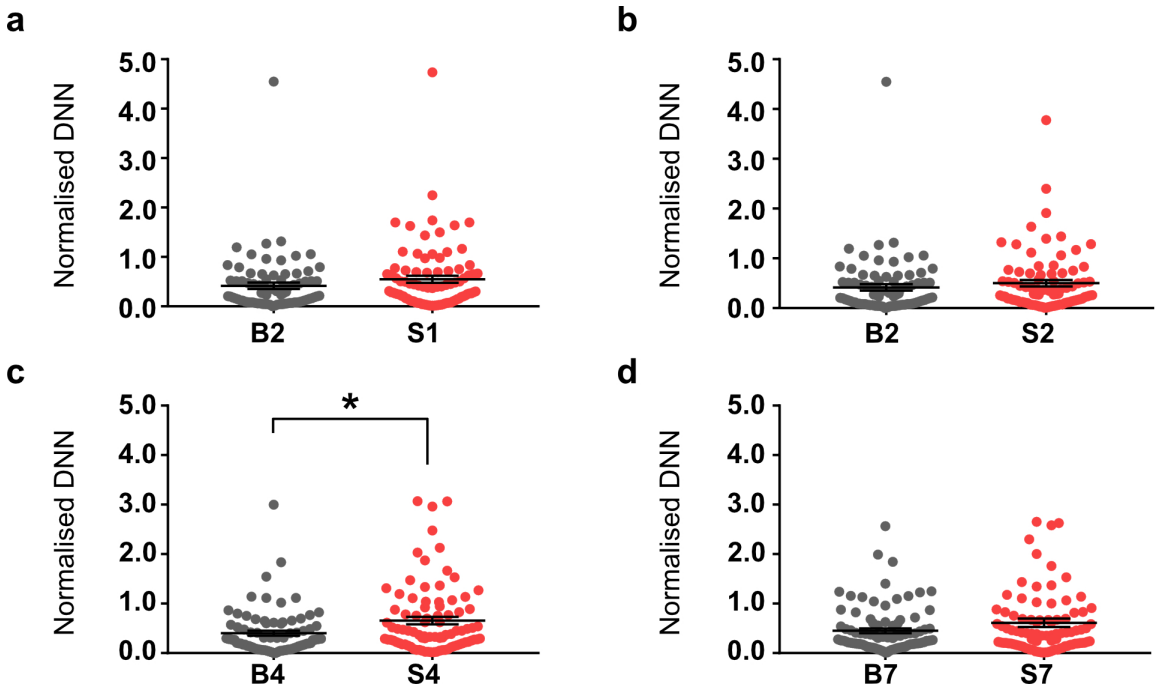


**Figure 4.15:** The effect of repeated 2h MMS on distances between lost and newborn spines per dendrite. Median DNN normalised by lost spine density per dendrite over a (a) 24 h period, B2 compared to S1, NS p = 0.1768; Wilcoxon matched pairs signed rank test (b) 24h period, B2 compared to S2, NS p = 0.2605; Wilcoxon matched pairs signed rank test (c) 48h period, B4 compared to S4, *p = 0.0116; Wilcoxon matched pairs signed rank test (d) 72h period, B7 compared to S7, NS p = 0.2015; Wilcoxon matched pairs signed rank test. n = 4 mice; n dendrites: Table A.6. Data presented as mean ± s.e.m. B2, baseline day 2, imaging day 2; B4 baseline day 4, imaging day 4; B7, baseline day 7, imaging day 7; S1, stress day 1, imaging day 8; S2, stress day 2, imaging day 9; S4, stress day 4, imaging day 11; S7, stress day 7, imaging day 14. Grey, baseline; red, stress.

#### 4.1.6.5 Clustering between lost and persistent spines per dendrite

Here I aimed to determine whether lost spines were more or less clustered to persistent spines after stress compared to baseline.

Density corrected median DNNs between lost and persistent spines were not affected by one 2h MMS exposure compared to the same baseline period in one cohort of mice (Figure 4.16a, NS p = 0.4234; Wilcoxon matched pairs signed rank test) but decreased in the other cohort (Figure 4.17a, **p = 0.0046; Wilcoxon matched pairs signed rank test).

Recovery exposure showed no effect on distances between lost and persistent spines when compared to the same baseline periods (Figure 4.16b-d, B2 compared to R1 NS, p = 0.4848; Wilcoxon matched pairs signed rank test; B4 compared to R3 NS, p = 0.5577; Wilcoxon matched pairs signed rank test and B7 compared to R6 NS, p = 0.3193; Wilcoxon matched pairs signed rank test).

4 repeated stress exposure increased distances between lost and persistent spines compared to

the same baseline periods (Figure 4.17c, B4 compared to S4 *p = 0.0181; Wilcoxon matched pairs signed rank test).

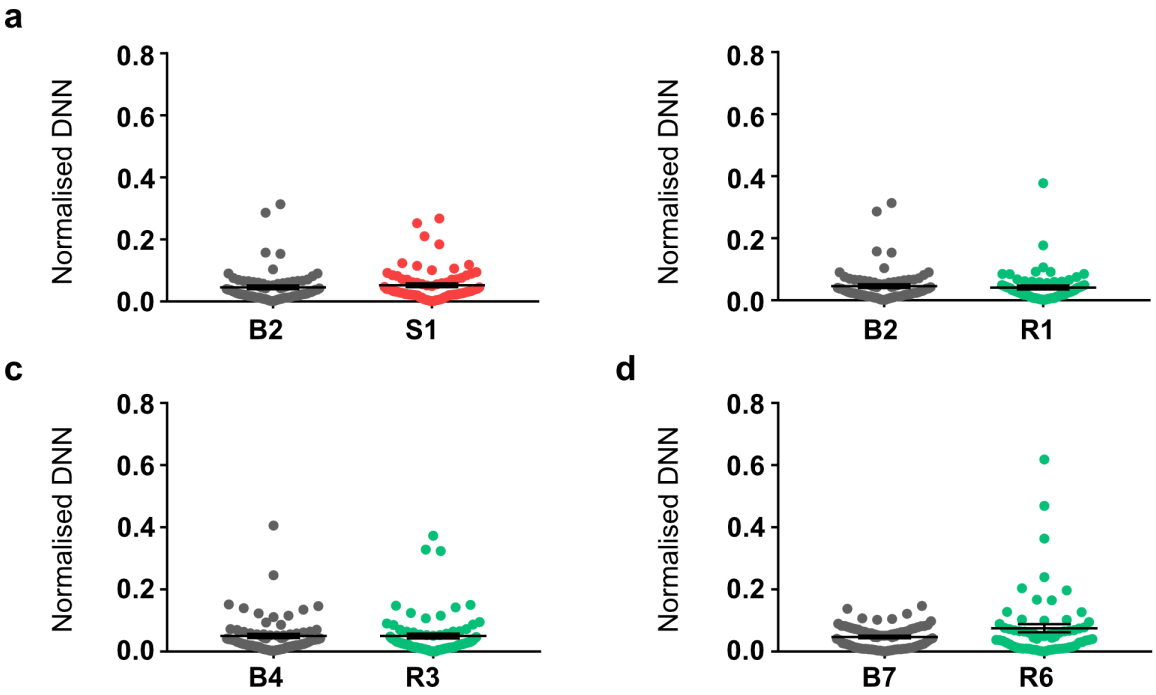


**Figure 4.16:** The effect of acute 2h MMS and recovery on distances between lost and persistent spines per dendrite. Median DNN normalised by lost spine density per dendrite over a (a) 24 h period, B2 compared to S1, NS p = 0.4234; Wilcoxon matched pairs signed rank test (b) 24h period, B2 compared to R1, NS p = 0.4848; Wilcoxon matched pairs signed rank test (c) 48h period, B4 compared to R3, NS p = 0.5577; Wilcoxon matched pairs signed rank test (d) 72h period, B7 compared to S7, NS p = 0.3193; Wilcoxon matched pairs signed rank test. n = 5 mice; n dendrites: Table A.7. Data presented as mean ± s.e.m. B2, baseline day 2, imaging day 2; B4 baseline day 4, imaging day 4; B7, baseline day 7, imaging day 7; S1, stress day 1, imaging day 8; R1, recovery day 1, imaging day 9; R3, recovery day 3, imaging day 11; R6, recovery day 6, imaging day 14. Grey, baseline; red, stress; green, recovery.

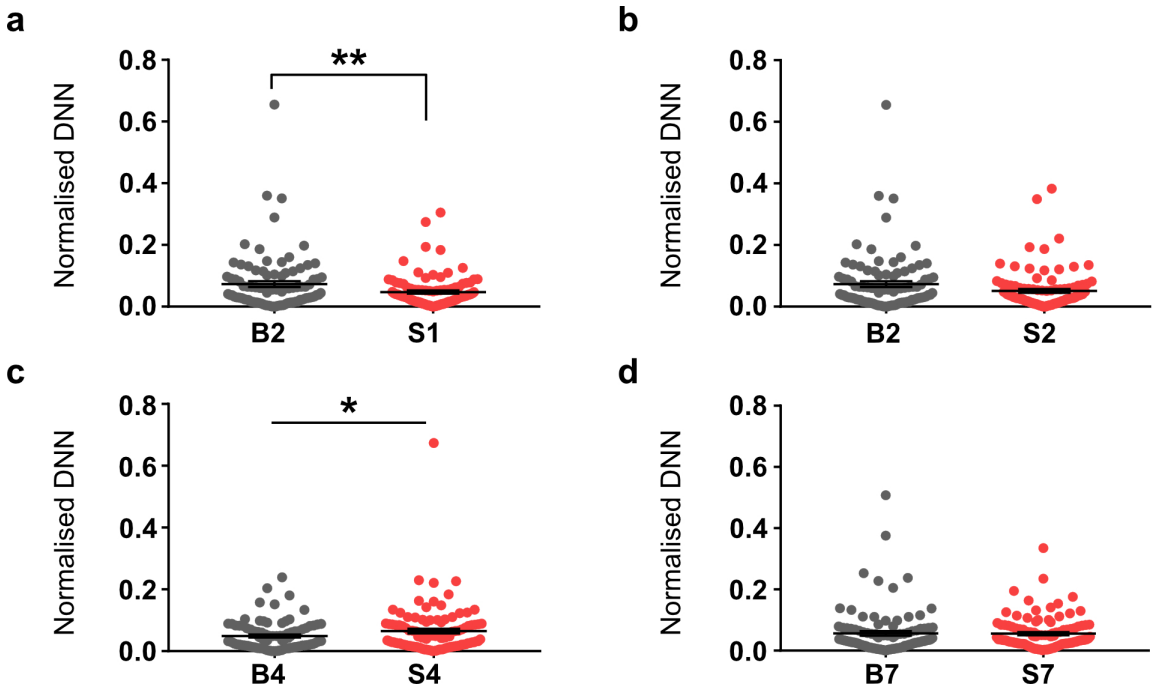


**Figure 4.17:** The effect of repeated 2h MMS on distances between lost and persistent spines per dendrite. Median DNN normalised by lost spine density per dendrite over a (a) 24 h period, B2 compared to S1, **p = 0.0046; Wilcoxon matched pairs signed rank test (b) 24h period, B2 compared to S2, NS p = 0.0596; Wilcoxon matched pairs signed rank test (c) 48h period, B4 compared to S4, *p = 0.0181; Wilcoxon matched pairs signed rank test (d) 72h period, B7 compared to S7, NS p = 0.7074; Wilcoxon matched pairs signed rank test. n = 4 mice; n dendrites: Table A.7. Data presented as mean ± s.e.m. B2, baseline day 2, imaging day 2; B4 baseline day 4, imaging day 4; B7, baseline day 7, imaging day 7; S1, stress day 1, imaging day 8; S2, stress day 2, imaging day 9; S4, stress day 4, imaging day 11; S7, stress day 7, imaging day 14. Grey, baseline; red, stress.

Although the analysis of DNNs so far takes into account the effects of density changes, this advantage also causes it to suffer from representing the DNNs as one main effect per dendrite. Therefore, any smaller or larger DNNs are not considered, inevitably resulting in a disregard of potential effects which may be driven differently to the median effect.
To gain a broader understanding of how DNNs change without being confined to median DNN behaviour, I analysed all DNNs per time point, comparing between baseline and stress conditions. The following results reflect the same structure as the per dendrite analysis, namely a consideration of clustering between

1. newborn spines
2. newborn and persistent spines
3. lost spines
4. lost and newborn spines
5. lost and persistent spines

#### 4.1.6.6 Clustering between newborn spines

Here I considered each individual newborn spine in turn and determined the distance to its nearest neighbouring newborn spine at each time point.
The distances between newborn spines increased after one 2h MMS exposure when compared to baseline (Figure 4.18a, ****p < 0.0001; Kolmogorov–Smirnov test). The opposite effect was observed with recovery, where the distances between newborn spines decreased after one day of recovery when compared to baseline (Figure 4.18b, ***p = 0.0001; Kolmogorov–Smirnov test).

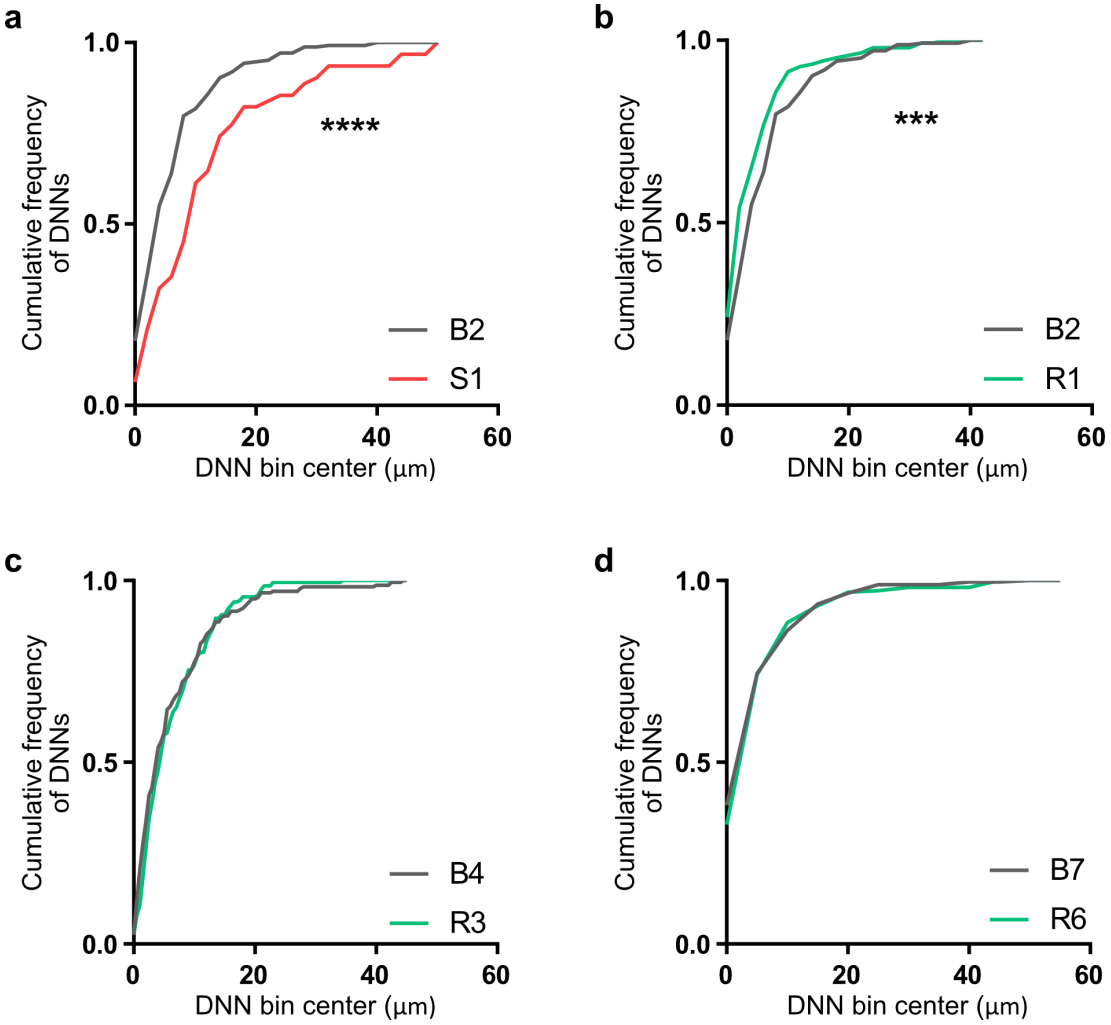


**Figure 4.18:** The effect of acute 2h MMS and recovery on distances between newborn spines. (a) 2h of MMS increased the distance between newborn spines compared to baseline, ****p < 0.0001; Kolmogorov–Smirnov test. (b) 24h of recovery decreased the distance between newborn spines, ***p = 0.0001; Kolmogorov–Smirnov test. (c) 3 days of recovery had no effect on distances between newborn spines, NS p = 0.2131; Kolmogorov–Smirnov test. (d) 6 days of recovery had no effect on distances between newborn spines, NS p = 0.1625; Kolmogorov–Smirnov test. n = 5 mice; n dendrites: Table A.8. B2, baseline day 2, imaging day 2; B4 baseline day 4, imaging day 4; B7, baseline day 7, imaging day 7; S1, stress day 1, imaging day 8; R1, recovery day 1, imaging day 9; R3, recovery day 3, imaging day 11; R6, recovery day 6, imaging day 14. Grey, baseline; red, stress; green, recovery.

Implementing the same analysis for the repeated stress cohort confirmed the increase in distance between newborn spines after one stress exposure (Figure 4.19a, ****p < 0.0001; Kolmogorov–Smirnov test). Contrasting to the recovery effect (Figure 4.18b, ***p = 0.0001; Kolmogorov–Smirnov test) seen with the acute cohort however, a second stress exposure continued to display an increase in the distance between newborn spines compared to baseline (Figure 4.19b, ****p < 0.0001; Kolmogorov–Smirnov test).

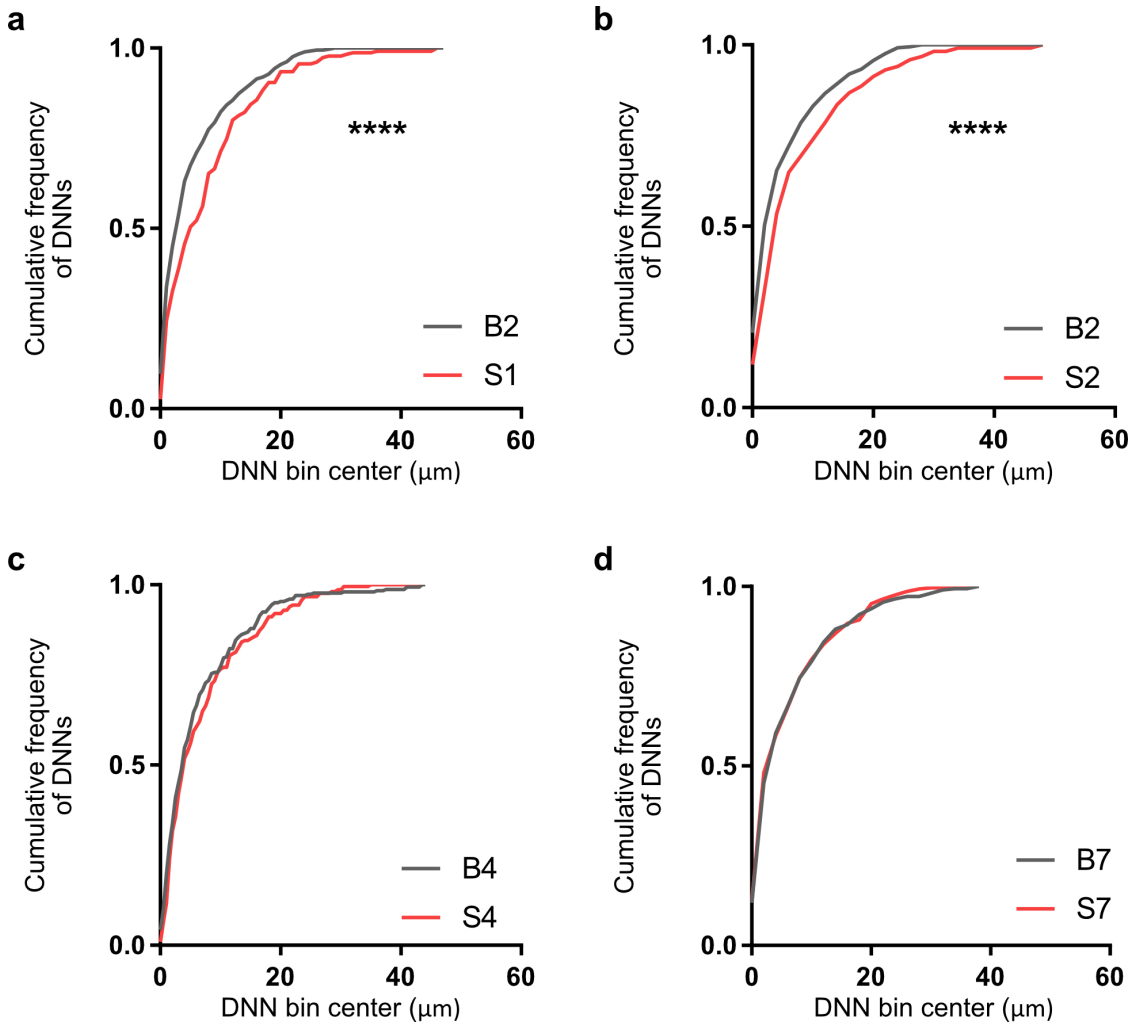


**Figure 4.19:** Cumulative distribution of DNNs between newborn spines during baseline and repeated 2h MMS exposure. (a) one 2h MMS exposure increased the distance between newborn spines compared to baseline, ****p < 0.0001; Kolmogorov–Smirnov test. (b) two 2h MMS exposures increased the distance between newborn spines compared to baseline, ****p < 0.0001; Kolmogorov–Smirnov test. (c) four repeated 2h MMS exposures had no effect on distances between newborn spines compared to baseline, NS p = 0.0776; Kolmogorov–Smirnov test. (d) seven repeated 2h MMS exposures had no effect on distances between newborn spines compared to baseline, NS p = 0.8043; Kolmogorov–Smirnov test. n = 4 mice; n dendrites: Table A.8. Grey, baseline; red, stress.

Therefore both an acute and repeated stress increased the distance between newborn spines. Recovery on the other hand, decreased the distance between newborn spines in comparison to baseline.

#### 4.1.6.7 Clustering between newborn and persistent spines

Here I considered each individual newborn spine in turn and determined the distance to its nearest neighbouring persistent spine at each time point.
The distances between newborn and persistent spines did not change significantly after one 2h MMS exposure when compared to baseline (Figure 4.20a, NS p = 0.7410 Kolmogorov–Smirnov test). The same was true after one (Figure 4.20b, NS p = 0.3478; Kolmogorov–Smirnov test), three (Figure 4.20c, NS p = 0.9474; Kolmogorov–Smirnov test) and six days (Figure 4.20d, NS p = 0.6324; Kolmogorov–Smirnov test) of recovery.

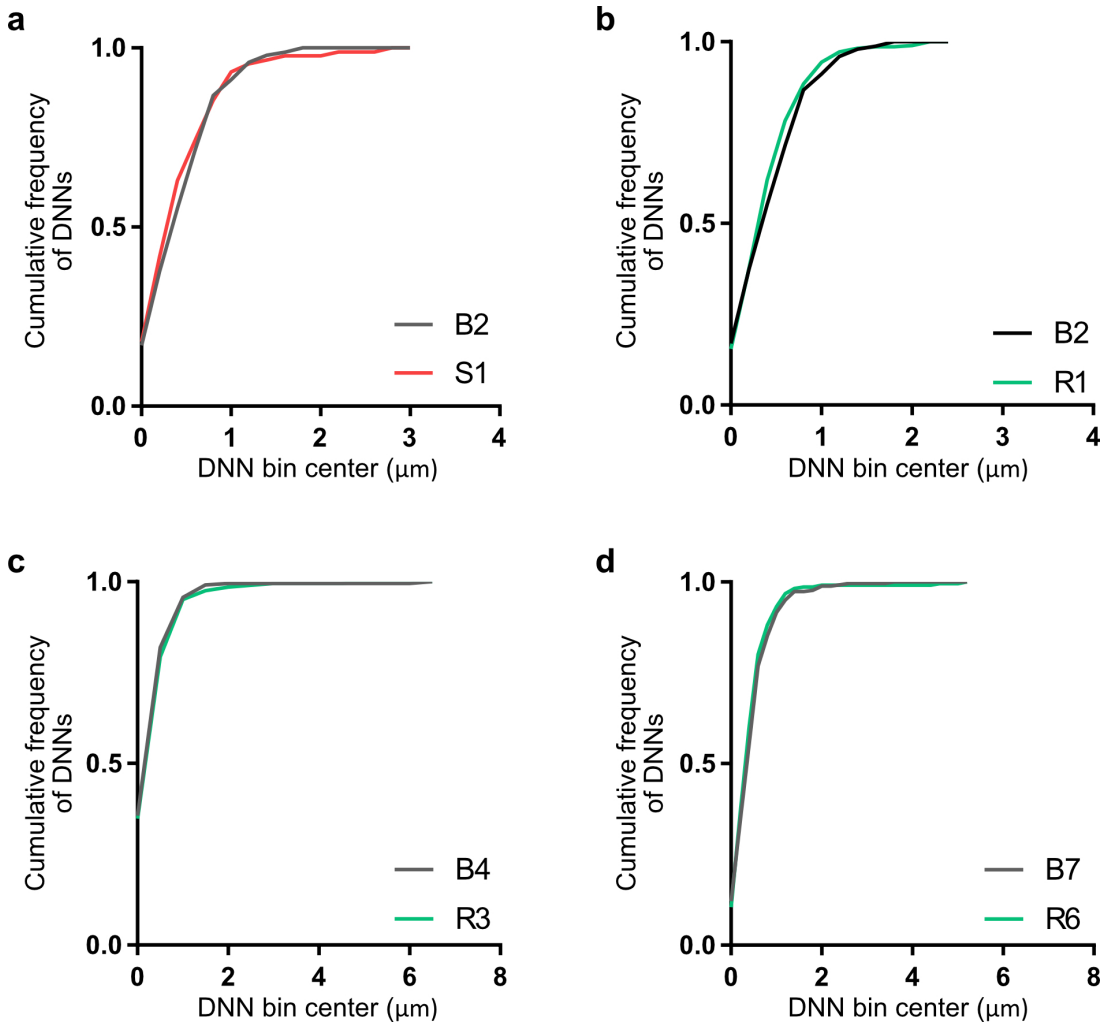


**Figure 4.20:** Cumulative distribution of DNNs between newborn and persistent spines during baseline, after acute 2h MMS exposure and during recovery. (a) 2h of MMS did not significantly change the newborn to persistent DNNs compared to baseline, NS p = 0.7410; Kolmogorov–Smirnov test. (b) 24h of recovery did not significantly change the newborn to persistent DNNs compared to baseline, NS p = 0.3478; Kolmogorov–Smirnov test. (c) three days of recovery did not significantly change the newborn to persistent DNNs compared to baseline, NS p = 0.9474; Kolmogorov–Smirnov test. (d) six days of recovery did not significantly change the newborn to persistent DNNs compared to baseline, NS p = 0.6324; Kolmogorov–Smirnov test. n = 5 mice; n dendrites: Table A.9. B2, baseline day 2, imaging day 2; B4 baseline day 4, imaging day 4; B7, baseline day 7, imaging day 7; S1, stress day 1, imaging day 8; R1, recovery day 1, imaging day 9; R3, recovery day 3, imaging day 11; R6, recovery day 6, imaging day 14. Grey, baseline; red, stress; green, recovery.

Distances between newborn and persistent spines were also not different between baseline and after the first stress exposure of the repeatedly stressed cohort (Figure 4.21a, NS p = 0.1443; Kolmogorov–Smirnov test), thus confirming the results of acute stress (4.20a, NS p = 0.7410 Kolmogorov–Smirnov test). Interestingly however, a second stress exposure significantly

decreased the distance between newborn and persistent spines (Figure 4.21b **p = 0.0058; Kolmogorov–Smirnov test).

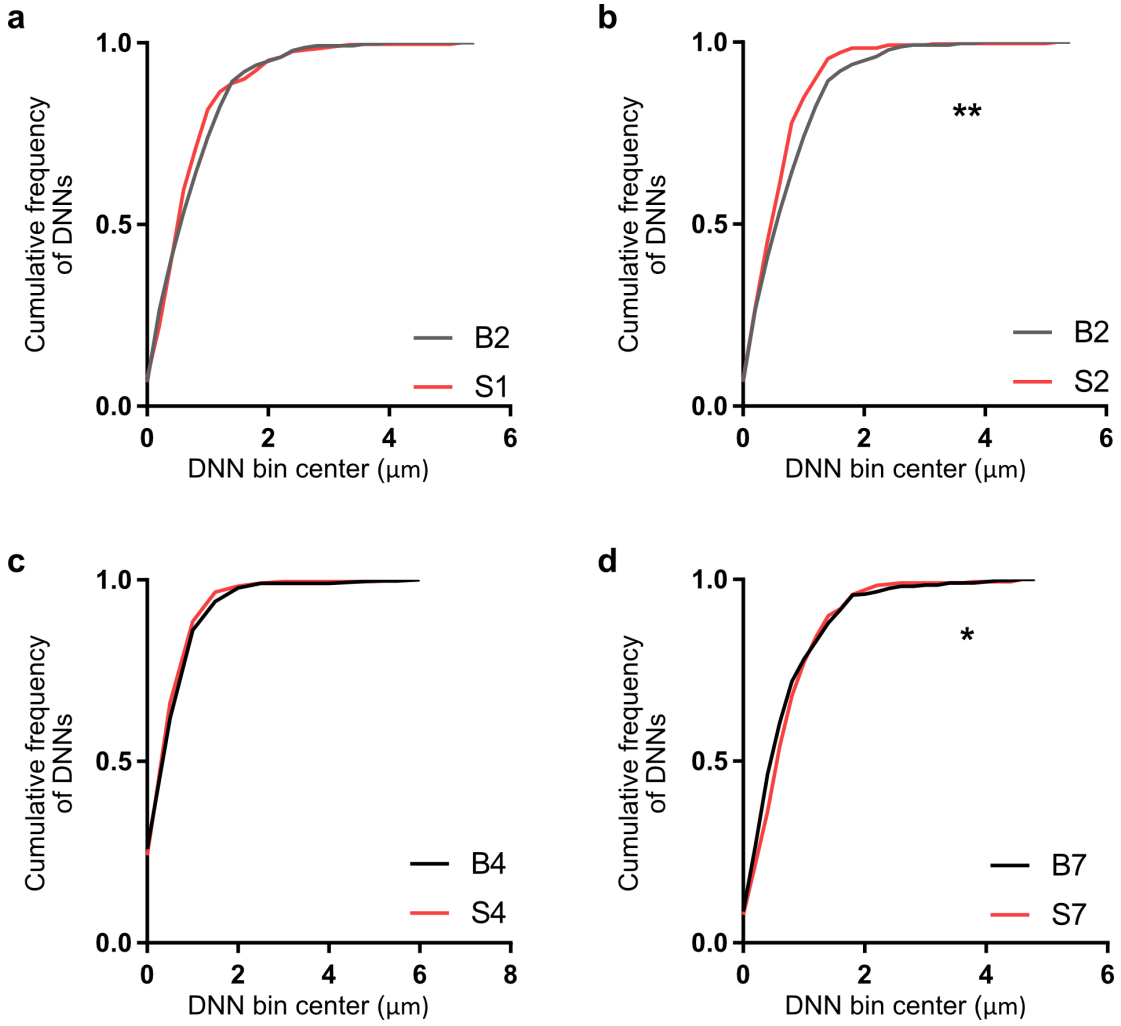


**Figure 4.21:** The effect of repeated 2h MMS on distances between newborn and persistent spines. (a) one 2h MMS exposure did not significantly change the newborn to persistent DNNs compared to baseline, NS p = 0.1443; Kolmogorov–Smirnov test. (b) two 2h MMS exposures decreased the distance between newborn and persistent spines compared to baseline, **p = 0.0058; Kolmogorov–Smirnov test. (c) four 2h MMS exposures did not affect the distance between newborn and persistent spines compared to baseline, NS p = 0.6791; Kolmogorov–Smirnov test. (d) seven 2h MMS exposures increased the distance between newborn and persistent spines compared to baseline, *p = 0.0262; Kolmogorov–Smirnov test. n = 4 mice; n dendrites: Table A.9. B2, baseline day 2, imaging day 2; B4 baseline day 4, imaging day 4; B7, baseline day 7, imaging day 7; S1, stress day 1, imaging day 8; S2, stress day 2, imaging day 9; S4, stress day 4, imaging day 11; S7, stress day 7, imaging day 14. Grey, baseline; red, stress.

#### 4.1.6.8 Clustering between lost spines

Distances between lost spines were not different between baseline and after one stress exposure (Figure 4.22a, NS p = 0.1537; Kolmogorov–Smirnov test). Exposure to recovery also did not change the distances between lost spines. (Figure 4.22b, NS p = 0.3190; Kolmogorov–Smirnov; Figure 4.22c, NS p = 0.2047; Kolmogorov–Smirnov test) except after 6 days of recovery (Figure 4.22d, NS p = 0.0076; Kolmogorov–Smirnov test;).
In the repeatedly stressed cohort, distances between lost spines were again not different between baseline and after one stress exposure (Figure 4.23a, NS p = 0.2766; Kolmogorov–Smirnov test), but 4 exposures resulted in smaller distances between lost spines (Figure 4.23c, *p = 0.0197; Kolmogorov–Smirnov test) compared to baseline. This effect did not extend to seven days of stress exposure when compared to baseline (Figure 4.23d, NS p = 0.0887; Kolmogorov–Smirnov test).

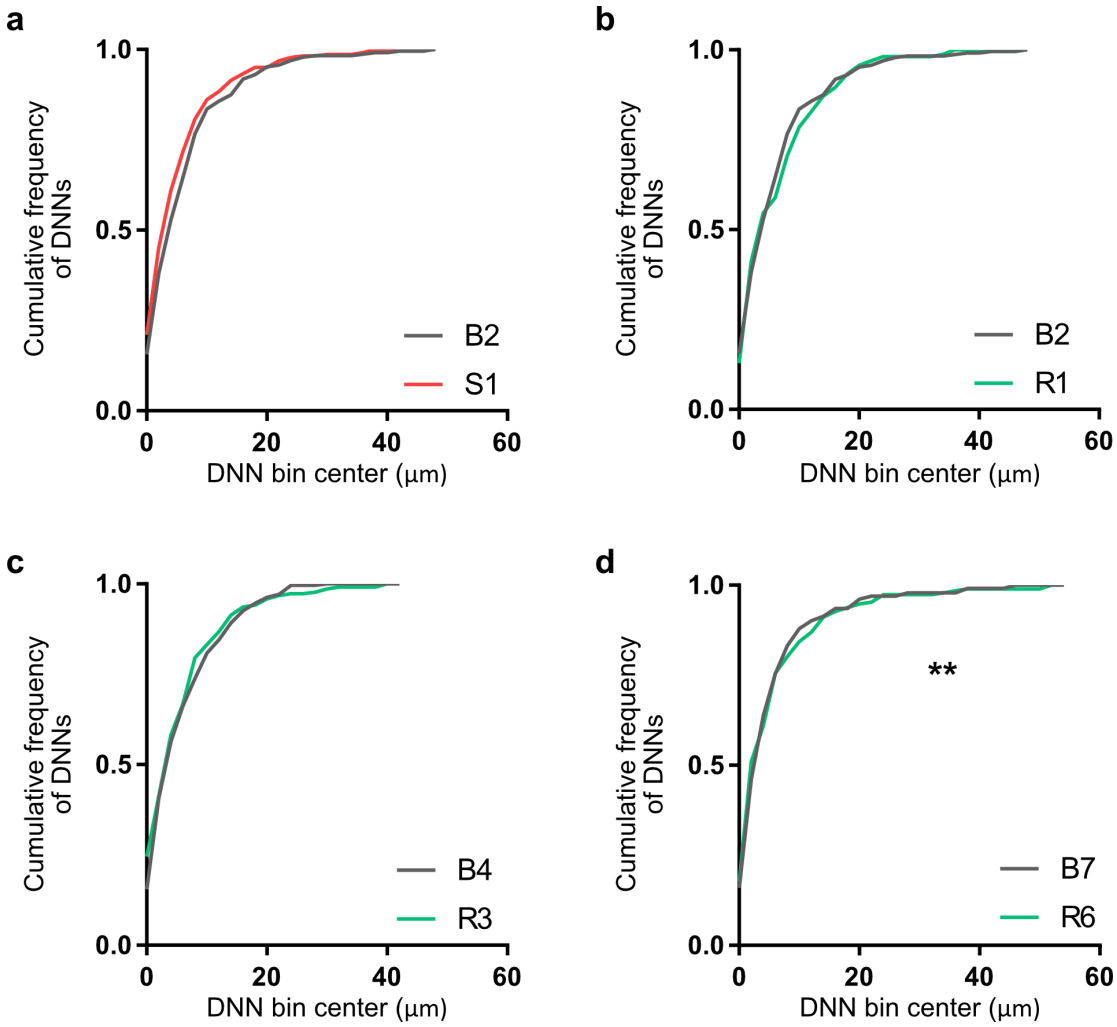


**Figure 4.22:** Cumulative distribution of DNNs between lost spines during baseline, after acute 2h MMS exposure and after recovery. (a) 2h of MMS did not significantly change the distances between lost spines compared to baseline, NS p = 0.1537; Kolmogorov–Smirnov test. (b) 24h of recovery did not significantly change the distances between lost spines compared to baseline, NS p = 0.3190; Kolmogorov–Smirnov test. (c) three days of recovery did not significantly change the distances between lost spines compared to baseline, NS p = 0.2047; Kolmogorov–Smirnov test. (d) six days of recovery significantly changed the distances between lost spines compared to baseline, **p = 0.0076; Kolmogorov–Smirnov test. n = 5 mice; n dendrites: Table A.10. B2, baseline day 2, imaging day 2; B4 baseline day 4, imaging day 4; B7, baseline day 7, imaging day 7; S1, stress day 1, imaging day 8; R1, recovery day 1, imaging day 9; R3, recovery day 3, imaging day 11; R6, recovery day 6, imaging day 14. Grey, baseline; red, stress; green, recovery.

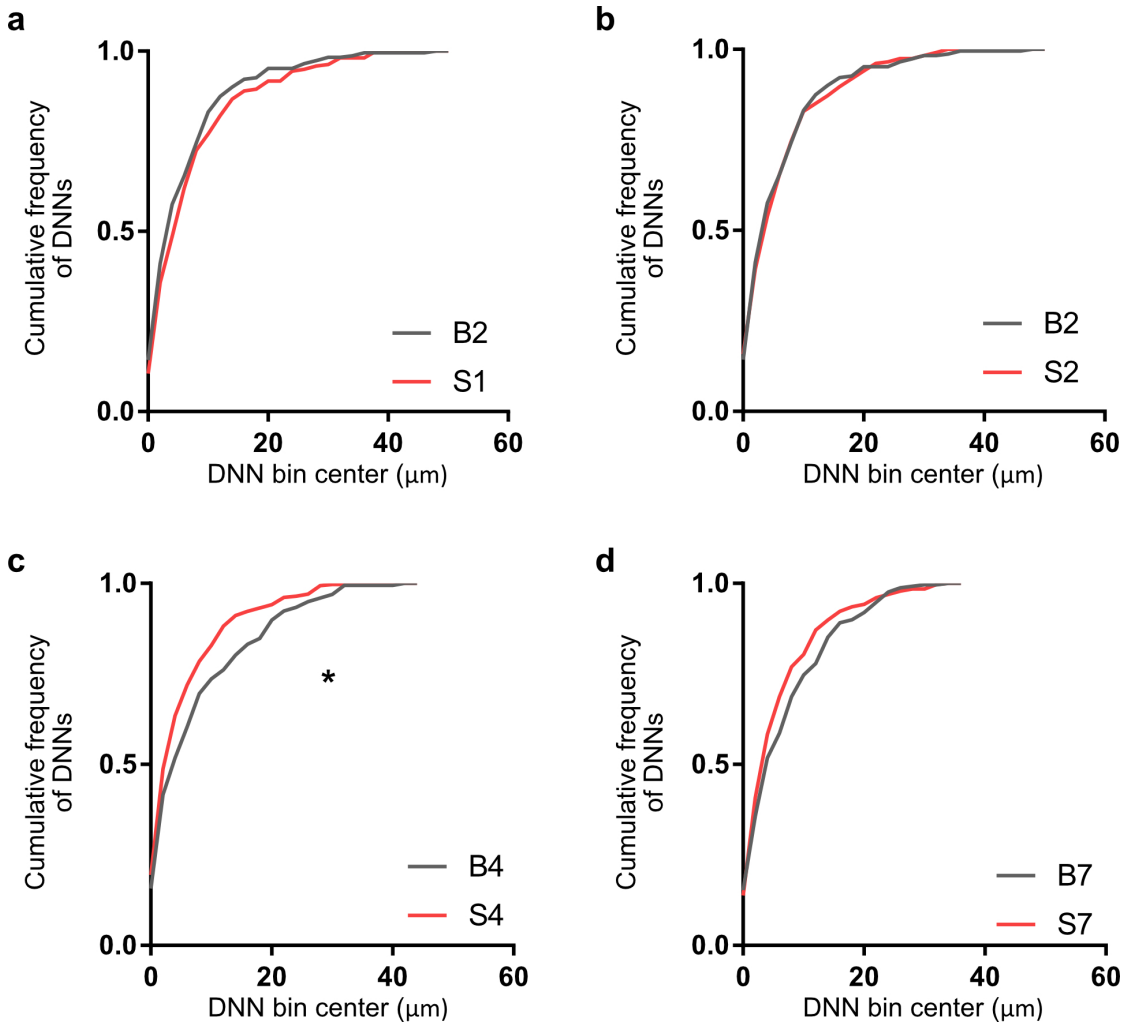


**Figure 4.23:** Cumulative distribution of DNNs between lost spines during baseline and repeated 2h MMS exposure. (a) 2h of MMS did not significantly change the distances between lost spines compared to baseline, NS p = 0.2766; Kolmogorov–Smirnov test. (b) two 2h MMS exposures did not significantly change the distances between lost spines compared to baseline, NS p = 0.8386; Kolmogorov–Smirnov test. (c) four 2h MMS exposures reduced the distances between lost spines compared to baseline, *p = 0.0197; Kolmogorov–Smirnov test. (d) seven 2h MMS exposures did not significantly alter the distances between lost spines compared to baseline, NS p = 0.0887; Kolmogorov–Smirnov test. n = 4 mice; n dendrites: Table A.10. B2, baseline day 2, imaging day 2; B4 baseline day 4, imaging day 4; B7, baseline day 7, imaging day 7; S1, stress day 1, imaging day 8; S2, stress day 2, imaging day 9; S4, stress day 4, imaging day 11; S7, stress day 7, imaging day 14. Grey, baseline; red, stress.

#### 4.1.6.9 Clustering between lost and newborn spines

Distances between lost and newborn spines increased after one 2h MMS exposure compared to baseline (Figure 4.24a, ****p < 0.0001; Kolmogorov–Smirnov test). Exposure to recovery did not change the distances between lost and newborn spines. (Figure 4.24b, NS p = 0.9281;

Kolmogorov–Smirnov; Figure 4.24c, NS p = 0.7083; Kolmogorov–Smirnov test and Figure 4.24d, NS p = 0.5256; Kolmogorov–Smirnov test).

In the repeatedly stressed cohort, distances between lost and newborn spines again increased after one stress exposure (Figure 4.25a, ***p = 0.0006; Kolmogorov–Smirnov test). In addition, the distances between lost and newborn spines also increased after two (Figure 4.25b, *p = 0.0239; Kolmogorov–Smirnov test) stress exposures. This effect did not extend to four and seven days of stress exposure when compared to baseline (Figure 4.25c, NS p = 0.0945; Kolmogorov–Smirnov test and Figure 4.25d, NS p = 0.5538; Kolmogorov–Smirnov test).

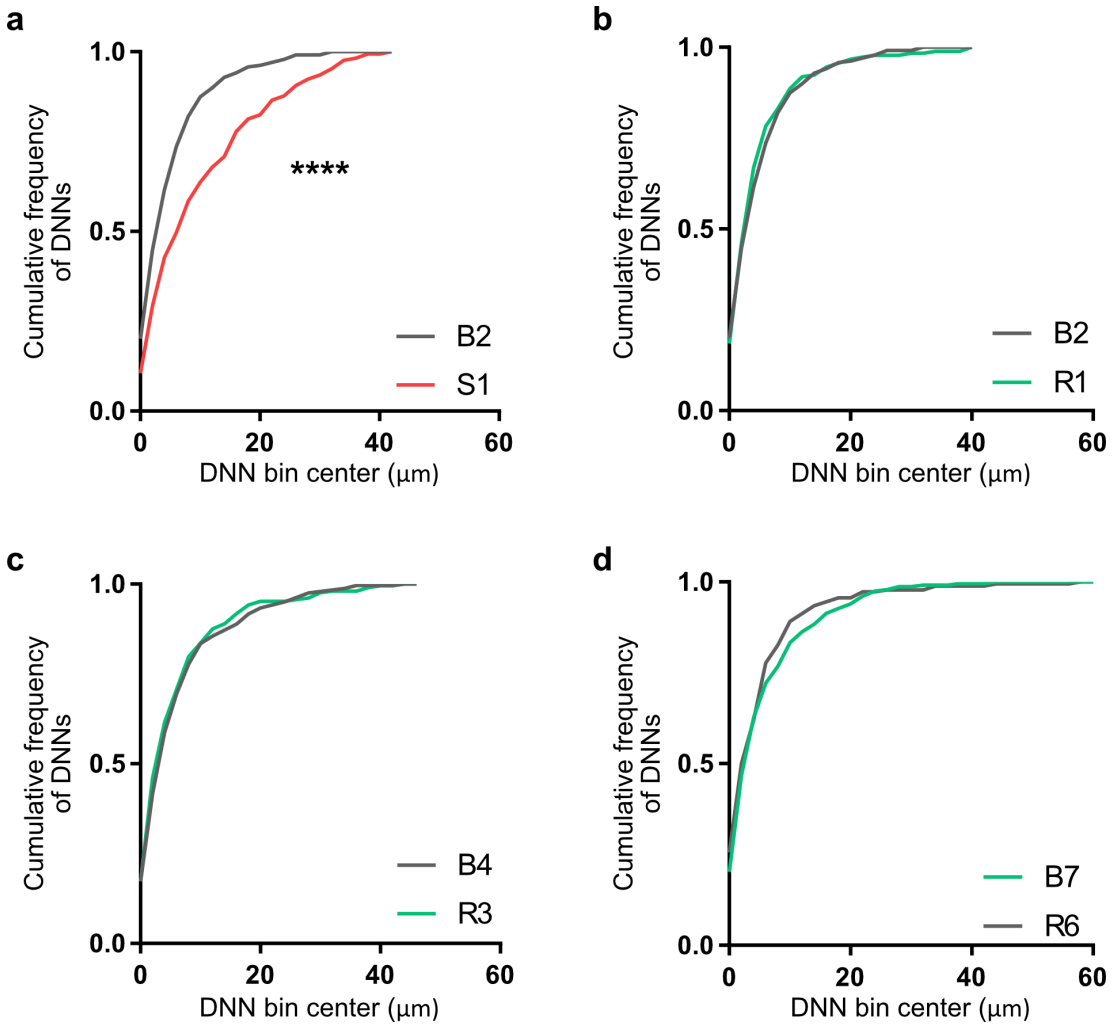


**Figure 4.24:** Cumulative distribution of DNNs between lost and newborn spines during baseline, after acute 2h MMS exposure and during recovery. (a) 2h of MMS increased the distances between lost and newborn spines compared to baseline, ****p < 0.0001; Kolmogorov–Smirnov test. (b) 24h of recovery did not significantly change the distances between lost and newborn spines compared to baseline, NS p = 0.9281; Kolmogorov–Smirnov test. (c) three days of recovery did not significantly change the distances between lost spines compared to baseline, NS p = 0.7083; Kolmogorov–Smirnov test. (d) six days of recovery did not significantly change the distances between lost and newborn spines compared to baseline, NS p = 0.5256; Kolmogorov–Smirnov test. n = 5 mice; n dendrites: Table A.11. B2, baseline day 2, imaging day 2; B4 baseline day 4, imaging day 4; B7, baseline day 7, imaging day 7; S1, stress day 1, imaging day 8; R1, recovery day 1, imaging day 9; R3, recovery day 3, imaging day 11; R6,recovery day 6, imaging day 14. Grey, baseline; red, stress; green, recovery.

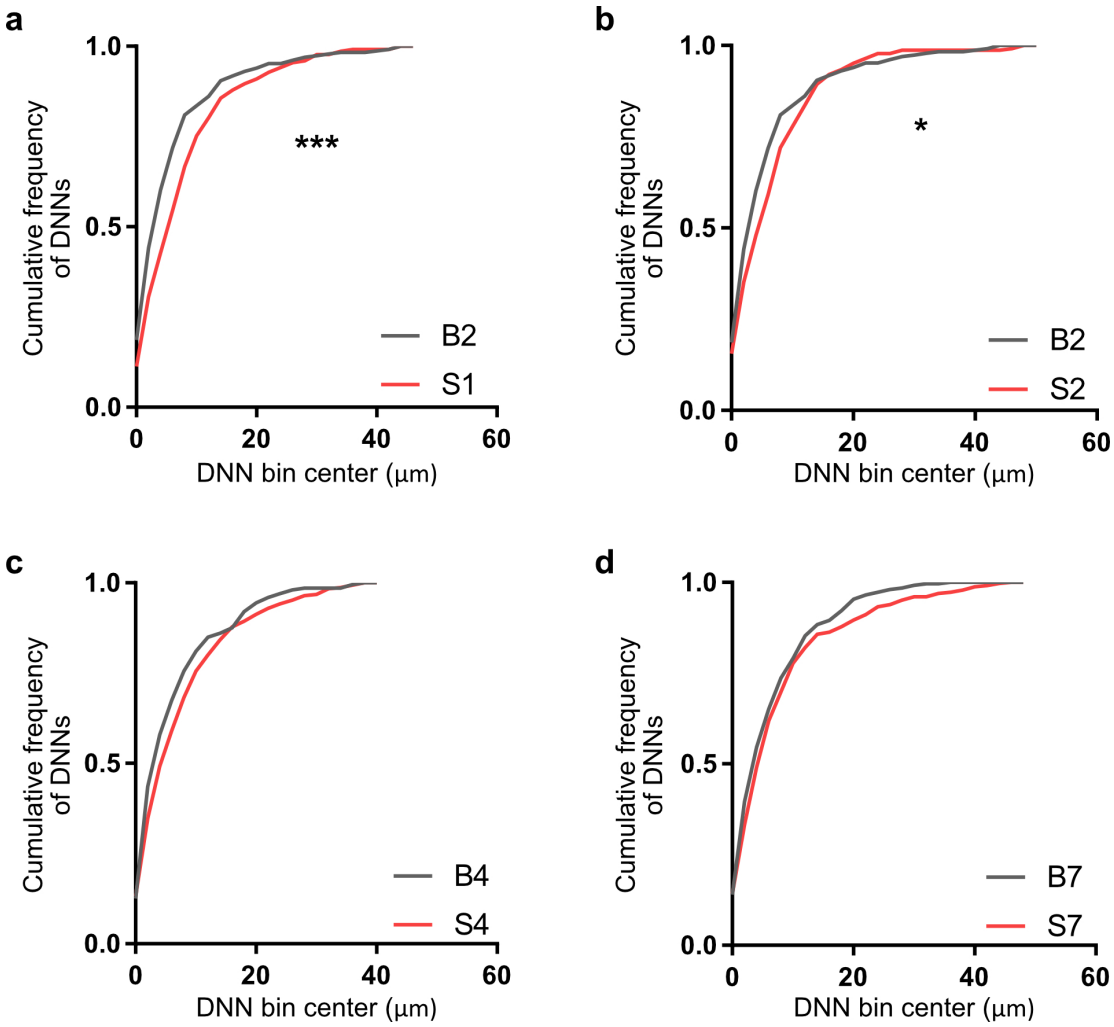


**Figure 4.25:** Cumulative distribution of DNNs between lost and newborn spines during baseline and repeated 2h MMS exposure. (a) 2h of MMS increased the distances between lost and newborn spines compared to baseline, ***p = 0.0006; Kolmogorov–Smirnov test. (b) two 2h MMS exposures increased the distances between lost and newborn spines compared to baseline,*p = 0.0239; Kolmogorov–Smirnov test. (c) four 2h MMS exposures did not significantly change the distances between lost and newborn spines compared to baseline, NS p = 0.0945; Kolmogorov–Smirnov test. (d) seven 2h MMS exposures did not significantly alter the distances between lost and newborn spines compared to baseline, NS p = 0.5538; Kolmogorov–Smirnov test. n = 4 mice; n dendrites: Table A.11. B2, baseline day 2, imaging day 2; B4 baseline day 4, imaging day 4; B7, baseline day 7, imaging day 7; S1, stress day 1, imaging day 8; S2, stress day 2, imaging day 9; S4, stress day 4, imaging day 11; S7, stress day 7, imaging day 14. Grey, baseline; red, stress.

#### 4.1.6.10 Clustering between lost and persistent spines

Distances between lost and persistent spines were unchanged after one 2h MMS exposure compared to baseline (Figure 4.26a, NS p = 0.8470; Kolmogorov–Smirnov test). Exposure to recovery did not change the distances between lost and persistent spines (Figure 4.26b, NS p = 0.7009; Kolmogorov–Smirnov test; Figure 4.26c, NS p = 0.8152; Kolmogorov–Smirnov test) except after 6 days of recovery where spines were lost further from peristent spines compared to baseline (Figure 4.26d, *p = 0.0455; Kolmogorov–Smirnov test).
In the repeatedly stressed cohort, distances between lost and persistent decreased after one (Figure 4.27a, *p = 0.0108; Kolmogorov–Smirnov test) and two (Figure 4.27b, *p = 0.0155; Kolmogorov–Smirnov test) 2h MMS exposures. The distances between lost and persistent spines were unchanged after four (Figure 4.27c, NS p = 0.7253; Kolmogorov–Smirnov test) and seven (Figure 4.27d, NS p = 0.7598; Kolmogorov–Smirnov test) stress exposures.

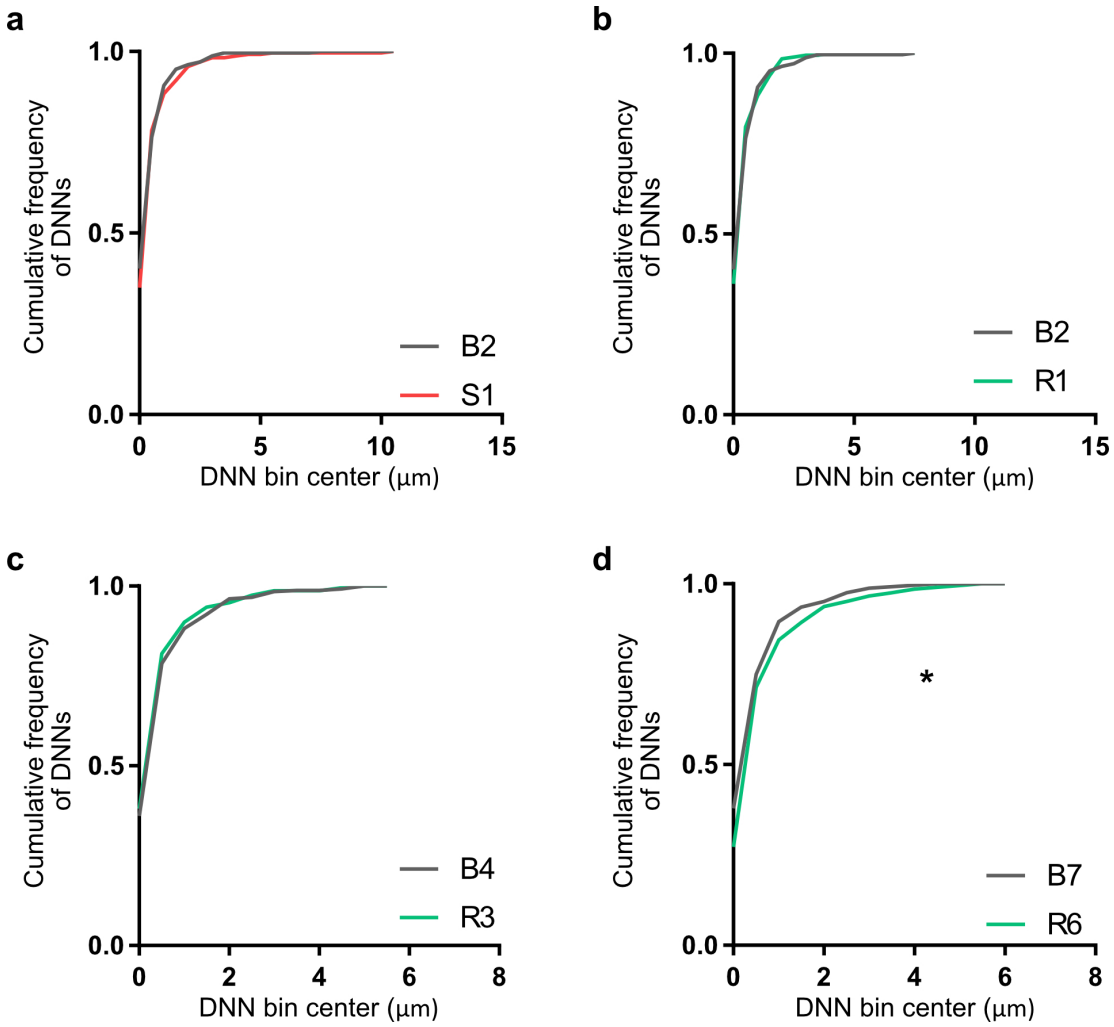


**Figure 4.26:** Cumulative distribution of DNNs between lost and persistent spines during baseline, after acute 2h MMS exposure and during recovery. (a) 2h of MMS did not significantly affect distances between lost and persistent spines compared to baseline, NS p = 0.8470; Kolmogorov–Smirnov test. (b) 24h of recovery did not significantly affect the distances between lost and persistent spines compared to baseline, NS p = 0.7009; Kolmogorov–Smirnov test. (c) three days of recovery did not significantly affect the distances between lost and persistent spines compared to baseline, NS p = 0.8152; Kolmogorov–Smirnov test. (d) six days of recovery increased the distances between lost and persistent spines compared to baseline, *p = 0.0455; Kolmogorov–Smirnov test. n = 5 mice; n dendrites: Table A.12. B2, baseline day 2, imaging day 2; B4 baseline day 4, imaging day 4; B7, baseline day 7, imaging day 7; S1, stress day 1, imaging day 8; R1, recovery day 1, imaging day 9; R3, recovery day 3, imaging day 11; R6, recovery day 6, imaging day 14. Grey, baseline; red, stress; green, recovery.

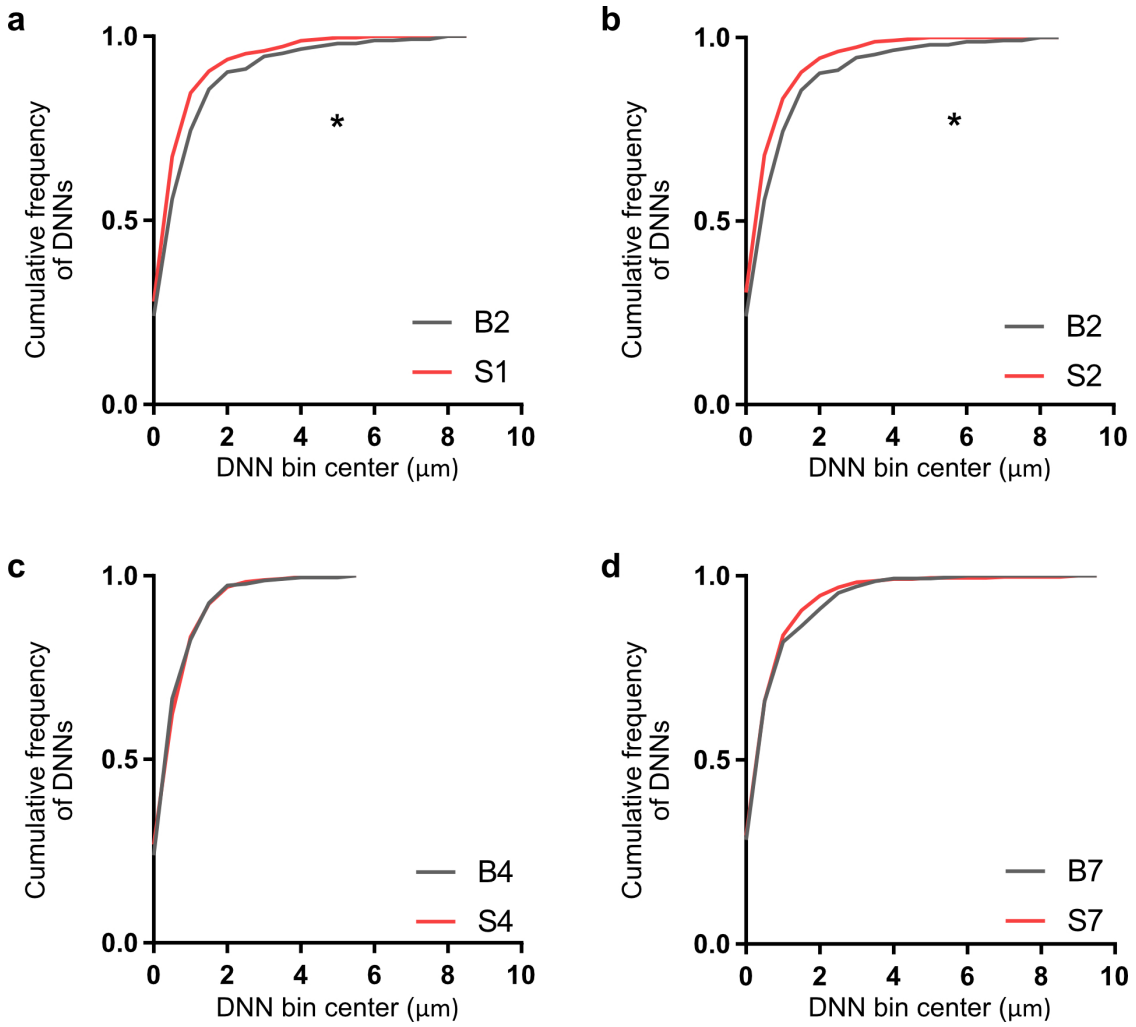


**Figure 4.27:** Cumulative distribution of DNNs between lost and persistent spines during baseline and repeated 2h MMS exposure. (a) 2h of MMS decreased the distances between lost and persistent spines compared to baseline, *p = 0.0108; Kolmogorov–Smirnov test. (b) two 2h MMS exposures decreased the distances between lost and persistent spines compared to baseline, *p = 0.0155; Kolmogorov–Smirnov test. (c) four 2h MMS exposures did not significantly affect the distances between lost and persistent spines compared to baseline, NS p = 0.7253; Kolmogorov–Smirnov test. (d) seven 2h MMS exposures did not significantly alter the distances between lost and persistent spines compared to baseline, NS p = 0.7598; Kolmogorov–Smirnov test. n = 4 mice; n dendrites: Table A.12. B2, baseline day 2, imaging day 2; B4 baseline day 4, imaging day 4; B7, baseline day 7, imaging day 7; S1, stress day 1, imaging day 8; S2, stress day 2, imaging day 9; S4, stress day 4, imaging day 11; S7, stress day 7, imaging day 14. Grey, baseline; red, stress.

## 4.2 Circulating corticosterone levels as a readout of stress

As an added measure to the highly internally controlled imaging experiments, I measured circulating corticosterone levels as a readout for the level of stress response in each animal.
To determine corticosterone levels, I collected tail blood from each animal 30 minutes and 90 minutes after the start of stress as described in section 3.11.2. Since corticosterone levels remained elevated between 30 minutes and 90 minutes after the exposure, indicating that mice remained stressed throughout the exposure, I averaged the two values for each mouse to obtain one readout of corticosterone per animal per measured time point.
In the acutely stressed cohort, MMS exposure resulted in increased corticosterone levels on the same day of exposure (Figure 4.28a, day 8, **p = 0.0031; Friedman test followed by post hoc Dunn's multiple comparison test, n = 5) when compared to baseline levels of corticosterone (Figure 4.28a, day 1, n = 5) in the same mice. By the last day of recovery, stress levels were reduced to baseline levels (Figure 4.28a, day 14, NS; Friedman test followed by post hoc Dunn's multiple comparison test, n = 5).
In the repeatedly stressed cohort, the first MMS exposure resulted in increased corticosterone, (Figure 4.28b, day 8, **p = 0.0027; Friedman test followed by post hoc Dunn's multiple comparison test, n = 8) when compared to baseline levels of corticosterone (Figure 4.28b, day 1, n = 8) in the same mice, thus confirming the result of the acutely stressed cohort. Mice remained responsive to the exposure as evidenced by the levels of corticosterone on the last day of stress which were still elevated (Figure 4.28b, day 14, *p = 0.0323; Friedman test followed by post hoc Dunn's multiple comparison test, n = 8), despite the cohort having been exposed to MMS 6 times prior.

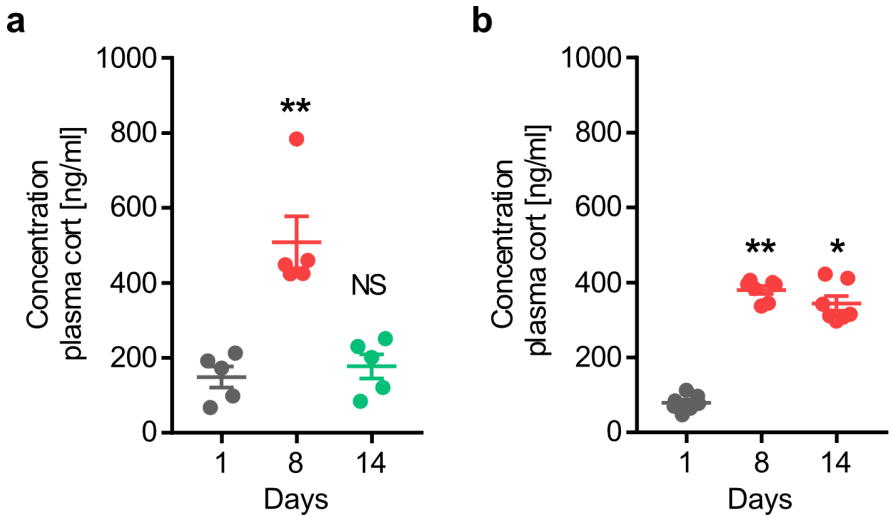


**Figure 4.28:** MMS increases levels of circulating corticosterone. (a) One exposure of 2h MMS significantly increased corticosterone levels: Day 8 **p = 0.0031, Friedman test with post hoc Dunn's multiple comparisons test. Following 6 days of recovery, corticosterone levels were not different to baseline: day 14, NS p = 0.2277, Friedman test with post hoc Dunn's multiple comparisons test. (b) One exposure of 2h MMS significantly increased corticosterone levels: Day 8 **p = 0.0027, Friedman test with post hoc Dunn's multiple comparisons test. After 7 repeated exposures, corticosterone still increased with stress exposure: Day 14 *p = 0.0323, Friedman test with post hoc Dunn's multiple comparisons test. Acute MMS, n = 5 mice; Repeated MMS, n = 8 mice. Data presented as mean ± s.e.m. Grey, baseline; red, stress; green, recovery.

## 4.3 Hippocampal dependent learning and memory

In order to study the effects of stress on dorsal hippocampal behaviour, I used the MWM learning task in 3 groups of mice.

Three cohorts of C57BL/6N mice were used to determine the effects of stress on dorsal hippocampal dependent learning and memory. The MWM task was used as described in section 3.12 on

1. a control group (n = 10) which underwent no stress.
2. an acute stress group (n = 10) in which mice were stressed with 2h of MMS. Learning commenced on the first day of the MWM task 1h after the end of stress.
3. a repeatedly stress group (n = 10) in which mice were stressed with 2h of MMS for 7 days, matching the learning period of the MWM. Learning commenced every day of the MWM learning period 1h after the end of stress.

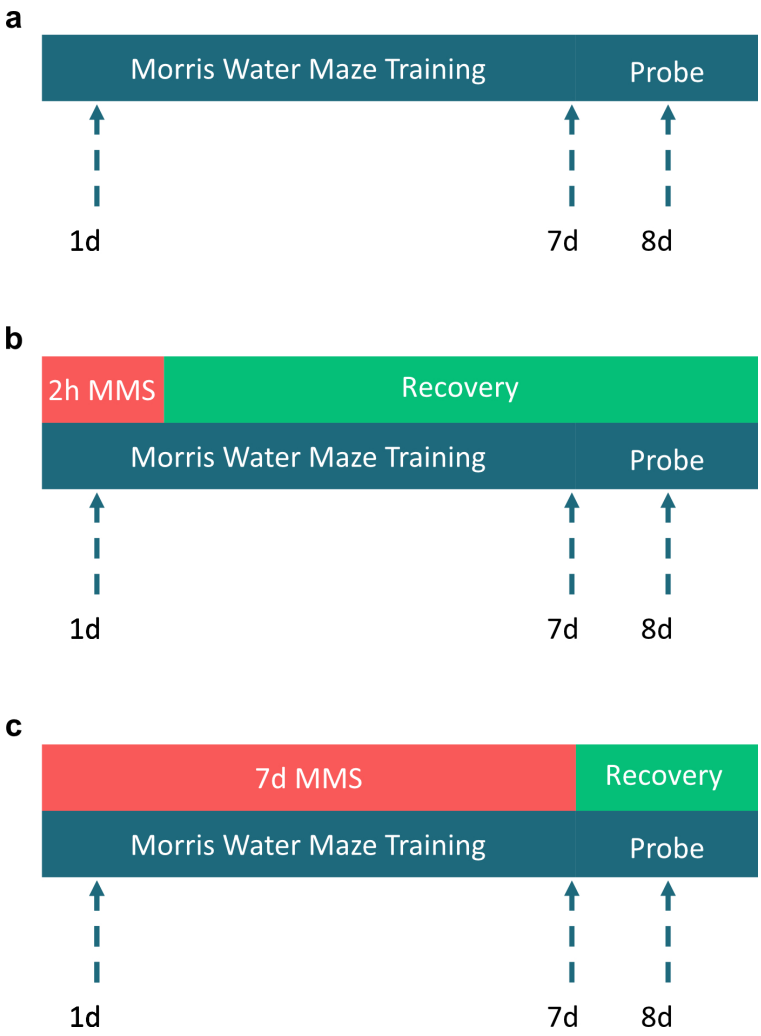


**Figure 4.29:** MWM cohorts to determine effect of acute and repeated MMS on hippocampal learning and memory (a) Control mice were unstressed (n = 10). (b) Acute 2h MMS mice were stressed once on the morning before the start of MWM training. (c) Repeated 2h MMS mice were stressed once every morning before the start of MWM training, totalling 7 stress exposures in parallel to the 7 training days. In all cases involving stress, MWM training began one hour after the end of stress.

MWM measures can be considered as both a readout of the ability to learn as well as of the extent of spatial memory recall. Here I will discuss these two aspects in turn.

### 4.3.1 Spatial Learning

The unstressed control cohort learned to navigate to the platform as expected over the 7 day learning period. This is demonstrated by the decrease in latency to platform entry with an increase in learning days (Figure 4.30, grey trace, ****$p < 0.0001$, 2way-ANOVA). Both stress groups demonstrated an impairment in learning as evidenced by their significantly higher

latencies compared to the control group. Mice stressed only once with 2h MMS showed a severe impairment in learning (Figure 4.30a, acute 2h MMS followed by recovery compared to baseline, **** p< 0.0001; 2-way ANOVA with post hoc Sidak's multiple comparisons test). Surprisingly however, the repeatedly stressed cohort had significantly lower latencies which were only slightly higher in comparison to controls (Figure 4.30b, repeated stress compared to baseline, *p < 0.05; 2-way ANOVA with post hoc Sidak's multiple comparisons test).

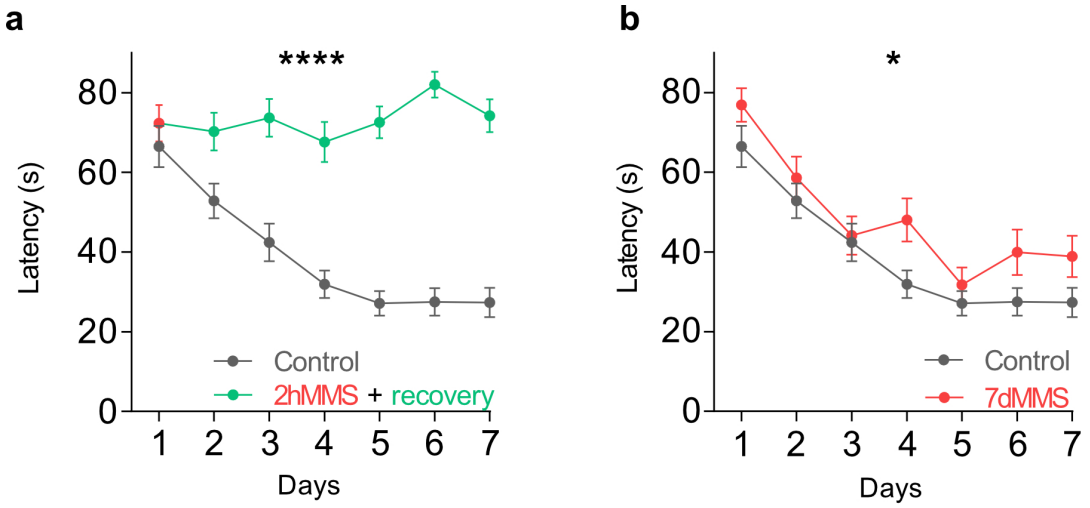


**Figure 4.30:** MMS impairs MWM learning. (a) One exposure of 2h MMS induced a significant impairment in learning which did not recover. ****p > 0.0001, 2 way ANOVA, Sidak's multiple comparisons test. (b) MMS exposure every day before learning induced a significant impairment in learning compared to baseline, although mice were still able to learn the task. *p <0.05, 2 way ANOVA, Sidak's multiple comparisons test. n = 10 mice per group. Data presented as mean ± s.e.m. Grey, baseline; red, stress; green, recovery.

In order to gain further insight into the learning approach of each group, I conducted a swim strategy analysis (refer to section 3.12 for a detailed description of strategies). Garthe et al. (2009) have previously demonstrated that mice adopt a progressive approach to finding the platform, starting at no learning (designated thigmotaxis) and progressing to direct swimming. I have given each of the strategies a number as indicated in Figure 4.31a with 1 being the least direct (i.e. thigmotaxis) and 7 being the most direct strategy and determined the average strategy per 4 trials of each learning day. Modifications to the original algorithm are as outlined in section 3.12. Control mice showed a progression in swim strategies (Figure 4.31b) over learning days and learned within the first four trials of training day 1 that they needed to find the platform. This was clear from the lack of thigmotaxis observed.

Mice stressed acutely with 2h MMS showed the opposite effect: most individuals continued to thigmotax throughout the learning period, with only a few learning the task, albeit at a slower rate of progression than control mice (Figure 4.31c).

Mice stressed repeatedly with 2h MMS fit into the middle of the spectrum in strategy progression

compared to control and acutely stressed groups. This was clearly seen in the adoption of lower strategies compared to the control group but less thigmotaxis in comparison to the acutely stressed group (Figure 4.31d).

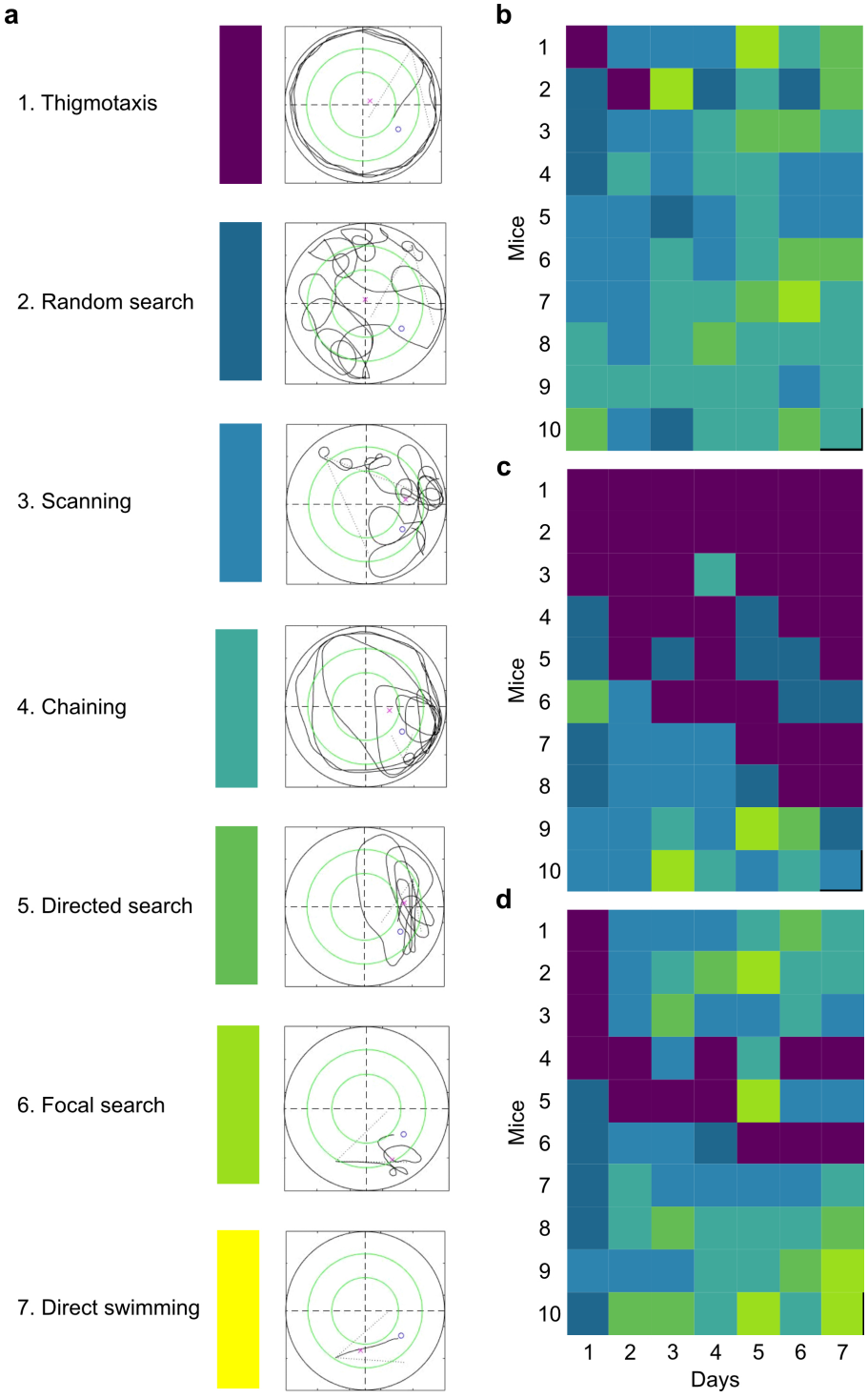


**Figure 4.31:** Acute and repeated MMS result in use of less direct swim strategies. (a) LEFT: Swim strategies. Each strategy was assigned a number from 1 to 7, with 1 being the least direct and 7 being the most direct strategy to reach the platform. MIDDLE: Colour code for each swim strategy. RIGHT: Example trace of each strategy. (b) Strategies employed by control mice. (c) Strategies employed by mice exposed to acute 2h MMS. (d) Strategies employed by mice stressed repeatedly, every day before learning. Each square in the heat maps of b-d represents the average strategy used per 4 trials of each training day.

### 4.3.2 Spatial Memory Recall

On the 8th day of the MWM, the platform was removed from the maze and the time spent in each quadrant (Figure 4.32) as well as the number of virtual platform crosses (Figure 4.33) was measured.

Control mice were able to distinguish the target quadrant from all other quadrants, as they spent a higher fraction of time in the target quadrant than all other quadrants (Figure 4.32a, target quadrant versus: SW ****p < 0.0001, paired t-test; SE **p = 0.0037, paired t-test; NW **p = 0.0039, paired t-test). Acutely stressed mice spent the most time in the start quadrant and could not distinguish the target quadrant from the remaining three quadrants (Figure 4.32b, target quadrant versus: SW NS, paired t-test; SE NS, paired t-test; NW *p = 0.0385, paired t-test). Mice stressed repeatedly were able to distinguish the quadrant furthest from the target quadrant, but did not spend significantly more time in the target quadrant compared to adjacent quadrants (Figure 4.32c, target quadrant versus: SW **p = 0.0017, paired t-test; SE **p NS, paired t-test; NW NS, paired t-test).

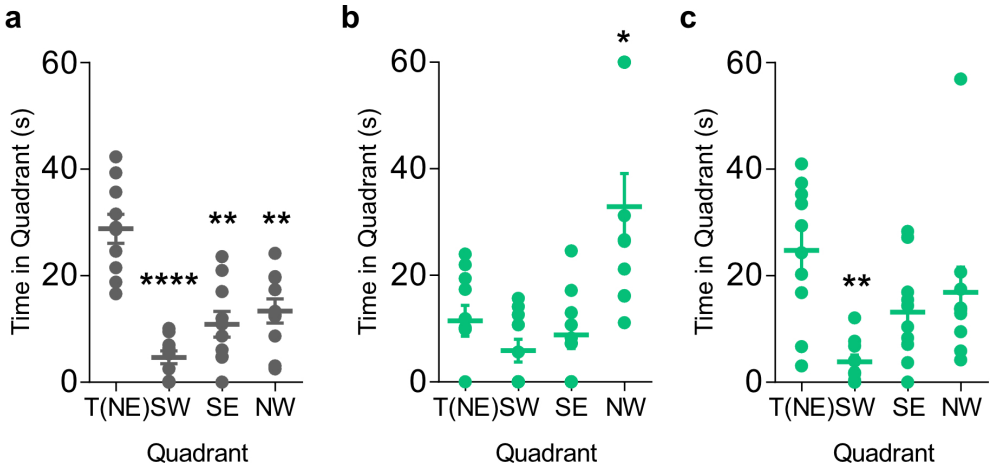


**Figure 4.32:** Acute and repeated MMS result in less time spent in the target quadrant during a MWM probe test. (a) Control mice spent more time in the target quadrant compared to the remaining quadrants. Target quadrant versus: SW ****p < 0.0001, paired t-test; SE **p = 0.0037, paired t-test; NW **p = 0.0039, paired t-test (b) Acutely stressed mice spent more time in the start quadrant and failed to discriminate between the remaining 3 quadrants. Target quadrant versus: SW NS p = 0.1153, paired t-test; SE NS p = 0.2481, paired t-test; NW *p = 0.0385, paired t-test (c) Repeatedly stressed mice distinguished between the quadrant furthest from the target quadrant and did not distinguish between the target quadrant and its adjacent quadrants. Target quadrant versus: SW **p = 0.0017, paired t-test; SE NS p = 0.0699, paired t-test; NW NS p = 0.3473, paired t-test. All mice were unstressed on day 8, MWM probe day. T(NE): Target (north east) quadrant); SW: south west quadrant; SE: south east quadrant; NW: north west quadrant (start quadrant). n = 10 mice per group. Data presented as mean ± s.e.m. Grey, baseline; green, recovery.

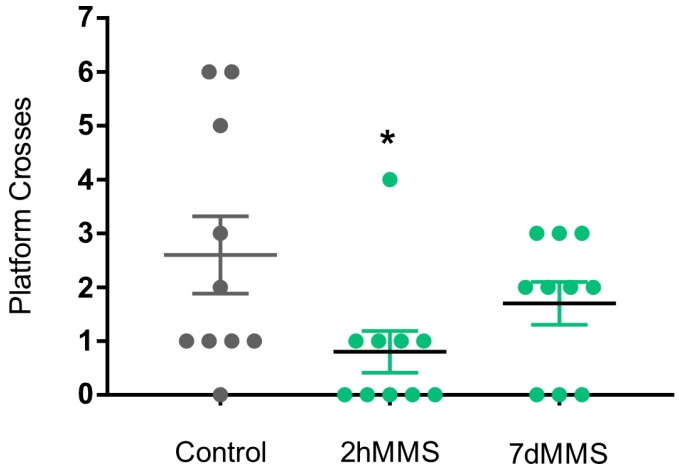


**Figure 4.33:** Acute 2h MMS exposure before learning resulted in fewer platform crosses at probe test. Control mice (grey) made the most platform crosses. Half of acutely stressed mice never crossed the platform area and those who did, made significantly fewer crosses than controls, *p = 0.0238; Mann-Whitney test. Mice stressed repeatedly did not make significantly fewer platform crosses than control mice, NS p = 0.6312, Mann-Whitney test. n = 10 mice per group. Data presented as mean ± s.e.m. Grey, baseline; green, recovery.

### 4.3.3 Memory recall of trace fear conditioning after stress exposure

To determine the effects of stress on hippocampal dependent memory of an already learned task, I used trace FC in two cohorts of mice.

The control cohort was not exposed to stress and the stress cohort was exposed to 5 days of repeated restraint stress for 2h/d, n = 10 mice per cohort.

The protocol (Figure 4.34) involved exposing both cohorts to a context for 3 minutes before administering tone shock pairings during conditioning. The conditioning context comprised a chamber with a square floor and metal grid placed on the floor. The chamber was scented with 70% EtOH in bedding below the grid. Walls were grey metal. A camera, dim light and a speaker were positioned at the top of the chamber and remained in fixed positions throughout the experiment and for all animals. After 3 minutes of undisturbed exploration time in the chamber, a 9kHz tone at 80dB was played for 20s followed by a 15s delay before a 1s shock of 0.7mA intensity was delivered. The tone-delay-shock pairings were repeated 5 times. Mice learned that a 15s delay preceded the onset of the shock and this learning has been shown (Misane et al. (2005)) to be dorsal hippocampal dependent. On the following day, mice were re-exposed to the chamber with all the same contextual cues and their freezing response was measured for 3 minutes.

After testing the ability of individual mice to learn and remember the trace FC task, I returned the control mice to their home cage for 5 days and the stress group were exposed to restraint stress for 2h/d for 5 consecutive days. Both cohorts were then re-exposed to the context in which they had been conditioned to the shock. The re-exposure served to determine the effect of stress on the acquired contextual memory as measured by freezing response.

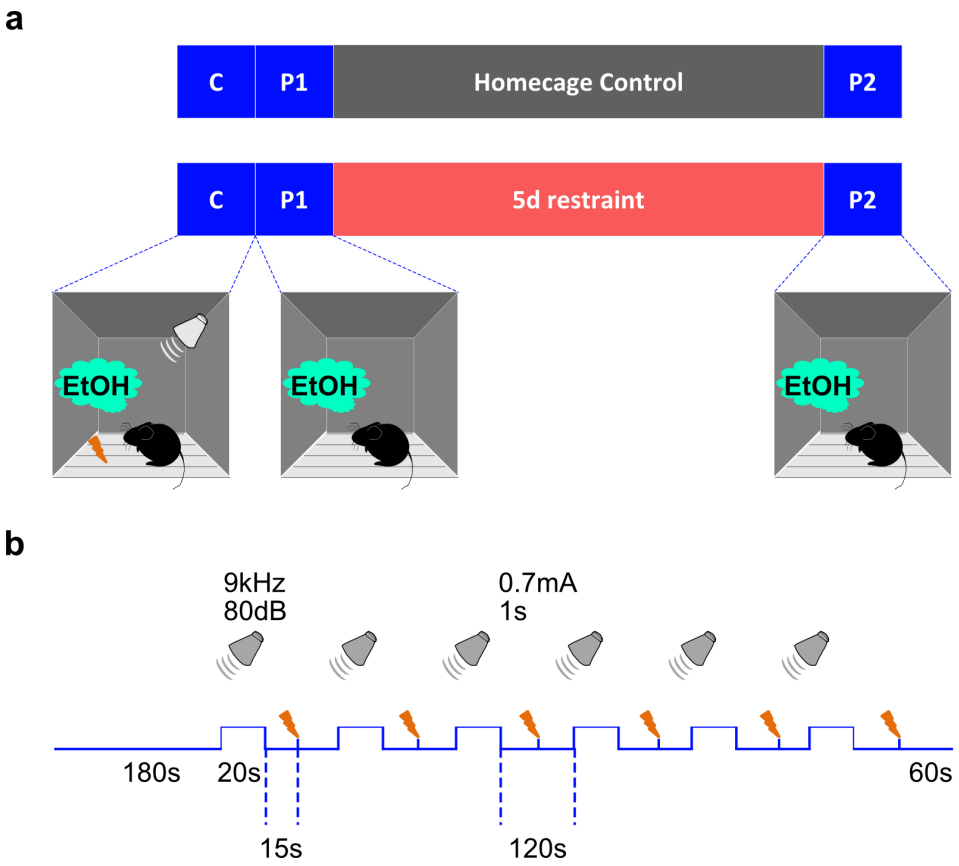


**Figure 4.34:** Pilot experiment determining stress effects on memory formed by trace FC. (a) 2 groups of WT mice were conditioned to tone-delay-shock pairing. Conditioning was the same between groups. Control mice were returned undisturbed to their home cages whilst stressed mice were exposed to 2h/d of restraint stress for 5 consecutive days. Both groups were then returned to the conditioning chamber and their freezing response measured for 3 minutes. (b) Trace FC protocol. Mice were allowed to explore the conditioning context for 3 minutes before a 9kHz, 80dB tone was played for 20s. 15s later a 0.7mA shock was administered via a metal grid for 1s duration. This was repeated 5 times with 120s between the end and start of each tone. After the last shock, mice were left in the chamber for 60s before being returned to their home cage. C, conditioning; P1, probe test 1; P2, probe test 2.

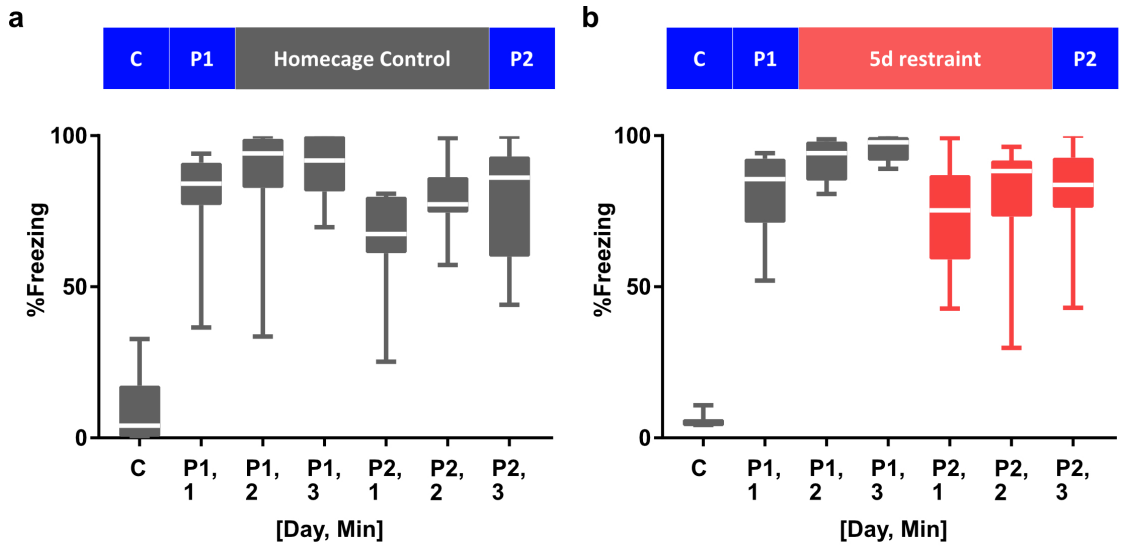


**Figure 4.35:** Repeated restraint does not impede memory of learned trace fear conditioning. (a) Mice were trace fear conditioned, placed back into their home cage for 5 days and then tested for their memory of the fear context. All mice learned to associate context with the shock and froze significantly more during the probe test minutes in comparison to the last minute of conditioning exploration. 5 days of´home cage housing post-learning neither strengthened nor weakened the memory of context since mice froze the same during the first and second probe. ****p < 0.0001; Friedman test; C compared to: P1,1 **p = 0.0056; P1,2 ****p < 0.0001; P1,3 ****p < 0.0001; C compared to: P2,1 NS p = 0.7230; P2,2 *p = 0.0312; P2,1 **p = 0.0017; post hoc Dunn's multiple comparisons test. Probe tests 1 and 2 compared for minutes 1 NS p = 0.1265, 2 NS p = 0.0505 and 3, NS p = 0.0695, Dunn's multiple comparisons test. ****p < 0.0001, Friedman test. (b) Mice were trace fear conditioned, stressed by restraint for 2h/d for 5 days and then tested for their memory of the fear context. All mice learned to associate context with the shock and froze significantly more during the probe test in comparison to the last minute of conditioning exploration. 5 days of´repeated restraint stress post-learning neither strengthened nor weakened the memory of context since mice froze the same during the first and second probe. ****p < 0.0001; Friedman test; C compared to: P1,1 NS p = 0.0580; P1,2 ****p < 0.0001; P1,3 ****p < 0.0001; C compared to: P2,1 NS p = 0.2306; P2,2 **p = 0.0080; P2,1 **p = 0.0021; post hoc Dunn's multiple comparisons test. Probe tests 1 and 2 compared for minutes 1 NS p > 0.9999, 2 NS p = 0.2828 and 3 NS p = 0.0505, Dunn's multiple comparisons test. ***p = 0.0003 Friedman test. C, conditioning minute 3; P1,1, Probe test 1 minute 1; P1,2, Probe test 1 minute 2; P1,3, Probe test 1 minute 3; P2,1 Probe test 2 minute 1; P2,2, Probe test 2 minute 2; P2,3 Probe test 2 minute 3. n = 10 mice per group. Data represented as min to max and average. Grey, baseline; red, stress.

Unsurprisingly, all mice from both cohorts displayed a freezing response at the first probe test one day after conditioning (Figure 4.35). However, stressed mice did not show any distinction to control mice after 5 days of repeated restraint stress at 2h/d, as seen by their freezing levels at the second probe test (Figure 4.35b, red bars), which were not significantly different to the percentage time spent freezing at the first probe test (Probe tests 1 and 2 compared for minutes 1 NS p > 0.9999, 2 NS p = 0.2828 and 3 NS p = 0.0505, Dunn's multiple comparisons test).

CHAPTER 5

# DISCUSSION

In this thesis I revealed that acute stress decreases spine formation. I further demonstrated an increase in survival of spines born after acute stress exposure when followed by recovery.
Moreover, I showed that the observed decrease in spine formation continues with repeated stress exposure, further associated with increased destabilisation of newborn spines.
In this context of dynamic structural changes, I elucidated stress effects on clustering of different spine populations and showed that stress decreases the distance between new spines and persistent spines. I also demonstrated that stress results in clustered spines loss which I showed to occur further from new spines.
Behaviourally, I demonstrated that acute stress severely impairs subsequent hippocampal dependent spatial learning whereas repeated exposure to stress before learning results in a comparatively smaller impairment.

In this chapter I will discuss my results in the context of published research.

## 5.1 Structural Synaptic Plasticity

In accordance with the aims of this thesis, I first tested whether structural dynamics in basal dendrites of dorsal hippocampal CA1 were affected by stress. For this purpose, *in vivo* 2-photon time lapse imaging was implemented in adult Thy1GFPm heterozygous male mice implanted with imaging cannulas.

### 5.1.1 MMS decreases the density of newborn spines

On a synaptic level, I aimed to discern any changes in spine dynamics which might occur with time, stress exposure and recovery.

First, I determined spine density under basal, stress and recovery conditions for populations of all, newborn and persistent spines, as outlined in section 4.1.
When all spines were considered as one population, no difference in spine density was detected after both acute and repeated MMS exposure (Figure 4.4a, c).
One study by Diamond et al. (2006) demonstrated an increase in stubby spines in basal dendrites of dCA1 induced by one day of MWM training in rats. This increase was not observed with 30 minutes of predator exposure before training. My data expands on this by showing a positive reduction in newborn spine density observed with one 2h MMS exposure as well as with repeated exposure. Stress has been reported to decrease spine density of CA1 apical dendrites (Shors et al. (2001, 2004)) and similar effects have been observed in basal dendrites but at smaller scales (Shors et al. (2004)). Given that newborn spines are a small fraction (around 10%) of all spines, if a drop in density is observed at the level of all spines, it is indeed expected to be a small effect.

In summary, the density of newborn spines was decreased after one stress exposure and was recoverable. Newborn spine density continued to display a decrease with up to four repeated MMS exposures.

### 5.1.2 Spine gain decreases after stress exposure and spine loss increases after multiple stress exposures

Next, I compared the fraction of spines gained and lost across successive times points of stress and equivalent baseline periods.
The data (Figures 4.5 and 4.6) points to a 2 phase progression in which first a reduction in gain is observed, followed by an increase in loss, the latter of which only becomes apparent after four stress exposures, as elucidated by the repeated stress cohort (Figures 4.6e and 4.6f). This effect was not simply due to time since it was not observed at the same time point of recovery in the acute MMS exposure cohort (Figures 4.6b-c). Moreover, data between acute and repeatedly stressed mice was consistent between cohorts, evidenced by equivalent reduction in gain after one stress exposure (Figures 4.5a and 4.5d, days 1-2 compared to days 7-8, acute 2h MMS cohort, ****$p < 0.0001$, repeated 2h MMS cohort, ***$p = 0.0001$; 1-way ANOVA, Dunn's multiple comparisons test) and no significant difference in loss after one stress exposure (Figures 4.6a and 4.6d, days 1-2 compared to days 7-8).
Although hippocampal spine loss in the CA1 has been studied under stress and observed mostly in apical dendrites (Maras et al. (2014); Patel et al. (2018)), no *in vivo* hippocampal data exists to examine stress effects on gain which, by definition, involves the addition of newborn spines. The data reported here showing a reduction in gain thus demonstrates for the first time a more passive mechanism of change which occurs prior to the active loss of spines.
Chen et al. (2008) demonstrated a causal role of CRH-mediated activation of corticotropin releasing factor receptor type 1 (CRFR1) in increasing the rate of spine elimination whilst spine

formation was unaffected in the CA3 after MMS exposure. This report supports differential mechanisms of spine formation and elimination which may act independently. I observed a significant increase in loss after four repeated stress exposures and a reduction in gain in the time leading up to this. This implies that the spines being lost are more likely 'older' or more mature synapses. Since CRH is abundantly expressed in interneurons of the CA1 and CRFR1 is expressed in spine heads, it is reasonable to assume that new spines are less responsive to potential effects of CRH because they may lack CRFR1 whilst still developing.

Few longitudinal *in vivo* studies on structural plasticity in the brain have been reported. One very recent study by Moda-Sava et al. (2019) examined the effects of chronic corticosterone exposure on structural synaptic dynamics *in vivo* in the PFC. They reported a decrease in spine formation and increase in spine elimination after 21 days of chronic exposure, with no intermediate dynamics recorded.
Chen et al. (2018) investigated the effects of different durations of restraint stress (2 days, 7 days and 14 days) on spine dynamics in the barrel cortex by *in vivo* 2-photon optical imaging. They reported no difference in spine formation after 7 days of repeated restraint stress compared to baseline but a robust increase in spine elimination which was not reduced to baseline levels after 2 days of recovery. No data on gain and loss at earlier time points of stress was reported, however, their observations match my hippocampal formation and elimination data after 7 days of repeated MMS.
Taken together, although these studies differ in brain region, duration and type of stress exposure, it is nonetheless interesting to observe similar dynamics in gain reduction and loss increase. Without intermittent imaging data from the reported experiments, it is not possible to directly compare the time courses of gain and loss to my own observation of a decrease in gain before the onset of loss, but the fact that we observe similar changes with repeated exposures suggests similar mechanisms and effects of elevated corticosterone on PFC, barrel cortex and CA1 structural dynamics.

Therefore my data demonstrates an initial reduction in gain which is evident within a matter of hours after one MMS exposure and continues for up to four MMS exposures. Increased elimination on the other hand only became apparent after four repeated MMS exposures. This data is in line with reports of formation and elimination in the PFC and barrel cortex.

### 5.1.3 MMS decreases spine survival in an exposure dependent and population specific manner

I next went on to investigate the survival of all, persistent and newborn spines.
Spine survival in basal dendrites of the CA1 has been shown to span 1-2 weeks under baseline conditions (Attardo et al. (2015)). In the cortex, stress has been shown to alter structural dynamics (Moda-Sava et al. (2019); Chen et al. (2018)), but survival of specific populations has so far not

been reported. As such, it is unknown how spine survival in the CA1 is affected by stress.
Here I have shown that all spines which exist at the first day of stress survive more after recovery (Figures 4.7a, ***p = 0.0007; 2-way ANOVA) and less with repeated stress when compared to the same span of time under baseline conditions (Figure 4.7e, **p = 0.0092; 2-way ANOVA).
By capitalising on the strength of *in vivo* time lapse imaging and separating all spines into persistent and newborn populations, it is evident that the two populations behave differently under acute and repeated stress conditions.
Persistent spines which exist at the first imaging time point after an acute 2h MMS exposure do not survive significantly differently (Figure 4.7b) in the recovery days following exposure. Since the days following exposure (days 9-14) are in fact recovery days, it is interesting to note the opposite effect with repeated stress exposure (Figure 4.7f, ***p = 0.0008; 2-way ANOVA). In the case of repeated MMS, persistent spines which exist after the first stress, instead demonstrate a reduction in survival over the following days in which they are repeatedly exposed to stress before each imaging session. Repeated stress thus decreases the survival of persistent spines, whereas an acute stress exposure does not affect their survival.
Interestingly, the newborn spine population in both acute and repeated stress cohorts was strongly affected. Spines born in the first few hours (1-6h) after an acute stress exposure and then allowed to recover in the 6 days to follow, showed an increased survival which was significantly different to baseline survival (Figure 4.7 c, ***p = 0.0009; 2-way ANOVA). In contrast, spines born after a 2h MMS stress exposure and then repeatedly exposed to stress thereafter, demonstrated a strong decrease in survival (Figure 4.7g, ****p < 0.0001; 2-way ANOVA) in comparison to baseline.
To further ascertain whether this was specific to the populations born after an initial exposure or whether it also affected spines born later, I also checked the survival of spines born on the first day of recovery for the acutely stressed cohort and the second day of stress for the repeatedly stressed cohort. Spines born in recovery showed no difference in survival compared to baseline newborn spine survival over an equivalent interval (Figure 4.7d; 2-way ANOVA). In contrast, spines born after the second stress exposure continued to exhibit a decrease in survival with continued exposure (Figure 4.7h, *p = 0.0353; 2-way ANOVA).
Of the two *in vivo* studies (Moda-Sava et al. (2019); Chen et al. (2018)) which consider stress effects on structural dynamics (albeit in the cortex), both implement only two imaging time points in relation to stress (one before and one after stress), thus lacking the insight into dynamics *during* stress. The same is true for recovery, with just one imaging time point before and one after recovery.
In contrast, I was able to follow a specific population of spines through stress and recovery periods to determine the effects of stress and recovery on the survival of these populations.
The increase in survival of spines born in the hours after acute stress exposure and then allowed to recover is an interesting and unexpected observation. All other readouts thus far were affected only on the first day of stress exposure, but here we see a lasting effect throughout recovery on

this specific population born in the 1-6h after stress. It has been demonstrated that newborn spines are important for encoding of new memories (Rogerson et al. (2014); Xu et al. (2009); Fu et al. (2012); De Roo et al. (2008a); Yang et al. (2009)). Here we see a reduction in gain of this important population of spines, but an increase in survival of those which *are* born. This population may well contribute to the encoding of the stress event. I will revisit this result in a later discussion in relation to the behavioural outcome in section 5.2.

### 5.1.4 MMS increases the distance between newborn spines and decreases the distance between newborn and persistent spines.

Given that formation and elimination dynamics were altered by stress, I was also interested in whether the spines being formed or lost after stress and recovery were more or less spatially clustered in relation to baseline.

To this aim, I first examined the distances between newborn spines by considering both median DNNs per dendrite as well as taking into account all DNNs.

Acute exposure to MMS did not alter the distance between newborn spines on a dendritic level (Figure 4.8a NS p = 0.1731; Wilcoxon matched pair signed rank test and Figure 4.9a NS p = 0.0628; Wilcoxon matched pair signed rank test) but a significant increase at the level of all DNNs was observed (Figure 4.18a ****p < 0.0001; Kolmogorov-Smirnov test, and Figure 4.19a ****p < 0.0001; Kolmogorov-Smirnov test).

Both recovery and further repeated stress exposure did not result in further changes in DNNs between newborn spines on a dendritic level (Figure 4.8b-d B2 compared to R1 NS p = 0.3286; Wilcoxon matched pair signed rank test; B4 compared to R3 NS p = 0.2680; Wilcoxon matched pair signed rank test and B7 compared to R6 NS, p = 0.2043; Wilcoxon matched pairs signed rank test; and Figure 4.9b-d B2 compared to S2 NS p = 0.2162; Wilcoxon matched pairs signed rank test; B4 compared to S4 NS p = 0.9607; Wilcoxon matched pairs signed rank test and B7 compared to S7 NS p = 0.5291; Wilcoxon matched pairs signed rank test). A consideration of all DNNs however, uncovered a decrease in the distance between newborn spines after the first day of recovery (Figure 4.18b ***p = 0.0001; Kolmogorov-Smirnov test) and a second stress exposure still demonstrated an increase in distance between newborn spines (Figure 4.19b, ****p < 0.0001). Whilst the increase in DNN between new spines could be motivated by the decrease in newborn spine density at this time point (Figure 4.4b, d), the decrease in DNN between new spines with recovery suggests the involvement of additional mechanisms (given that the density of new spines is not significantly different in recovery compared to baseline (Figure 4.4b).

Taken together, this data suggests a recovery mechanism favouring the closer proximity of newborn spines than that observed under normal conditions. Fu et al. (2012) demonstrated increased clustering of newborn spines with motor learning and the subsequent stabilisation of these clusters with prolonged learning. It is interesting that we see the opposite effect with stress in the hippocampus.

DNNs between newborn and persistent spines decreased with one stress exposure in comparison to baseline (Figure 4.10a ****p < 0.0001; Wilcoxon matched pairs signed rank test and Figure 4.11a **p = 0.0049; Wilcoxon matched pairs signed rank test). This observation was made at a dendritic level, but not at the level of all spines.
Recovery had no effect on the distances between newborn and persistent spines on both a dendritic (Figure 4.10b-d B2 compared to R1 NS p = 0.7561; Wilcoxon signed rank test; B4 compared to R3 NS p = 0.8306; Wilcoxon signed rank test and B7 compared to R6 NS p = 0.0900; Wilcoxon signed rank test) and spine (Figure 4.21b-d B2 compared to R1 NS p = 0.3478; Kolmogorov-Smirnov test; B4 compared to R3 NS p = 0.9474; Kolmogorov-Smirnov test and B7 compared to R6 NS p = 0.6324; Kolmogorov-Smirnov test) level.
After two stress exposures, median DNNs per dendrite decreased compared to baseline (Figure 4.11b ***p = 0.0001; Wilcoxon signed rank test), as did all DNNs between newborn and persistent spines (Figure 4.21b **p = 0.0058; Kolmogorov-Smirnov test) compared to baseline. Four stress exposures still demonstrated a decrease on a dendritic (Figure 4.11c *p = 0.01; Wilcoxon signed rank test) but not all spine (Figure 4.21b NS p = 0.0.6791; Kolmogorov-Smirnov test) level.

Experience dependent synaptic remodeling is dependent upon the biophysical and anatomical properties of the dendrites on which they reside. Dendrites propagate and integrate synaptic activity onto the soma and, as such, support compartmentalised plasticity (Branco and Häusser (2010)). The clustered plasticity hypothesis posits spatially confined synaptic remodeling, or clusters, which have been proposed to encode for memories related closely in time or space in the context of overlapping neuronal populations (Kastellakis et al. (2015)). The biological relevance of clustered activity is supported by cortical data demonstrating the involvement of clustered spine formation in learning and experience dependent plasticity (Fu et al. (2012); Gökçe et al. (2016)). Interestingly, I have shown here that stress effects in the hippocampus produce the opposite effect to learning in the cortex - namely a decrease in spatial clustering of new spines and increase in clustering of new spines to persistent spines. I will discuss this result in more detail in the context of stress effects on spatial learning in section 5.2.

### 5.1.5 Spines are lost in clusters with repeated stress

On top of investigating the effects of stress and recovery on newborn spine proximity to newborn and persistent spines, I aimed to determine whether spine loss was more or less clustered during stress compared to the same durations of baseline.
To address this question, I measured distances between lost spines, using location data from the previous time point relative to the time point of interest.
We have already observed that the amount of loss that occurs with stress is not different between baseline and stress within 24h periods (Figure 4.6a, Figure 4.6d). Further, loss was neither more nor less clustered compared to baseline after acute stress exposure (Figures 4.12a NS p = 0.4052;

Wilcoxon matched pairs signed rank test and Figure 4.13a, NS p = 0.7507; Wilcoxon matched pairs signed rank test).
The same held true for all time points of recovery (Figure 4.12b-d, B2 compared to R1 NS p = 0.0946; Wilcoxon matched pairs signed rank test; B4 compared to R3 NS p = 0.6011; Wilcoxon matched pairs signed rank test and B7 compared to R6 NS p = 0.0844), except at the level of all spines (Figure 4.22d **p = 0.0076; Kolmogorov-Smirnov test).
Two 2h MMS exposures also had no effect on the distances between lost spines (Figure 4.13b NS p = 0.8231; Wilcoxon matched pairs signed rank test and Figure 4.23b NS p = 0.8386; Kolmogorov-Smirnov test). However, loss was observed to be more clustered after 4 stress exposures (Figure 4.23c *p = 0.0197; Kolmogorov-Smirnov test), corresponding to the time point of increased fraction of loss compared to baseline. Since this effect is not observed when normalising by density (Figure 4.13c NS p = 0.1047; Wilcoxon matched pairs signed rank test), it may be attributed to the increase in spine elimination.
Since the previous imaging time point is 2 days prior, there is a greater difference in spine 'age' within the population of spines born over 48h (days 2-4 and 9-11) than there is for the population of spines born over 24h (days 1-2, 7-8 and 8-9). We have also observed that during stress, gain decreases (days 2-4 compared to 9-11, Figure 4.5e, **p = 0.0022; Wilcoxon matched pairs signed rank test), thus making the population of spines which are lost in this period potentially 'older' compared to the baseline population.
Spine ages become more mixed the longer the duration between imaging time points, thus making the last 72h period the one in which ages are most variable. This may also be why spines do not cluster more (or less) at days 11-14 compared to baseline (Figure 4.13d NS p = 0.8809; Wilcoxon matched pairs signed rank test and Figure 4.23d NS p = 0.0887; Kolmogorov-Smirnov test). Of course, it may well be that some habituation effect occurs after repeated exposure and that this is reflected in the structural dynamics, but we cannot state this definitively.
The increase in clustered loss is suggestive of a local regulatory mechanism. Evidence in the cortex suggests spine competition for limited resources such as ß-catenin, an intra-cellular binding partner forming part of the cadherin-catenin complex which is crucial for synapse formation and plasticity (Bian et al. (2015)). Reduced levels of ß-catenin after chronic stress, such as was demonstrated in the cortex (Teo et al. (2018); Chen et al. (2012c)), would account for increased competition and could explain clustered regions with low levels that would enable clustered loss. Both Moda-Sava et al. (2019) and Chen et al. (2018) demonstrated an increase in clustered loss after exposure to chronic corticosterone and repeated restraint stress respectively, drawing yet another parallel between cortical and hippocampal CA1 structural effects of stress.

### 5.1.6 Spines are lost further away from newborn neighbours after MMS exposure

I examined yet another level of complexity by considering the proximity of lost spines to newborn spines.

A single exposure to 2h MMS did not change the distance between lost and newborn spines on a dendritic level (Figure 4.14a NS p = 0.0993; Wilcoxon matched pairs signed rank test; Figure 4.15a NS p = 0.1768; Wilcoxon matched pairs signed rank test) but resulted in an increase in DNNs at the level of all spines (Figure 4.24a ****p < 0.0001; Kolmogorov-Smirnov test and Figure 4.25a ***p = 0.0006; Kolmogorov-Smirnov test). An analysis of all lost to newborn DNNs uncovered a continuation of this effect after two (Figure 4.25b *p = 0.0239; Kolmogorov-Smirnov test) stress exposures. The closest observation to this in the literature was reported in the motor cortex where spines which were further from newly formed clusters were preferentially pruned (Fu et al. (2012)). Although I am not comparing spine loss to newborn clusters, I would speculate that the underlying mechanisms driven by scaffolding protein availability are similar between new spines and clusters of new spines. I will revisit this concept in a later summary of all clustering observations within the context of literature in section 5.1.8.

### 5.1.7 Spines are lost in closer proximity to persistent spines after 2 stress exposures

In the repeated stress cohort of mice, one (Figure 4.27a *p = 0.0108; Kolmogorov-Smirnov test) and two (Figure 4.27b *p = 0.0155; Kolmogorov-Smirnov test) stress exposures were observed to decrease the distance between lost and persistent spines, that is to say that spines were being lost closer to persistent spines after stress than during baseline. The acutely stressed cohort did not display a decrease in distance between lost and persistent spines after exposure (Figure 4.26a NS 0.8470; Kolmogorov-Smirnov test). Since the effect is small, this could simply be due to a difference between the two cohorts of mice.

No effect on distances between lost and persistent spines was observed during recovery (Figure 4.16b-d B2 compared to R1 NS p = 0.4848; Wilcoxon matched pairs signed rank test; B4 compared to R3 NS 0.5577; Wilcoxon matched pairs signed rank test; B7 compared to R6 NS p = 0.3193; Wilcoxon matched pairs signed rank test) at a dendritic level, but increased 6 days of recovery increased DNNs between lost and persistent spines Figure 4.26d B7 compared to R6 *p = 0.0455; Kolmogorov-Smirnov test).

### 5.1.8 Clustering summary

Clustering is a complex and highly regulated cellular mechanism which reflects, amongst others, how spine populations may potentially interact with each other due to their proximity and allow for processes such as non-linear summation of synaptic inputs.

Stress has been demonstrated to decrease LTP and increase LTD (Alfarez and Krugers (2003); Artola et al. (2006); Kavushansky et al. (2006); Xu et al. (1997); Zhou et al. (2000); Chaouloff et al. (2007)). Conversely, LTP has been shown to increase in the CA1 as a result of learning (Whitlock et al. (2006); Nicoll (2017)). In slice, potentiated spines were stabilised and newborn spines were shown to form in close proximity (within 1.5µm) to potentiated spines. New spines in these 'hotspots' (De Roo et al. (2008b)) were more likely to become stabilised, whereas those born outside of these regions tended to be pruned, especially with consolidation of learning, suggesting the local spread of intracellular mechanisms along the dendrite concomitantly influencing multiple spines in unique dendritic sub-domains.

Accordingly, I observed

1. decreased survival of persistent spines with repeated stress (persistent spines are the more likely candidates for functional synapses and hence subjected to LTP and LTD mechanisms)

2. a concomitant decreased survival of newborn spines as well as an decreased distance of newborn to persistent spines

3. clustered spine elimination

In theory, there exists the possibility of measuring spine size as a proxy for LTP strength. However, given the resolution limit of our *in vivo* technique, we would be limited in accuracy.
Taken together, these observations support the hypothesis that stress effects, by decreasing synaptic LTP and increasing synaptic LTD (or in addition to these), might impact the intracellular mechanisms which coordinate spine dynamics at the level of dendritic sub-domains.

The larger the distance between newborn spines, the more likely the chance of each spine making distinct pre-synaptic contact. If this held true and they formed functional synapses, it would hold the prospect for non-linear integration of inputs from potentially different neurons thus enhancing the computational capability of the circuit. The increased stabilisation of spines born after acute stress and subsequent recovery support this notion. To confirm this would most likely require post hoc electron microscopy imaging of the same regions acquired *in vivo*. To add to the complexity, we do not know the effect of acute (or repeated) MMS on axonal boutons, which may affect the location of spine formation along the dendrite. Although a decrease in PV interneuron boutons in the cortex has been shown with 7 days of repeated restraint stress (Ng et al. (2018)), little is known about the effect of concurrent stressors on potential pre-synpatic inputs in the CA1. Thus, what appears to be an active avoidance between newborn spines may well be simply based on availability and system allocation of regulatory molecular signals which govern spinogenesis under stress, much of which is still largely unknown. Both 'avoidance' and clustering tendencies may depend on either post- and/or pre-synaptic regulatory mechanisms. Signalling molecules such as guanosine triphosphatases (GTPase) Ras and RhoA for instance, have been shown to spread from activated spines, supporting a promotion of clustered dynamics

(Nicoll (2017); Murakoshi et al. (2011)).
Taken together, clustered behaviour between the various spine populations after acute stress may facilitate robust encoding of stress exposure. Subsequent recovery and the additional associated increase in spine survival of the population of spines formed after stress, may further contribute towards the salience of this memory, reflective of typical strong encoding of post traumatic stress disorder (PTSD) events.
Repeated stress on the other hand demonstrates further homeostatic disruptions coupled with decreased survival of newborn spines. This continued remodeling and disruption of stability of spines formed after the first exposure may partly explain adaptive responses to repeated (same stress) exposures.

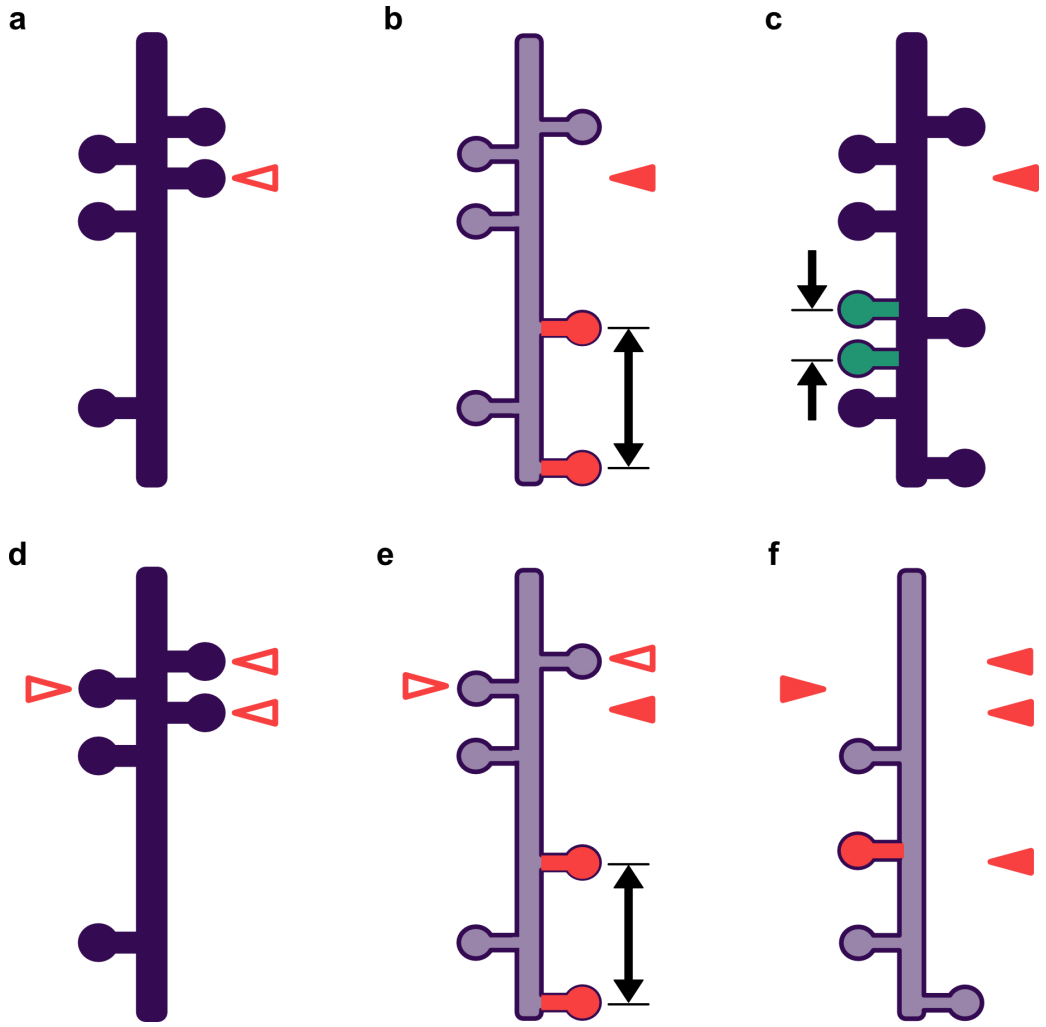


**Figure 5.1:** Summarised effects of stress and recovery on structural plasticity. (a, d) Under baseline conditions dendrites may be strongly potentiated. (b, e) after an acute exposure to MMS, few new spines are gained and are born further from each other (black arrows). Spines are lost further from newborn spines (red arrow). (c) New spines gained at 'b' are stabilised during recovery. New spines born at the first day of recovery are born closer to other new spines. (f) repeated stress reduces the fraction of newborn spines. Loss is clustered. Survival of spines born after the first exposure at 'e' is reduced. Purple, persistent spines; red, stress; green recovery; red arrows, lost spines.

### 5.1.9 Corticosterone levels increase in mice exposed to MMS

Although we fully expected MMS to activate the HPA axis response, I measured corticosterone levels to

1. confirm HPA axis response
2. determine whether recovery could rescue the expected response
3. determine whether repeatedly stressed animals remained responsive to the last exposure

In all imaged mice, I collected trunk blood at baseline and after the first and last stress exposure/last recovery, corresponding to days 1, 8 and 14 of the imaging experiments.
As was predicted, MMS exposure resulted in an increase in corticosterone levels measured from trunk blood. It is worth noting that corticosterone levels still increased at the 7th stress exposure for the repeated stress cohort, thus supporting no habituation to MMS, at least on a corticosterone level, over the duration of repeated exposure.
MMS exposure thus increased corticosterone levels both acutely and after repeated exposure and levels could be reduced to baseline with recovery.
Corticosterone increase during acute exposure was comparable to the original protocol (Chen et al. (2016)). I collected samples at 30 and 90 minutes after the start of MMS, whereas the original protocol reported collection 60 minutes after the onset of MMS.
To my knowledge there are no published reports of repeated MMS exposure.

## 5.2 MMS impairs hippocampal dependent learning and memory

With the aim of determining the behavioural aspects of acute MMS and recovery and repeated MMS, I implemented a 7 day MWM protocol on three separate groups of mice as described in section 4.3.
The MWM experiments conducted in this work have shown that

1. Acute MMS impairs hippocampal dependent MWM learning (Figure 4.30a).
2. Acute MMS results in the use of less direct spatial learning strategies in comparison to unstressed controls (Figure 4.31).
3. Acute MMS results in less time spent in the target quadrant (Figure 4.32b) and fewer platform crosses during a MWM probe test (Figure 4.33).
4. Repeated MMS impairs hippocampal dependent MWM learning (Figure4.30b).
5. Repeated MMS results in the use of less direct spatial learning strategies in comparison to unstressed controls (Figure 4.31).

6. Repeated MMS results in less time spent in the target quadrant (4.32c).

7. The acutely stressed cohort performed worse than the repeatedly stressed cohort during both learning and memory tasks (Figures 4.30, 4.31, 4.32 and 4.33).

The MWM is an incremental learning task requiring multiple trials over days for mice to learn. It is possible that hippocampal dependent tasks with different time dependencies may produce alternative results. I showed that repeated MMS exposure impairs learning and recall but the nature of the task does not allow us to distinguish whether this effect is on the encoding or consolidation phase of learning. However, given the incremental changes in synaptic dynamics I observed with stress, we can speculate that repeated MMS at least affects memory encoding and at most additionally impairs consolidation and recall. Chronic stress exposure in the weeks prior to MWM learning has also been shown to result in a slight impairment in learning (Conrad (2010)), further supporting the observation reported here.

Mechanistically, stress might influence memory encoding in multiple ways such as (but not limited to) decreased LTP and increased LTD. Here, I provided the first characterization of how stress influences spine dynamics in the hippocampus - the neural system playing a pivotal role in memory formation. In this respect, I have shown compelling evidence that repeated stress changes dCA1 synaptic dynamics by decreasing spine formation and survival, decreasing proximity of new spines to each other and increasing clustered spine elimination. To further understand how these results affect learning, we would require knowledge of synaptic dynamics in dCA1 in association with learning.

Little is known in this regard primarily due to inaccessibility of the region for *in vivo* tracking at the required micrometer level spatial resolution. In a recent study, Schmid and colleagues (Schmid et al. (2016)) analyzed structural remodeling of GABA-ergic somatostatin (SOM) positive interneurons in an association learning paradigm and demonstrated that learning is associated with new spine formation in this neuronal sub-population. The mechanism was absent in an Alzheimer disease mouse model. This was the first and only longitudinal study which associates some changes in hippocampal synaptic dynamics with learning. However, to the best of my knowledge, this question has not been addressed in pyramidal neurons, the principal cells of hippocampal CA1, and the major candidate to encode memory content (Tonegawa et al. (2015)). In contrast, the cortex has been better characterised in this regard (Chklovskii et al. (2004)). Increased spine formation and elimination have been shown to be associated with learning and novel sensory exposure and to correlate with improved learning. New spines formed in association with learning have also been shown to be stabilised and to be important for long term memories (Xu et al. (2009); Yang et al. (2009); Moczulska et al. (2013); Fu and Zuo (2011)) whereas stress has been demonstrated to increase spine loss in L5 pyramidal neurons of the barrel cortex (Chen et al. (2018)).

Interestingly, I observed the opposite effect to that of motor learning: I observed newborn spines being born further apart after stress exposure, whereas Fu et al. (2012) reported the preva-

lence of paired, clustered newborn spines in L5 of the motor cortex during the acquisition phase of a motor learning task. Furthermore, they reported that newborn spines which were clustered demonstrated an increased survival and non-clustered newborn spines had a reduced survival. In this work, newborn spines born after the first stress demonstrated an increased survival during recovery but repeated stress decreased newborn spine survival as well as continued reduction of clustering of newborn spines. Fu et al. (2012) showed that repeated learning was required for the stabilisation of clusters. Here, repeated stress continued to decrease survival and clustering of newborn spines. Under control conditions in the motor cortex, newborn spines were reported to 'avoid' clustering to persistent spines unless born in clusters with other newborn spines and later to be born in closer proximity to persistent spines. I observed the opposite effect: a preference of newborn spines to be born closer to persistent spines when compared to control conditions, but overall survival was evidently also reduced (Figure 4.7h). Despite the open question of how learning affects dCA1 synaptic dynamics, my results, for the first time and to the best of our knowledge, link stress induced pyramidal neuron spine dynamics with learning impairment.

I have further shown that acute MMS exposure before learning results in a severe impairment in the ability of mice to learn an incremental spatial MWM task. MMS, intended as a PTSD model, has also been shown to impair hippocampal dependent learning and recall (Chen et al. (2016); Maras et al. (2014); Chen et al. (2010)) of non-incremental tasks such as novel object recognition. Despite not yet fully understanding the underlying mechanisms involved, the characterisation of hippocampal spine dynamics of this process can provide some useful insight to the changes associated with acute MMS exposure. To briefly recapitulate these: I observed an increased survival throughout recovery of the population of spines born in the hours after stress. I postulated that this population was involved in encoding of the MMS experience. Assuming this same effect would occur in the mice exposed to MMS before MWM training, we could expect either increased LTP due to exposure to a learning experience or the perception of the mice to consider the task as stressful (reasonable considering they were naive to the MWM on the first day of training) and instead to induce similar dynamics as with stress exposure. Interestingly, although fear episodic-memory is well known to be dependent on the amygdala in addition to the hippocampus, it has been shown that only by manipulating hippocampal circuitry activity (in the DG) is it possible for a past experience, to interfere with the valence of a new experience (Redondo et al. (2014). This suggests that a stable memory trace of a previous stressful experience in the hippocampus might indeed interfere with the valence association of new hippocampal-dependent experiences. Accordingly, acutely stressed mice mainly exhibited an emotional, instinctive response (thigmotaxis) during MWM training (Garthe et al. (2009)).

Cai et al. (2016) reported that prior activation of cells prime them for later inclusion into an engram. Repeated stress may activate the network enough for learning to occur, although it clearly also has deleterious effects on learning compared to controls. Based on sharing of neuronal ensembles to link memories close in time (Cai et al. (2016)), I would posit that in acutely stressed

mice on the day of stress followed by MWM training, the two experiences (stress and MWM) may share an ensemble. Each re-exposure to the MWM thereafter would re-activate this ensemble and hence also the associated stress memory resulting in 'panic' reactions in which mice are seen to swim around the edges of the maze in an effort to escape. Following the same line of argument, repeated stress and MWM would form the same association on the first day, but with each MMS re-exposure, network activation would be less synchronised and the association to the MWM not reactivated as strongly. Unpublished evidence from our lab has shown that stress reduces the synchrony of activation in the dCA1. Even if all of these hypotheses were to hold true, it would be a long way before we could fully understand the mechanisms that link stress dynamics, activation and behaviour, as hinted at by the tome of literature on these topics.

In summary, both acute and repeated exposure to MMS resulted in spatial learning impairment and recall. The mechanisms underlying this result cannot be fully explained by the structural dynamic changes observed (for to do this would require imaging also during learning), but when taken together, contribute important evidence that stress contrasts learning effects by many of the same structural correlates as observed in the cortex.

### 5.2.1 Repeated restraint stress does not affect contextual memory of trace fear conditioning

Stress has been shown to disrupt learning as well as memory recall (Conrad (2010); Schwabe et al. (2010); Park et al. (2008); Raju (2000)). After investigating stress effects on incremental learning in the MWM, I further conducted a pilot experiment which aimed to determine whether repeated stress affects recall of a previously encoded dCA1 dependent contextual fear memory. Restraint stress for 2h/day for 5 days did not affect the contextual memory of a trace FC task as the stressed cohort remembered the stress comparably to home cage controls.

A recent study in rats (Rahman et al. (2018)) published after these experiments were conducted, considered the effect of 10 days of chronic immobilisation stress on the memory of a learned FC task. Stress exposure after the encoding of a FC task did not change the freezing response of rats compared to home cage controls. This effect mirrors the result presented here in mice exposed to 5 days of repeated restraint stress.

Although this is a hippocampal-dependent learning paradigm, other brain regions such as the amygdala (Paré et al. (2004); Misane et al. (2005); Haubensak et al. (2010)) are involved in the encoding of this aversive task and could contribute to the recall. Therefore, despite any synaptic changes which may occur in the dCA1 with repeated stress exposure, it is likely that plasticity in these additional regions also influence recall. It is also possible that synaptic remodeling akin to what I have demonstrated, have no effect on already consolidated aversive memories. Moreover, we cannot exclude that the difference in stress paradigms (restraint stress rather than MMS) might differentially affect dynamics.

We took the result from this pilot experiment as an indication that repeated restraint stress does not affect memory recall of a previously encoded hippocampal dependent aversive learning episode, a result which is in line with recent literature.

CHAPTER 6

# CONCLUSIONS

In conclusion, I found that both acute and repeated stress affect structural synaptic plasticity in basal dendrites of dorsal hippocampal CA1. The results presented here extend the field of knowledge by demonstrating the susceptibility of newborn spines to stress. Acute and repeated MMS were shown to involve the same dynamic changes with the exception of newborn spine survival which was increased during recovery and reduced with repeated stress exposure. Spines also tended to form further away from each other after stress and repeated stress increased clustered spine elimination which occurred further away from newborn spines. This is the first known report of *in vivo* dCA1 structural dynamics and, importantly, also the first determination of structural changes *during* stress and recovery.

Behaviourally, both acute and repeated stress were shown to impede spatial learning. Surprisingly, repeatedly stressed mice were able to learn the Morris Water Maze task almost as well as controls, whereas acute stress resulted in no spatial learning, supporting interactivity of the neuronal mechanisms underlying learning and stress. Structural dynamic changes during concurrent stress and learning would ultimately shed light on the *in vivo* mechanisms which motivate this result.

Our ability to detect and characterise dynamic longitudinal changes under the influence of stress and recovery in a deep brain structure such as the hippocampus is an essential part of understanding neuronal stress pathology in relation to learning and memory mechanisms. In conjunction with genetic models and anti-depressant treatments, this will lay a strong foundation for clarification of the etiology of synaptic dysregulation in stress and related psychiatric disorders and their putative effects on learning and memory.

It is nonetheless important to note that neuronal changes due to stress may encompass a complex sequential or parallel host of circuit feedback mechanisms, much of which remains

to be elucidated. The influence of such convoluted interactions on behaviour are slowly being uncovered. Only by considering stress and learning as dynamic processes can we begin to dissect the pathways for manipulation that may lead to effective treatments.

CHAPTER 7

# OUTLOOK

This chapter describes follow up experiments currently being conducted to further elucidate the effects of stress on dCA1 dendritic morphology as well as the role of GRs in structural synaptic plasticity changes observed with stress.

## 7.1 *In vivo* dendritic tracing of 2-photon acquired images at short and long time intervals

So far, I have analysed dCA1 spine dynamics and demonstrated a multitude of stress-related changes. However, structural remodeling due to stress is not solely limited to spine dynamics and stress has in fact, been associated with dendritic remodeling.
Evidence suggests that dendritic morphology plays an essential role in the modulation of firing patterns (Mainen and Sejnowski (1996); Van Ooyen et al. (2002); Chen (2010); Bailey and Kandel (1993)). van Elburg and van Ooyen (2010) for instance, used computational modeling of neocortical pyramidal cells to demonstrate that changes in dendritic morphology, such as those that occur with chronic stress, alter neuronal burst firing and hence downstream information processing and cognitive performance.
With the aim of determining whether potential changes in dendritic length could be captured and quantified with *in vivo* 2-photon laser scanning microscopy, I conducted a pilot experiment and established methods of dendritic length quantification.
This pilot experiment aimed to

1. determine the feasibility of measuring potential changes in dendritic length with longitudinal 2-photon imaging

2. quantify tracing noise

3. quantify baseline biological fluctuations.

I implanted Thy1GFPm male mice with imaging cannulas and imaged over two consecutive days as well as 6 weeks later (Figure 7.1) in order to glean changes over a short and long time window. Dendritic tracing was done using Imaris filament tracer and dendritic branching levels were assigned according to the definition of the software. Briefly, branching level was based on dendrite thickness and bifurcation angle. Thicker dendrites and smaller bifurcation angles retained lower levels at branching points.

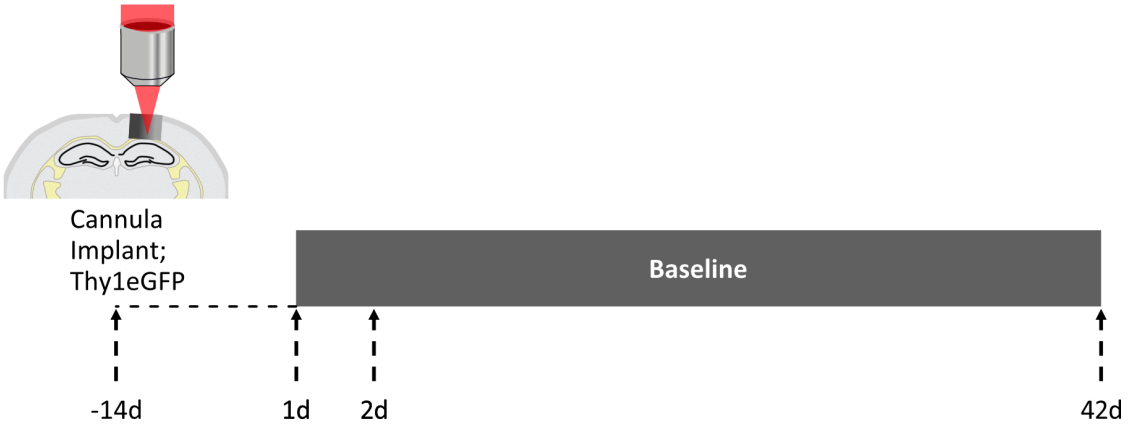


**Figure 7.1:** 2-photon imaging pilot experiment to determine feasibility of dendritic tracing. Thy1GFPm male mice were implanted with imaging cannulas and allowed to recover for 2 weeks. Mice were imaged on days 1, 2 and 42 in order to determine dendritic length fluctuation over short and long time periods.

It is difficult to decide what makes a change in dendritic length of significance. In order to remain as unbiased as possible, I took dendritic changes in length that lay outside of 2 standard deviations of the change in length distribution as notable. Dendrites traced over 2 days (Figure 7.2a, b, e) showed a high stability, with only 4% of dendrites falling outside 2 standard deviations of the mean change in dendrite length over two days.
Dendrites that were traced over 6 weeks (42 days) (Figure 7.2c, d, e) also showed a high level of stability with 5% of changes in dendrite length landing outside of 2 standard deviations (Figure 7.2e). Of those outliers, 80% were terminal dendrites.

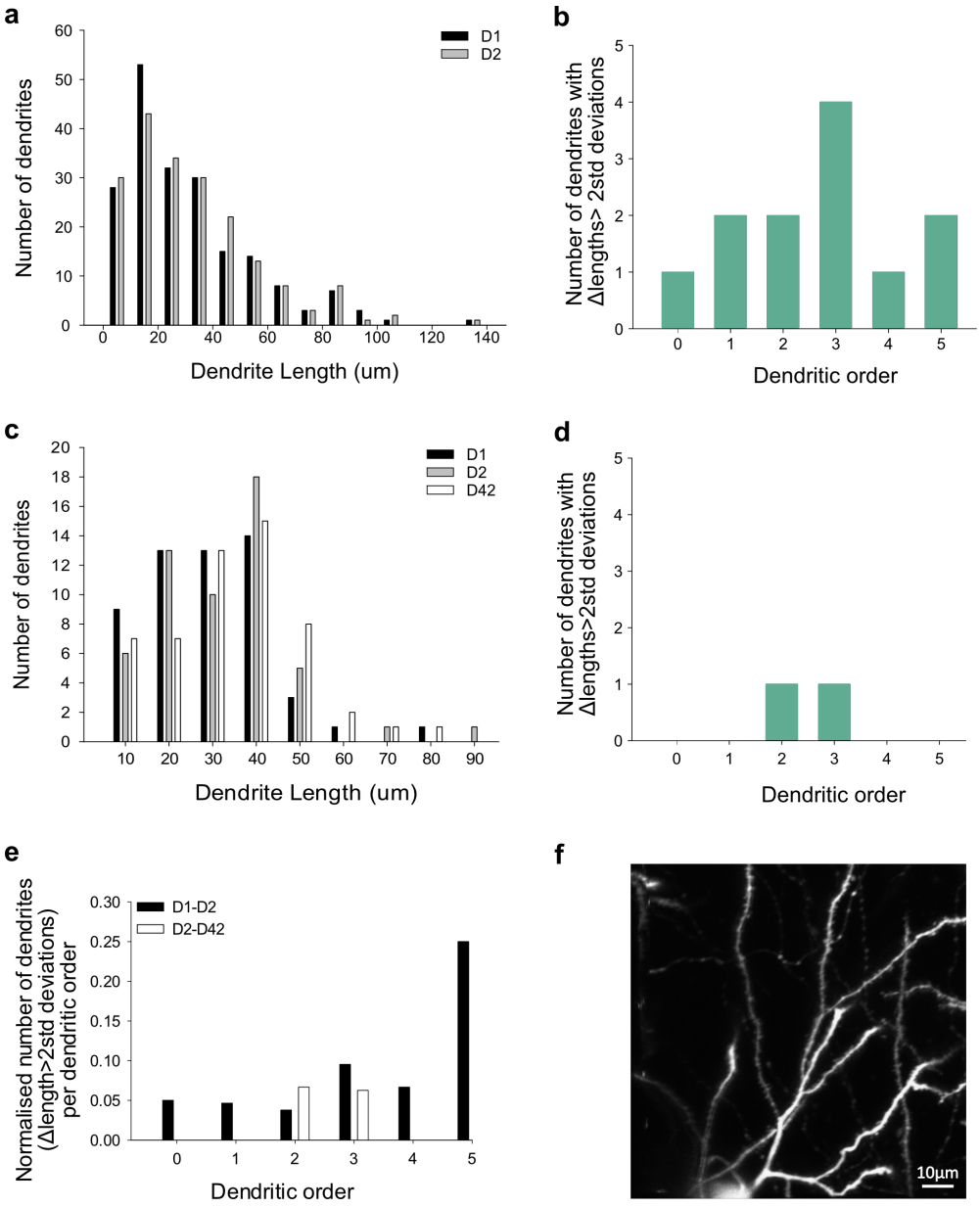


**Figure 7.2:** Characterisation of dendritic tracing over time. (a) Distribution of dendritic lengths over two consecutive days. (b) Dendritic order distribution of dendrites whose change in length fall outside of 2 standard deviations of the distribution of change in length over two consecutive days. These comprised 4% (9/206) of dendrites. (c) Distribution of dendritic lengths over three time points, days 1, 2 and 42. (d) Dendritic order distribution of dendrites whose change in length fall outside of 2 standard deviations of the distribution of change in length over 42 days. These comprised 2% (2/104) of dendrites. (e) Distribution of dendrites with differences larger than 2 standard deviations from the mean of the length changes, normalised by dendritic order. Differences in dendritic lengths across days 1, 2 and 42. Higher order dendrites (terminal branches) were most variable. (f) Representative figure of dendritic branching of basal CA1 dendrites acquired with galvonometric raster scanning. Regions were mapped and the same regions imaged across 3 time points in order to follow the same dendrites through time. a-c, n = 3 mice, 13 cells, 206 dendrites; d-f, n = 1 mouse, 5 cells, 104 dendrites. Black, day 1; grey, day 2; white, day 42.

The quantification of baseline fluctuation in dendritic length over short and long time spans demonstrated that such information could be gleaned and quantified from an *in vivo* hippocampal preparation and that small fluctuations in dendritic length are measurable under baseline conditions.

Chronic stress exposure has been shown to result in retraction of apical CA1 dendrites, an effect found to be dependent on upstream CA3 NMDAR activation (Christian et al. (2011)). It should be further noted that the literature presents some confounding effects in this regard. Whilst others have repeatedly shown CA3 apical dendritic retraction after chronic stress exposure (Sousa et al. (2000); Magarin and McEwen (1995); McEwen (1999); Sapolsky (2000); Woolley et al. (1990)), few studies support CA1 dendritic alterations (Christian et al. (2011); Lambert et al. (1998); Sousa et al. (2000); Alfarez et al. (2008)). Stress effects on CA1 structure have mostly been observed in animals which were exposed to chronic stress and then later exposed to an acute stressor (Alfarez et al. (2008)). One recent study reported the retraction of CA1 basal dendrites in rats after repeated chronic social defeat stress and only in the rats that had been defeated (Patel et al. (2018)) and another (Gourley et al. (2013)) observed reduced and unrecoverable dendritic arborisation in (amongst others) CA1 basal dendrites in adolescent mice after 20 days of chronic corticosterone exposure. This was not evident in adult mice.

It is well known that inputs onto dendritic arbours differ depending on proximity to the cell body. Different interneurons have for instance been shown to send afferents to pyramidal cell dendritic arbours in a compartment-specific manner. This is illustrated by, for example, parvalbumin positive interneurons which inhibit perisomatic regions and somatostatin positive interneurons which inhibit more distal dendrites (Bloss et al. (2016)). In this context, a further aim of *in vivo* dCA1 dendritic tracing would be to determine whether stress differentially affects dendritic orders or distances away from the cell body.

Scant observations in CA1 dendritic changes could further be due to small effect sizes which are difficult to catch with between cohort analyses. The experimental design used in this thesis for *in vivo* tracking of structural dynamics is aimed at maximising the ability to observe small differences by comparing the very same structures repeatedly through time and under various conditions. It is further interesting to note from the literature that acute MMS had the same effects of CA3 dendritic retraction as chronic stress exposure, suggesting that in addition to duration of exposure, severity of stress exposure is also a factor which drives rapid structural changes (Chen et al. (2008)).

We therefore next aim to determine *in vivo* dCA1 potential changes in dendritic length with MMS exposure.

## 7.2 Mechanistic determinant of *in vivo* structural changes under stress

I have shown that a single 2h exposure to MMS results in recoverable changes in structural plasticity and severe impairments in spatial learning and memory. Dissecting the mechanisms which underlie these changes could eventually allow for rescue interventions.
Given that MMS elevates corticosterone levels (Figure 4.28) and that the hippocampus has an abundance of GR's, we are interested in determining whether the changes we see are GR dependent. A multitude of tools exist which enable us to answer this question.
To this aim, we plan to knock out (KO) GR's in a subset of cells while keeping the rest in tact (or wild type - WT). The same imaging experiment and stress paradigms as outlined in Figure 4.2 will be followed. Differences in transgenes and the use of viral vectors to obtain an internally controlled comparison of WT and GR-KO cells are described below.
Figure 7.3 outlines the approaches we are establishing to achieve this aim.

### 7.2.1 Tamoxifen dependent GR-KO in Thy1GFPm-NexCreERT2-GRfl/fl;Ai9 line

The first approach (Figure 7.3a) makes use of a quadruple transgenic mouse line in which a random subset of cells are labelled with GFP under the Thy1 promoter. Under the Nex promoter, another overlapping subset of cells express a tamoxifen-dependent Cre, denoted CreERT2. In addition, GRfl/fl cells and a housekeeping tdTomato allow for the control of GR expression. Upon the administration of tamoxifen (TAM), Cre is activated and GR knocked out. Cells in which Cre is activated become tdTomato positive. Depending on the TAM titration, it is possible to control the proportion of GR-KO cells such that I can achieve double (eGFP and tdTomato) positive cells. WT cells (with GR in tact) will be only GFP positive and GR-KO cells will be either tdtomato positive or eGFP-tdTomato positive. Double positive cells are necessary because tdTomato expression on its own is not bright enough to image at spine resolution *in vivo* using the 2-photon set up we employ. I would thus identify GR-KO cells by tdTomato expression but image their spines by exciting GFP in these cells. The tdTomato in this instance, serves only as a marker for GR-KO and spines of these cells will be imaged by exciting eGFP in these cells to compare to WT cell structural changes under stress. Utilising the same set up as before, we will be able track cells both before and after stress exposure and determine whether stress has a differential effect on cells which have their GRs in tact and those which do not.
Although this approach provides all the necessary aspects for control and manipulation of the cells of interest, the requirement of 4 transgenes is a timely one to pursue, especially given that I aim to compare this to the collected data in male, 3 month old mice (thus also enforcing a sex and age criteria).

#### 7.2.1.1 Determination of tamoxifen titration for sparse expression

In the meantime, I have tested the titration of TAM required for sparse expression in the dCA1. To this aim, I used 12 NexCreERT2 3 month old male mice and administered TAM by intraperitoneal (i.p.) injection in the following concentrations (dissolved in corn oil)

1. 0mg/kg
2. 10mg/kg
3. 50mg/kg
4. 100mg/kg once per day for 1 day
5. 100mg/kg once per day for 2 days
6. 100mg/kg once per day for 5 days

1 administration of 100mg/kg of TAM resulted in sparse labeling of 20% of cells (Figure 7.4, n = 2 mice).

#### 7.2.1.2 *In vivo* characterisation of tamoxifen dependent expression and overlap with GFP positive cells

Based on the expression pattern obtained in the NexCreERT2 mice of the experiment in section 7.2.1.1 , we next used Thy1GFPm;GRfl/fl mice infected with AAV1/2-ESynCreERT2 and AAV1/2-CAG-DIO-tdTomato (ratio 1:3) *in vivo* and i.p. administration of 100mg/kg TAM to check the percentage overlap of tdTomato positive and GFP positive cells (Figure 7.4b, n = 3). Surprisingly, no overlap between the two populations of cells was observed. It should be noted that although this experiment can provide insight into the overlap of double positive and WT cells, it cannot provide any information on how many cells are GR-KO since Cre is untagged.

### 7.2.2 Non-tamoxifen dependent GR-KO virus approach

Given that

1. the GR-KO is highly TAM titration dependent and
2. it takes a significant amount of time to obtain quadruple transgenic animals,

We also considered a second approach to achieving a sparse labeling of GR-KO cells by a TAM independent viral approach in Thy1GFPm-GRfl/fl;Ai9 mice (Figure 7.3). In this case, mice were infected with 2 viruses: AAV8-CamKII-Cre-mCherry and AAV1/2-CAG-DIO-tdTomato (ratio 1:3). The results remain to be characterised and this will form the basis for the experiment outlined in Figure 7.3c.

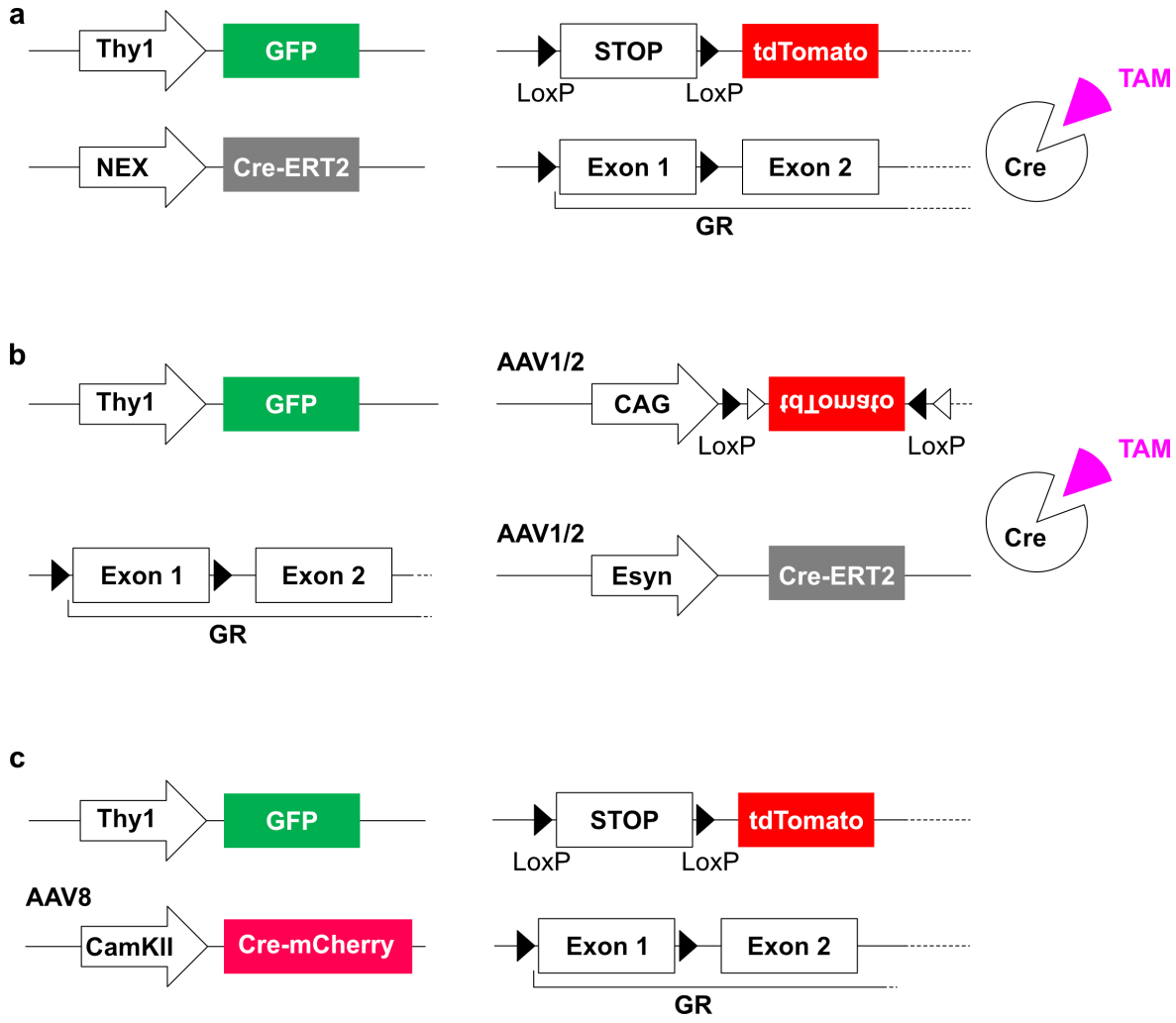


**Figure 7.3:** Methods of obtaining WT and GR-KO cells in the same animals. (a) Quadruple transgenic line containing sparse Thy1GFPm labeled cells and GR fl/fl. Cre is TAM dependent. Cells express tdTomato when Cre is activated. The aim is to achieve WT (only GFP positive cells) and GR-KO (GFP positive and tdTomato positive cells) for *in vivo* imaging. (b) Double transgenic line containing sparse Thy1GFPm labeled cells and GR fl/fl. AAV1/2-CAG-DIO-tdTomato (3 volumes) and AAV1/2-ESyn-CreERT2 (1 volume) allow for GR-KO and TAM dependent labeling without the need for four transgenes (as in (a)) Cre is untagged in this case. This experiment was used to check the ratio of double positive cells to WT cells. (c) Double transgenic line containing sparse Thy1GFPm labeled cells and GR fl/fl. Cre is not TAM dependent and is fused to mCherry as a marker. AAV1/2-CAG-DIO-tdTomato (3 volumes) and AAV8-CamKII-Cre-mCherry (1 volume) allow for GR-KO and TAM independent labeling without the need for four transgenes (as in (a)).

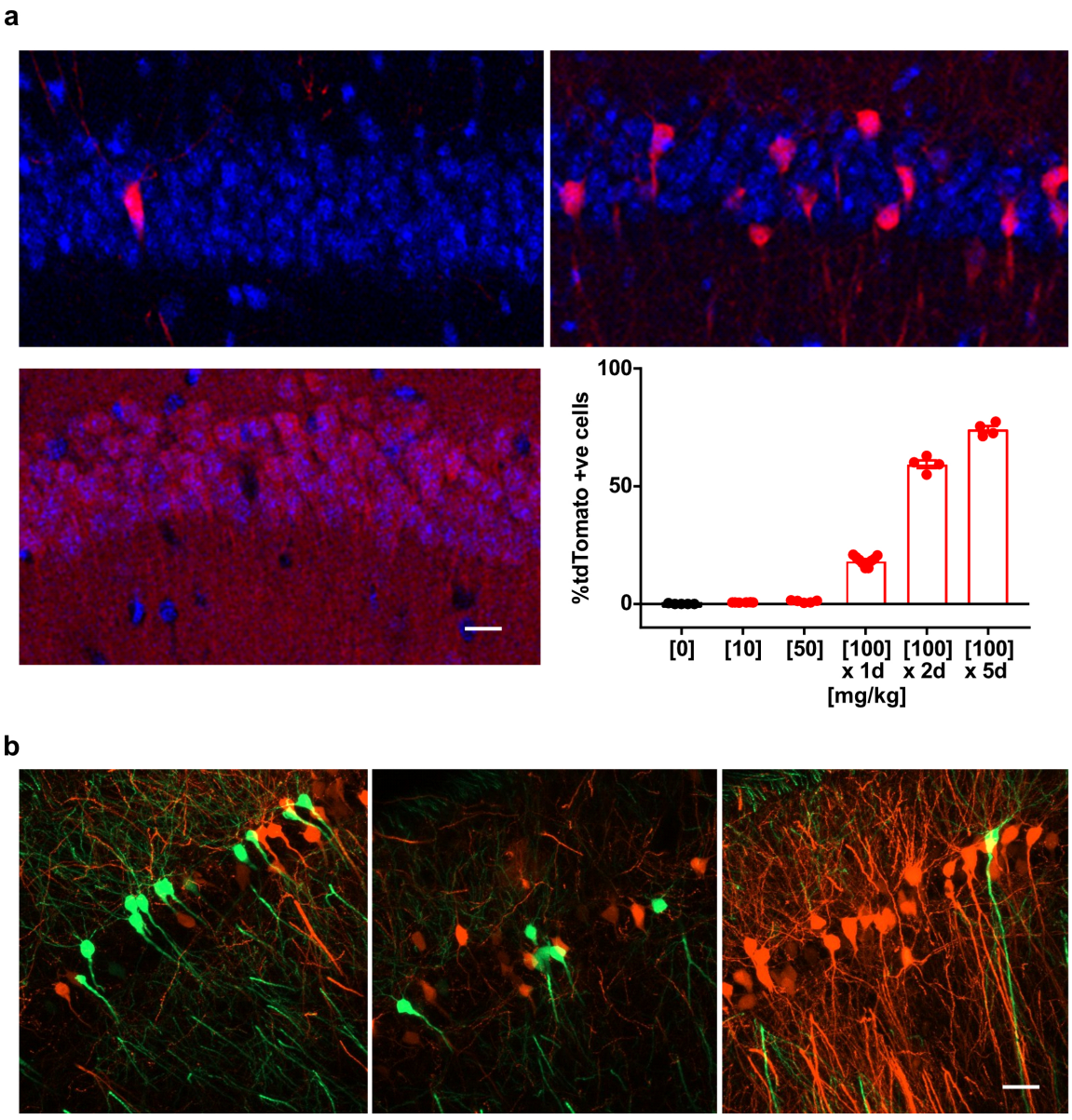


**Figure 7.4:** *In vivo* characterisation of TAM dependent Cre expression in dorsal hippocampal CA1. (a) Determination of TAM titration to achieve sparse labeling in NexCreERT2 male mice. TOP LEFT: 0mg/kg TAM. Some leakage exists within the system, resulting in < 1% of tdTomato positive cells without CreERT2 activation by TAM. TOP RIGHT: 100mg/kg TAM administered once. Approximately 20% of cells have CreERT2 activated by this concentration of TAM. Given the sparsity of Thy1GFPm labeling, this presented a viable option for achieving a 50% overlap between WT and GR-KO cells. BOTTOM LEFT: 100mg/kg administered for 5 days. 80% of cells were labelled. BOTTOM RIGHT: Quantification of tdTomato positive cells as a percentage of DAPI positive cells. Five concentrations were tested; n = 12 mice, 2 per TAM concentration; data presented as mean ± s.e.m.; d, days; scale bar 20µm. (b) 100mg/kg TAM administered in Thy1GFPm-GRfl/fl mice infected with AAV1/2-ESynCreERT2 and AAV1/2-CAG-DIO-tdTomato (ratio 1:3) There was no overlap between GFP positive and tdTomato positive cells, n = 3 mice; scale bar 30µm.


# APPENDIX A

This appendix provides detailed sample sizes for survival fraction and clustering data. Samples sizes are based on the number of dendrites which contain spine populations of interest. Additional DNN sample sizes for data in which the median DNN per dendrite was not used are also included here.

**Table A.1:** Dendrite sample size for survival fraction, Acute 2hMMS cohort

| Spine Population | Day 1 | Day 2 | Day 3 |
|---|---|---|---|
| All | 88 | 88 | 88 |
| Newborn at Day 2 and Day 8 | - | 83 | 59 |
| Persistent | - | 88 | 88 |
| Newborn at Day 2 and Day 9 | - | 82 | 77 |

**Table A.2:** Dendrite sample size for survival fraction, Repeated 2hMMS cohort

| Spine Population | Day 1 | Day 2 | Day 3 |
|---|---|---|---|
| All | 124 | 124 | 124 |
| Newborn at Day 2 and Day 8 | - | 106 | 104 |
| Persistent | - | 124 | 124 |
| Newborn at Day 2 and Day 9 | - | 85 | 65 |

**Table A.3:** Dendrite sample size for DNNs between newborn spines, Acute and Repeated 2hMMS cohort

| Imaging days | Acute 2h MMS and Recovery | Repeated 2h MMS |
|---|---|---|
| 2 | 68 | 86 |
| 4 | 63 | 81 |
| 7 | 65 | 87 |
| 8 | 27 | 72 |
| 9 | 66 | 65 |
| 11 | 53 | 68 |
| 14 | 55 | 79 |

**Table A.4:** Dendrite sample size for DNNs between newborn and persistent spines, Acute and Repeated 2hMMS cohort

| Imaging days | Acute 2h MMS and Recovery | Repeated 2h MMS |
|---|---|---|
| 2 | 83 | 106 |
| 4 | 75 | 106 |
| 7 | 80 | 105 |
| 8 | 59 | 104 |
| 9 | 77 | 99 |
| 11 | 71 | 98 |
| 14 | 72 | 108 |

**Table A.5:** Dendrite sample size for DNNs between lost spines, Acute and Repeated 2hMMS cohort

| Imaging days | Acute 2h MMS and Recovery | Repeated 2h MMS |
|---|---|---|
| 2 | 63 | 68 |
| 4 | 66 | 62 |
| 7 | 57 | 73 |
| 8 | 58 | 67 |
| 9 | 41 | 72 |
| 11 | 58 | 82 |
| 14 | 52 | 81 |

**Table A.6:** Dendrite sample size for DNNs between lost and newborn spines, Acute and Repeated 2hMMS cohort

| Imaging days | Acute 2h MMS and Recovery | Repeated 2h MMS |
|---|---|---|
| 2 | 74 | 80 |
| 4 | 69 | 81 |
| 7 | 67 | 91 |
| 8 | 53 | 88 |
| 9 | 61 | 84 |
| 11 | 62 | 88 |
| 14 | 56 | 95 |

**Table A.7:** Dendrite sample size for DNNs between lost and persistent spines, Acute and Repeated 2hMMS cohort

| Imaging days | Acute 2h MMS and Recovery | Repeated 2h MMS |
|---|---|---|
| 2 | 78 | 95 |
| 4 | 77 | 95 |
| 7 | 73 | 103 |
| 8 | 75 | 103 |
| 9 | 68 | 103 |
| 11 | 77 | 109 |
| 14 | 66 | 108 |

**Table A.8:** Number of DNNs between newborn spines

| Imaging days | Acute 2h MMS and Recovery | Repeated 2h MMS |
|---|---|---|
| 2 | 247 | 373 |
| 4 | 237 | 305 |
| 7 | 262 | 321 |
| 8 | 62 | 230 |
| 9 | 290 | 219 |
| 11 | 203 | 214 |
| 14 | 216 | 291 |

**Table A.9:** Number of DNNs between newborn and persistent spines

| Imaging days | Acute 2h MMS and Recovery | Repeated 2h MMS |
|---|---|---|
| 2 | 248 | 377 |
| 4 | 233 | 317 |
| 7 | 264 | 325 |
| 8 | 89 | 252 |
| 9 | 284 | 243 |
| 11 | 204 | 236 |
| 14 | 220 | 312 |

**Table A.10:** Number of DNNs between lost spines

| Imaging days | Acute 2h MMS and Recovery | Repeated 2h MMS |
|---|---|---|
| 2 | 231 | 231 |
| 4 | 240 | 197 |
| 7 | 232 | 249 |
| 8 | 223 | 218 |
| 9 | 163 | 234 |
| 11 | 220 | 339 |
| 14 | 192 | 326 |

**Table A.11:** Number of DNNs between lost and newborn spines

| Imaging days | Acute 2h MMS and Recovery | Repeated 2h MMS |
|---|---|---|
| 2 | 239 | 231 |
| 4 | 242 | 200 |
| 7 | 233 | 258 |
| 8 | 171 | 222 |
| 9 | 184 | 225 |
| 11 | 208 | 311 |
| 14 | 184 | 328 |

**Table A.12:** Number of DNNs between lost and persistent spines

| Imaging days | Acute 2h MMS and Recovery | Repeated 2h MMS |
|---|---|---|
| 2 | 246 | 258 |
| 4 | 255 | 230 |
| 7 | 248 | 279 |
| 8 | 240 | 254 |
| 9 | 196 | 265 |
| 11 | 239 | 366 |
| 14 | 206 | 353 |

# BIBLIOGRAPHY


W. C. Abraham and M. F. Bear.
Metaplasticity: the plasticity of synaptic plasticity.
*Trends in Neurosciences*, 19(4):126–130, 1996.

D. Acker, S. Paradis, and P. Miller.
Stable memory and computation in randomly rewiring neural networks.
*Journal of Neurophysiology*, 2019.

F. I. Aguayo, M. Tejos-Bravo, G. Díaz-Véliz, A. Pacheco, G. García Rojo, W. Corrales, F. A. Olave, E. Aliaga, J. L. Ulloa, A. M. Avalos, L. Román-Albasini, P. S. Rojas, and J. L. Fiedler.
Hippocampal memory recovery after acute stress: A behavioral, molecular and morphological study.
*Frontiers in Molecular Neuroscience*, 11:283, 2018.

D. N. Alfarez, H. Karst, E. H. Velzing, M. Joels, and H. J. Krugers.
Opposite effects of glucocorticoid receptor activation on hippocampal ca1 dendritic complexity in chronically stressed and handled animals.
*Hippocampus*, 18(1):20–28, 2008.

M. Alfarez, D. N .and Joëls and H. J. Krugers.
Chronic unpredictable stress impairs long-term potentiation in rat hippocampal ca1 area and dentate gyrus in vitro.
*European Journal of Neuroscience*, 17(9):1928–1934, 2003.

A. Artola, J. C. Von Frijtag, P. C. J. Fermont, W. H. Gispen, L. H. Schrama, A. Kamal, and B. M. Spruijt.
Long-lasting modulation of the induction of ltd and ltp in rat hippocampal ca1 by behavioural stress and environmental enrichment.
*European Journal of Neuroscience*, 23(1):261–272, 2006.

A. Attardo, J. E. Fitzgerald, and M. J. Schnitzer.
Impermanence of dendritic spines in live adult ca1 hippocampus.
*Nature*, 523(7562):592, 2015.

C. H. Bailey and E. R. Kandel.
Structural changes accompanying memory storage.
*Annual Review of Physiology*, 55(1):397–426, 1993.

M. F. Bear and R. C. Malenka.
Synaptic plasticity: Ltp and ltd.
*Current Opinion in Neurobiology*, 4(3):389–399, 1994.

A. V. Beylin and T. J. Shors.
Stress enhances excitatory trace eyeblink conditioning and opposes acquisition of inhibitory conditioning.
*Behavioral Neuroscience*, 112(6):1327, 1998.

A. Bhargava, R. S. Mathias, J. A. McCormick, M. F. Dallman, and D. Pearce.
Glucocorticoids prolong ca2+ transients in hippocampal-derived h19-7 neurons by repressing the plasma membrane ca2+-atpase-1.
*Molecular Endocrinology*, 16(7):1629–1637, 2002.

W. Bian, W. Miao, S. He, Z. Qiu, and X. Yu.
Coordinated spine pruning and maturation mediated by inter-spine competition for cadherin/catenin complexes.
*Cell*, 162(4):808–822, 2015.

T. V. P. Bliss and G. L. Collingridge.
A synaptic model of memory: long-term potentiation in the hippocampus.
*Nature*, 361(6407):31, 1993.

E. B. Bloss, M. S. Cembrowski, B. Karsh, J. Colonell, R. D. Fetter, and N. Spruston.
Structured dendritic inhibition supports branch-selective integration in ca1 pyramidal cells.
*Neuron*, 89(5):1016–1030, 2016.

T. Branco and M. Häusser.
The single dendritic branch as a fundamental functional unit in the nervous system.
*Current opinion in neurobiology*, 20(4):494–502, 2010.

J. D. Bremner, P. Randall, E. Vermetten, L. Staib, R. A. Bronen, C. Mazure, S. Capelli, G. McCarthy, R. B. Innis, and D. S. Charney.
Magnetic resonance imaging-based measurement of hippocampal volume in posttraumatic stress disorder related to childhood physical and sexual abuse—a preliminary report.
*Biological Psychiatry*, 41(1):23–32, 1997.

J. D. Bremner, M. Narayan, E. R. Anderson, L. H. Staib, H. L. Miller, and D. S. Charney.
Hippocampal volume reduction in major depression.

*American Journal of Psychiatry*, 157(1):115–118, 2000.

E. S. Brown, A. J. Rush, and B. S. McEwen.
Hippocampal remodeling and damage by corticosteroids: implications for mood disorders.
*Neuropsychopharmacology*, 21(4):474–484, 1999.

D. J. Cai, D. Aharoni, T. Shuman, J. Shobe, J. Biane, W. Song, B. Wei, M. Veshkini, M. La-Vu, J. Lou, S. E. Flores, I. Kim, Y. Sano, M. Zhou, K. Baumgaertel, A. Lavi, M. Kamata, M. Tuszynski, M. Mayford, P. Golshani, and A.J. Sila.
A shared neural ensemble links distinct contextual memories encoded close in time.
*Nature*, 534(7605):115, 2016.

S. R. Y. Cajal.
La retine des vertebres.
*Cellule*, 9:119–255, 1893.

J. J. Cerqueira, F. Mailliet, O. F. X. Almeida, T. M. Jay, and N. Sousa.
The prefrontal cortex as a key target of the maladaptive response to stress.
*Journal of Neuroscience*, 27(11):2781–2787, 2007.

P. Chameau, Y. Qin, S. Spijker, G. Smit, and M. Joëls.
Glucocorticoids specifically enhance l-type calcium current amplitude and affect calcium channel subunit expression in the mouse hippocampus.
*Journal of Neurophysiology*, 97(1):5–14, 2007.

F. Chaouloff, A. Hémar, and O. Manzoni.
Acute stress facilitates hippocampal ca1 metabotropic glutamate receptor-dependent long-term depression.
*Journal of Neuroscience*, 27(27):7130–7135, 2007.

C. Chen, J. Lu, R. Yang, J. B. Ding, and Y. Zuo.
Selective activation of parvalbumin interneurons prevents stress-induced synapse loss and perceptual defects.
*Molecular Psychiatry*, 23(7):1614, 2018.

D. Y. Chen, D. Bambah-Mukku, G. Pollonini, and C. M. Alberini.
Glucocorticoid receptors recruit the camkii$\alpha$-bdnf-creb pathways to mediate memory consolidation.
*Nature Neuroscience*, 15(12):1707, 2012a.

J. Chen.
A simulation study investigating the impact of dendritic morphology and synaptic topology on neuronal firing patterns.

*Neural computation*, 22(4):1086–1111, 2010.

J. L. Chen, K. L. Villa, J. W. Cha, P. T. C. So, Y. Kubota, and E. Nedivi.
Clustered dynamics of inhibitory synapses and dendritic spines in the adult neocortex.
*Neuron*, 74(2):361–373, 2012b.

Y. Chen, C. M. Dubé, C. J. Rice, and T. Z. Baram.
Rapid loss of dendritic spines after stress involves derangement of spine dynamics by corticotropin-releasing hormone.
*Journal of Neuroscience*, 28(11):2903–2911, 2008.

Y. Chen, C. S. Rex, C. J. Rice, C. M. Dubé, C. M. Gall, G. Lynch, and T. Z. Baram.
Correlated memory defects and hippocampal dendritic spine loss after acute stress involve corticotropin-releasing hormone signaling.
*Proceedings of the National Academy of Sciences*, 107(29):13123–13128, 2010.

Y. Chen, J. Molet, J. C. Lauterborn, B. H. Trieu, J. L. Bolton, K. P. Patterson, C. M. Gall, G. Lynch, and T. Z. Baram.
Converging, synergistic actions of multiple stress hormones mediate enduring memory impairments after acute simultaneous stresses.
*Journal of Neuroscience*, 36(44):11295–11307, 2016.

Y. C Chen, Q. R. Tan, W. Dang, H. N. Wang, R. B. Zhang, Z. Y. Li, H. Lin, and R. Liu.
The effect of citalopram on chronic stress-induced depressive-like behavior in rats through gsk3$\beta$/$\beta$-catenin activation in the medial prefrontal cortex.
*Brain Research Bulletin*, 88(4):338–344, 2012c.

D. B. Chklovskii, B. W. Mel, and K. Svoboda.
Cortical rewiring and information storage.
*Nature*, 431(7010):782, 2004.

K. M. Christian, A. D. Miracle, C. L. Wellman, and K. Nakazawa.
Chronic stress-induced hippocampal dendritic retraction requires ca3 nmda receptors.
*Neuroscience*, 174:26–36, 2011.

G. L. Collingridge, S. Peineau, J. G. Howland, and Y. T. Wang.
Long-term depression in the cns.
*Nature reviews Neuroscience*, 11(7):459, 2010.

C. D. Conrad.
A critical review of chronic stress effects on spatial learning and memory.
*Progress in Neuro-Psychopharmacology and Biological Psychiatry*, 34(5):742–755, 2010.

C. D. Conrad, S. J. Lupien, and B. S. McEwen.
Support for a bimodal role for type ii adrenal steroid receptors in spatial memory.
*Neurobiology of Learning and Memory*, 72(1):39–46, 1999.

E. R. de Kloet, M. S. Oitzl, and M. Joëls.
Stress and cognition: are corticosteroids good or bad guys?
*Trends in Neurosciences*, 22(10):422–426, 1999.

M. De Roo, P. Klauser, P. M. Garcia, L. Poglia, and D. Muller.
Spine dynamics and synapse remodeling during ltp and memory processes.
*Progress in brain research*, 169:199–207, 2008a.

M. De Roo, P. Klauser, and D. Muller.
Ltp promotes a selective long-term stabilization and clustering of dendritic spines.
*PLoS Biology*, 6(9):e219, 2008b.

W. Denk, J. H. Strickler, and W. W. Webb.
Two-photon laser scanning fluorescence microscopy.
*Science*, 248(4951):73–76, 1990.

D. M. Diamond, M. Fleshner, N. Ingersoll, and G. Rose.
Psychological stress impairs spatial working memory: relevance to electrophysiological studies of hippocampal function.
*Behavioral Neuroscience*, 110(4):661, 1996.

D. M. Diamond, C. R. Park, K. L. Heman, and G. M. Rose.
Exposing rats to a predator impairs spatial working memory in the radial arm water maze.
*Hippocampus*, 9(5):542–552, 1999.

D. M. Diamond, C. R. Park, A. M. Campbell, and J. C. Woodson.
Competitive interactions between endogenous ltd and ltp in the hippocampus underlie the storage of emotional memories and stress-induced amnesia.
*Hippocampus*, 15(8):1006–1025, 2005.

D. M. Diamond, A. M. Campbell, C. R. Park, J. C. Woodson, C. D. Conrad, A. D. Bachstetter, and R. F. Mervis.
Influence of predator stress on the consolidation versus retrieval of long-term spatial memory and hippocampal spinogenesis.
*Hippocampus*, 16(7):571–576, 2006.

J. F. Dominique, B. Roozendaal, and J. L. McGaugh.
Stress and glucocorticoids impair retrieval of long-term spatial memory.
*Nature*, 394(6695):787, 1998.

Z. Dong, Y. Bai, X. Wu, H. Li, B. Gong, J. G. Howland, Y. Huang, W. He, T. Li, and Y. T. Wang.
Hippocampal long-term depression mediates spatial reversal learning in the morris water maze.
*Neuropharmacology*, 64:65–73, 2013.

M. P. Donley, J. Schulkin, and J. B. Rosen.
Glucocorticoid receptor antagonism in the basolateral amygdala and ventral hippocampus interferes with long-term memory of contextual fear.
*Behavioural Brain Research*, 164(2):197–205, 2005.

H. S. Donohue, P. L. A. Gabbott, H. A. Davies, J. J. Rodriguez, M. I. Cordero, C. Sandi, N. I. Medvedev, V. I. Popov, F. M. Colyer, C. J. Peddie, and M. G. Stewart.
Chronic restraint stress induces changes in synapse morphology in stratum lacunosum-moleculare ca1 rat hippocampus: a stereological and three-dimensional ultrastructural study.
*Neuroscience*, 140(2):597–606, 2006.

S. Druckmann, L. Feng, B. Lee, C. Yook, T. Zhao, J. C. Magee, and J. Kim.
Structured synaptic connectivity between hippocampal regions.
*Neuron*, 81(3):629–640, 2014.

Y. Dudai.
The neurobiology of consolidations, or, how stable is the engram?
*Annu. Rev. Psychol.*, 55:51–86, 2004.

H. Eichenbaum.
A cortical–hippocampal system for declarative memory.
*Nature Reviews Neuroscience*, 1(1):41, 2000.

M. S. Fanselow and H. Dong.
Are the dorsal and ventral hippocampus functionally distinct structures?
*Neuron*, 65(1):7–19, 2010.

G. Feng, R. H. Mellor, M. Bernstein, C. Keller-Peck, Q. T. Nguyen, M. Wallace, J. M. Nerbonne, J. W. Lichtman, and J. R. Sanes.
Imaging neuronal subsets in transgenic mice expressing multiple spectral variants of gfp.
*Neuron*, 28(1):41–51, 2000.

M. R. Foy, M. E. Stanton, S. Levine, and R. F. Thompson.
Behavioral stress impairs long-term potentiation in rodent hippocampus.
*Behavioral and Neural Biology*, 48(1):138 – 149, 1987.
ISSN 0163-1047.

D. D. Francis, M. D. Zaharia, N. Shanks, and H. Anisman.
Stress-induced disturbances in morris water-maze performance: interstrain variability.
*Physiology & Behavior*, 58(1):57–65, 1995.

A. C. Frank, S. Huang, M. Zhou, A. Gdalyahu, G. Kastellakis, T. K. Silva, E. Lu, X. Wen, P. Poirazi, J. T. Trachtenberg, and A. J. Silva.
Hotspots of dendritic spine turnover facilitate clustered spine addition and learning and memory.
*Nature Communications*, 9(1):422, 2018.

M. Fu and Y. Zuo.
Experience-dependent structural plasticity in the cortex.
*Trends in neurosciences*, 34(4):177–187, 2011.

M. Fu, X. Yu, J. Lu, and Y. Zuo.
Repetitive motor learning induces coordinated formation of clustered dendritic spines in vivo.
*Nature*, 483(7387):92, 2012.

R. Garcia, W. Musleh, G. Tocco, R. F. Thompson, and M. Baudry.
Time-dependent blockade of stp and ltp in hippocampal slices following acute stress in mice.
*Neuroscience Letters*, 233(1):41–44, 1997.

A. Garthe, J. Behr, and G. Kempermann.
Adult-generated hippocampal neurons allow the flexible use of spatially precise learning strategies.
*PloS One*, 4(5):e5464, 2009.

J. Gilabert-Juan, C. Bueno-Fernandez, E. Castillo-Gomez, and J. Nacher.
Reduced interneuronal dendritic arborization in ca1 but not in ca3 region of mice subjected to chronic mild stress.
*Brain and Behavior*, 7(2):e00534, 2017.

O. Gökçe, T. Bonhoeffer, and V. Scheuss.
Clusters of synaptic inputs on dendrites of layer 5 pyramidal cells in mouse visual cortex.
*Elife*, 5:e09222, 2016.

M. Göppert-Mayer.
Über elementarakte mit zwei quantensprüngen.
*Annalen der Physik*, 401(3):273–294, 1931.

A. M. Gouirand and L. Matuszewich.
The effects of chronic unpredictable stress on male rats in the water maze.
*Physiology & Behavior*, 86(1-2):21–31, 2005.

S. L. Gourley, A. M. Swanson, and A. J. Koleske.
Corticosteroid-induced neural remodeling predicts behavioral vulnerability and resilience.
*Journal of Neuroscience*, 33(7):3107–3112, 2013.

L. Groc, D. Choquet, and F. Chaouloff.
The stress hormone corticosterone conditions ampar surface trafficking and synaptic potentiation.
*Nature neuroscience*, 11(8):868, 2008.

J. Grutzendler, N. Kasthuri, and W. Gan.
Long-term dendritic spine stability in the adult cortex.
*Nature*, 420(6917):812, 2002.

Ligang Gu, Stefanie Kleiber, Lena Schmid, Felix Nebeling, Miriam Chamoun, Julia Steffen, Jens Wagner, and Martin Fuhrmann.
Long-term in vivo imaging of dendritic spines in the hippocampus reveals structural plasticity.
*Journal of Neuroscience*, 34(42):13948–13953, 2014.

J. P. Hartner and L. A. Schrader.
Interaction of norepinephrine and glucocorticoids modulate inhibition of principle cells of layer ii medial entorhinal cortex in male mice.
*Frontiers in Synaptic Neuroscience*, 10:3, 2018.

W. Haubensak, P. S. Kunwar, H. Cai, S. Ciocchi, N. R. Wall, R. Ponnusamy, J. Biag, H. Dong, K. Deisseroth, E. M. Callaway, M. S. Fanselow, A. Lüthi, and D. J. Anderson.
Genetic dissection of an amygdala microcircuit that gates conditioned fear.
*Nature*, 468(7321):270, 2010.

D. O. Hebb.
*The organization of behavior*.
Wiley, New York, 1949.

M. Joels and E. R. De Kloet.
Effects of glucocorticoids and norepinephrine on the excitability in the hippocampus.
*Science*, 245(4925):1502–1505, 1989.

M. Joëls, R. Karst, H.and DeRijk, and E. R. de Kloet.
The coming out of the brain mineralocorticoid receptor.
*Trends in Neurosciences*, 31(1):1–7, 2008.

S. A. Josselyn, S. Köhler, and P. W. Frankland.
Finding the engram.
*Nature Reviews Neuroscience*, 16(9):521, 2015.

H. Karst and M. Joëls.
Corticosterone slowly enhances miniature excitatory postsynaptic current amplitude in mice ca1 hippocampal cells.
*Journal of neurophysiology*, 94(5):3479–3486, 2005.

H. Karst and M. Joëls.
Brief ru 38486 treatment normalizes the effects of chronic stress on calcium currents in rat hippocampal ca1 neurons.
*Neuropsychopharmacology*, 32(8):1830, 2007.

H. Karst, W. J. Wadman, and M. Joëls.
Corticosteroid receptor-dependent modulation of calcium currents in rat hippocampal ca1 neurons.
*Brain Research*, 649(1-2):234–242, 1994.

G. Kastellakis, D. J. Cai, S. C. Mednick, A. J. Silva, and P. Poirazi.
Synaptic clustering within dendrites: An emerging theory of memory formation.
*Progress in Neurobiology*, 126:19–35, 2015.

A. Kavushansky, R. Vouimba, H. Cohen, and G. Richter-Levin.
Activity and plasticity in the ca1, the dentate gyrus, and the amygdala following controllable vs. uncontrollable water stress.
*Hippocampus*, 16(1):35–42, 2006.

T. Keck, T. D. Mrsic-Flogel, M. V. Afonso, U. T. Eysel, T. Bonhoeffer, and M. Hübener.
Massive restructuring of neuronal circuits during functional reorganization of adult visual cortex.
*Nature Neuroscience*, 11(10):1162, 2008.

M. Khaksari, A. Rashidy-Pour, and A. A. Vafaei.
Central mineralocorticoid receptors are indispensable for corticosterone-induced impairment of memory retrieval in rats.
*Neuroscience*, 149(4):729–738, 2007.

J. J. Kim and D. M. Diamond.
The stressed hippocampus, synaptic plasticity and lost memories.
*Nature Reviews Neuroscience*, 3(6):453, 2002.

J. J. Kim and K. S. Yoon.
Stress: metaplastic effects in the hippocampus.
*Trends in Neurosciences*, 21(12):505–509, 1998.

C. Kirschbaum, O. T. Wolf, M. May, W. Wippich, and D. H. Hellhammer.
Stress-and treatment-induced elevations of cortisol levels associated with impaired declarative memory in healthy adults.
*Life sciences*, 58(17):1475–1483, 1996.

H. J. Krugers, P. M. Goltstein, S. Van Der Linden, and M. Joels.
Blockade of glucocorticoid receptors rapidly restores hippocampal ca1 synaptic plasticity after exposure to chronic stress.
*European Journal of Neuroscience*, 23(11):3051–3055, 2006.

K. G. Lambert, S. K. Buckelew, G. Staffiso-Sandoz, S. Gaffga, W. Carpenter, J. Fisher, and C. H. Kinsley.
Activity-stress induces atrophy of apical dendrites of hippocampal pyramidal neurons in male rats.
*Physiology & Behavior*, 65(1):43–49, 1998.

X. Liu, S. Ramirez, P. T. Pang, C. B. Puryear, A. Govindarajan, K. Deisseroth, and S. Tonegawa.
Optogenetic stimulation of a hippocampal engram activates fear memory recall.
*Nature*, 484(7394):381, 2012.

V. N. Luine, R. L. Spencer, and B. S. McEwen.
Effects of chronic corticosterone ingestion on spatial memory performance and hippocampal serotonergic function.
*Brain Research*, 616(1-2):65–70, 1993.

A. M. Magarin and B. S. McEwen.
Stress-induced atrophy of apical dendrites of hippocampal ca3c neurons: involvement of glucocorticoid secretion and excitatory amino acid receptors.
*Neuroscience*, 69(1):89–98, 1995.

A. M. Magariños, B. S. McEwen, G. Flügge, and E. Fuchs.
Chronic psychosocial stress causes apical dendritic atrophy of hippocampal ca3 pyramidal neurons in subordinate tree shrews.
*Journal of Neuroscience*, 16(10):3534–3540, 1996.

A. M. Magariños, J. M. G. Verdugo, and B. S. McEwen.
Chronic stress alters synaptic terminal structure in hippocampus.
*Proceedings of the National Academy of Sciences*, 94(25):14002–14008, 1997.

Z. F. Mainen and T. J. Sejnowski.
Influence of dendritic structure on firing pattern in model neocortical neurons.
*Nature*, 382(6589):363, 1996.

R. C. Malenka and M. F. Bear.
Ltp and ltd: an embarrassment of riches.
*Neuron*, 44(1):5–21, 2004.

P. M. Maras, J. Molet, Y. Chen, C. Rice, S. G. Ji, A. Solodkin, and T. Z. Baram.
Preferential loss of dorsal-hippocampus synapses underlies memory impairments provoked by short, multimodal stress.
*Molecular Psychiatry*, 19(7):811, 2014.

S. J. Martin and R. G. M. Morris.
New life in an old idea: the synaptic plasticity and memory hypothesis revisited.
*Hippocampus*, 12(5):609–636, 2002.

S. J. Martin, P. D. Grimwood, and R. G. M. Morris.
Synaptic plasticity and memory: an evaluation of the hypothesis.
*Annual review of Neuroscience*, 23(1):649–711, 2000.

R. I. Martínez-Téllez, E. Hernández-Torres, C. Gamboa, and G. Flores.
Prenatal stress alters spine density and dendritic length of nucleus accumbens and hippocampus neurons in rat offspring.
*Synapse*, 63(9):794–804, 2009.

M. Matsuzaki, N. Honkura, G. C. R. Ellis-Davies, and H. Kasai.
Structural basis of long-term potentiation in single dendritic spines.
*Nature*, 429(6993):761, 2004.

B. S. McEwen.
Stress and hippocampal plasticity.
*Annual Review of Neuroscience*, 22(1):105–122, 1999.

B. S. McEwen.
Effects of adverse experiences for brain structure and function.
*Biological Psychiatry*, 48(8):721–731, 2000.

B. S. McEwen and R. M. Sapolsky.
Stress and cognitive function.
*Current opinion in Neurobiology*, 5(2):205–216, 1995.

J. L. McGaugh.
Memory–a century of consolidation.
*Science*, 287(5451):248–251, 2000.

C. Mirescu, J. D. Peters, and E. Gould.

Early life experience alters response of adult neurogenesis to stress.
*Nature neuroscience*, 7(8):841, 2004.

I. Misane, P. Tovote, M. Meyer, J. Spiess, S. O. Ögren, and O. Stiedl.
Time-dependent involvement of the dorsal hippocampus in trace fear conditioning in mice.
*Hippocampus*, 15(4):418–426, 2005.

K. E. Moczulska, J. Tinter-Thiede, M. Peter, L. Ushakova, T. Wernle, B. Bathellier, and S. Rumpel.
Dynamics of dendritic spines in the mouse auditory cortex during memory formation and memory recall.
*Proceedings of the National Academy of Sciences*, 110(45):18315–18320, 2013.

R. N. Moda-Sava, M. H. Murdock, P. K. Parekh, R. N. Fetcho, B. S. Huang, T. N. Huynh, J. Witztum, D. C. Shaver, D. L. Rosenthal, E. J. Alway, K. Lopez, Y. Meng, L. Nellissen, L. Grosenick, T. A. Milner, K. Deisseroth, H. Bito, H. Kasai, and C. Liston.
Sustained rescue of prefrontal circuit dysfunction by antidepressant-induced spine formation.
*Science*, 364(6436):eaat8078, 2019.

R. G. M. Morris.
Spatial localization does not require the presence of local cues.
*Learning and Motivation*, 12(2):239–260, 1981.

R. G. M. Morris, P. Garrud, J. N. P. Rawlins, and J. O'Keefe.
Place navigation impaired in rats with hippocampal lesions.
*Nature*, 297(5868):681, 1982.

R. G. M. Morris, E. Anderson, G. S. a Lynch, and M. Baudry.
Selective impairment of learning and blockade of long-term potentiation by an n-methyl-d-aspartate receptor antagonist, ap5.
*Nature*, 319(6056):774, 1986.

E. I. Moser, K. A. Krobert, M. Moser, and R. G. M. Morris.
Impaired spatial learning after saturation of long-term potentiation.
*Science*, 281(5385):2038–2042, 1998.

M. Moser and E. I. Moser.
Functional differentiation in the hippocampus.
*Hippocampus*, 8(6):608–619, 1998.

H. Murakoshi, H. Wang, and R. Yasuda.
Local, persistent activation of rho gtpases during plasticity of single dendritic spines.
*Nature*, 472(7341):100, 2011.

M. S. Murmu, S. Salomon, Y. Biala, M. Weinstock, K. Braun, and J. Bock.
Changes of spine density and dendritic complexity in the prefrontal cortex in offspring of mothers exposed to stress during pregnancy.
*European Journal of Neuroscience*, 24(5):1477–1487, 2006.

B. Myers, J. M. McKlveen, and J.P Herman.
Glucocorticoid actions on synapses, circuits, and behavior: implications for the energetics of stress.
*Frontiers in Neuroendocrinology*, 35(2):180–196, 2014.

L. H. L. Ng, Y. Huang, L. Han, R. C. Chang, Y. S. Chan, and C. S. W. Lai.
Ketamine and selective activation of parvalbumin interneurons inhibit stress-induced dendritic spine elimination.
*Translational Psychiatry*, 8(1):272, 2018.

R. A. Nicoll.
A brief history of long-term potentiation.
*Neuron*, 93(2):281–290, 2017.

M. S. Oitzl and E. R. De Kloet.
Selective corticosteroid antagonists modulate specific aspects of spatial orientation learning.
*Behavioral Neuroscience*, 106(1):62, 1992.

M. S. Oitzl, M. Fluttert, and E. Ron de Kloet.
The effect of corticosterone on reactivity to spatial novelty is mediated by central mineralocorticosteroid receptors.
*European Journal of Neuroscience*, 6(7):1072–1079, 1994.

M. S. Oitzl, H. M. Reichardt, M. Joëls, and E. R. de Kloet.
Point mutation in the mouse glucocorticoid receptor preventing dna binding impairs spatial memory.
*Proceedings of the National Academy of Sciences*, 98(22):12790–12795, 2001.

J. O'Keefe and J. Dostrovsky.
The hippocampus as a spatial map: Preliminary evidence from unit activity in the freely-moving rat.
*Brain Research*, 1971.

J. O'Keefe and L. Nadel.
*The hippocampus as a cognitive map*.
Oxford: Clarendon Press, 1978.

J. E. Olijslagers, E. R. De Kloet, Y. Elgersma, G. M. Van Woerden, M. Joëls, and H. Karst.
Rapid changes in hippocampal ca1 pyramidal cell function via pre-as well as postsynaptic membrane mineralocorticoid receptors.
*European Journal of Neuroscience*, 27(10):2542–2550, 2008.

D. Paré, G. J. Quirk, and J. E. Ledoux.
New vistas on amygdala networks in conditioned fear.
*Journal of neurophysiology*, 92(1):1–9, 2004.

C. R. Park, P. R. Zoladz, C. D. Conrad, M. Fleshner, and D. M. Diamond.
Acute predator stress impairs the consolidation and retrieval of hippocampus-dependent memory in male and female rats.
*Learning & memory*, 15(4):271–280, 2008.

N. Pasricha, M. Joels, and H. Karst.
Rapid effects of corticosterone in the mouse dentate gyrus via a nongenomic pathway.
*Journal of Neuroendocrinology*, 23(2):143–147, 2011.

D. Patel, S. Anilkumar, S. Chattarji, and B. Buwalda.
Repeated social stress leads to contrasting patterns of structural plasticity in the amygdala and hippocampus.
*Behavioural Brain Research*, 347:314–324, 2018.

C. Pavlides, S. Ogawa, A. Kimura, and B. S. McEwen.
Role of adrenal steroid mineralocorticoid and glucocorticoid receptors in long-term potentiation in the ca1 field of hippocampal slices.
*Brain Research*, 738(2):229–235, 1996.

T. Pfeiffer, S. Poll, S. Bancelin, J. Angibaud, V. V. G. K. Inavalli, K. Keppler, M. Mittag, M. Fuhrmann, and U. V. Nägerl.
Chronic 2p-sted imaging reveals high turnover of dendritic spines in the hippocampus in vivo.
*eLife*, 7:e34700, 2018.

C. R. Pugh, D. Tremblay, M. Fleshner, and J. W. Rudy.
A selective role for corticosterone in contextual-fear conditioning.
*Behavioral Neuroscience*, 111(3):503, 1997.

M. Quan, C. Zheng, N. Zhang, D. Han, Y. Tian, T. Zhang, and Z. Yang.
Impairments of behavior, information flow between thalamus and cortex, and prefrontal cortical synaptic plasticity in an animal model of depression.
*Brain Research Bulletin*, 85(3-4):109–116, 2011.

J. J. Radley, A. B. Rocher, M. Miller, W. G. M. Janssen, C. Liston, P. R. Hof, B. S. McEwen, and J. H. Morrison.
Repeated stress induces dendritic spine loss in the rat medial prefrontal cortex.
*Cerebral cortex*, 16(3):313–320, 2005.

M. M. Rahman, A. Shukla, and S. Chattarji.
Extinction recall of fear memories formed before stress is not affected despite higher theta activity in the amygdala.
*eLife*, 7:e35450, 2018.

T Raju.
Chronic restraint stress impairs acquisition and retention of spatial memory task in rats.
*Current science*, 79(11):1581, 2000.

S. Ramirez, X. Liu, C. J. MacDonald, A. Moffa, J. Zhou, R. L. Redondo, and S. Tonegawa.
Activating positive memory engrams suppresses depression-like behaviour.
*Nature*, 522(7556):335, 2015.

R. L. Redondo, J. Kim, A. L. Arons, S. Ramirez, X. Liu, and S. Tonegawa.
Bidirectional switch of the valence associated with a hippocampal contextual memory engram.
*Nature*, 513(7518):426, 2014.

T. Rogerson, D. J. Cai, A. Frank, Y. Sano, J. Shobe, M. F. Lopez-Aranda, and A. J. Silva.
Synaptic tagging during memory allocation.
*Nature Reviews Neuroscience*, 15(3):157, 2014.

B. Roozendaal.
Stress and memory: opposing effects of glucocorticoids on memory consolidation and memory retrieval.
*Neurobiology of Learning and Memory*, 78(3):578–595, 2002.

S. Saito, S. Kimura, N. Adachi, T. Numakawa, A. Ogura, and K. Tominaga-Yoshino.
An in vitro reproduction of stress-induced memory defects: Effects of corticoids on dendritic spine dynamics.
*Scientific Reports*, 6:19287, 2016.

C. Sandi, M. Loscertales, and journal=European Journal of Neuroscience volume=9 number=4 pages=637–642 year=1997 publisher=Wiley Online Library Guaza, C.
Experience-dependent facilitating effect of corticosterone on spatial memory formation in the water maze.

C. Sandi, J. J. Merino, M. I. Cordero, K. Touyarot, and C. Venero.

Effects of chronic stress on contextual fear conditioning and the hippocampal expression of the neural cell adhesion molecule, its polysialylation, and l1.
*Neuroscience*, 102(2):329–339, 2001.

C. Sandi, H. A. Davies, M. I. Cordero, J. J. Rodriguez, V. I. Popov, and M. G. Stewart.
Rapid reversal of stress induced loss of synapses in ca3 of rat hippocampus following water maze training.
*European Journal of Neuroscience*, 17(11):2447–2456, 2003.

R. M. Sapolsky.
*Stress, the aging brain, and the mechanisms of neuron death.*
the MIT Press, 1992.

R. M. Sapolsky.
Glucocorticoids and hippocampal atrophy in neuropsychiatric disorders.
*Archives of General Psychiatry*, 57(10):925–935, 2000.

L. C. Schmid, M. Mittag, S. Poll, J. Steffen, J. Wagner, H. Geis, I. Schwarz, B. Schmidt, M. K. Schwarz, S. Remy, and M. Fuhrmann.
Dysfunction of somatostatin-positive interneurons associated with memory deficits in an alzheimer's disease model.
*Neuron*, 92(1):114–125, 2016.

L. Schwabe, H. Schächinger, E. R. de Kloet, and M. S. Oitzl.
Stress impairs spatial but not early stimulus–response learning.
*Behavioural brain research*, 213(1):50–55, 2010.

W. B. Scoville and B. Milner.
Loss of recent memory after bilateral hippocampal lesions.
*Journal of Neurology, Neurosurgery, and Psychiatry*, 20(1):11, 1957.

T. J. Shors and E. Dryver.
Effects of stress and long-term potentiation (ltp) on subsequent ltp and the theta burst response in the dentate gyrus.
*Brain Research*, 666(2):232–238, 1994.

T. J. Shors, T. B. Seib, S. Levine, and R. F. Thompson.
Inescapable versus escapable shock modulates long-term potentiation in the rat hippocampus.
*Science*, 244(4901):224–226, 1989.

T. J. Shors, C. Weiss, and R. F. Thompson.
Stress-induced facilitation of classical conditioning.
*Science*, 257(5069):537–539, 1992.

T. J. Shors, C. Chua, and J. Falduto.
Sex differences and opposite effects of stress on dendritic spine density in the male versus female hippocampus.
*Journal of Neuroscience*, 21(16):6292–6297, 2001.

T. J. Shors, J. Falduto, and B. Leuner.
The opposite effects of stress on dendritic spines in male vs. female rats are nmda receptor-dependent.
*European Journal of Neuroscience*, 19(1):145–150, 2004.

T. Smeets, O. T. Wolf, T. Giesbrecht, K. Sijstermans, S. Telgen, and M. Joëls.
Stress selectively and lastingly promotes learning of context-related high arousing information.
*Psychoneuroendocrinology*, 34(8):1152–1161, 2009.

J. S. Snyder, A. Soumier, M. Brewer, J. Pickel, and H. A. Cameron.
Adult hippocampal neurogenesis buffers stress responses and depressive behaviour.
*Nature*, 476(7361):458, 2011.

N. Sousa, N. V. Lukoyanov, M. D. Madeira, O. F. X. Almeida, and M. M. Paula-Barbosa.
Reorganization of the morphology of hippocampal neurites and synapses after stress-induced damage correlates with behavioral improvement.
*Neuroscience*, 97(2):253–266, 2000.

L. R. Squire and S. Zola-Morgan.
The medial temporal lobe memory system.
*Science*, 253(5026):1380–1386, 1991.

M. N. Starkman, S. S. Gebarski, S. Berent, and D. E. Schteingart.
Hippocampal formation volume, memory dysfunction, and cortisol levels in patients with cushing's syndrome.
*Biological Psychiatry*, 32(9):756–765, 1992.

M. G. Stewart, H. A. Davies, C. Sandi, I. V. Kraev, V. V. Rogachevsky, C. J. Peddie, J. J. Rodriguez, M. I. Cordero, H. S. Donohue, P. L. A. Gabbott, and V. I. Popov.
Stress suppresses and learning induces plasticity in ca3 of rat hippocampus: a three-dimensional ultrastructural study of thorny excrescences and their postsynaptic densities.
*Neuroscience*, 131(1):43–54, 2005.

Sunanda, M. S. Rao, T. R. Raju, et al.
Effect of chronic restraint stress on dendritic spines and excrescences of hippocampal ca3 pyramidal neurons—a quantitative study.
*Brain Research*, 694(1-2):312–317, 1995.

L. W. Swanson and W. M. Cowan.
An autoradiographic study of the organization of the efferent connections of the hippocampal formation in the rat.
*Journal of Comparative Neurology*, 172(1):49–84, 1977.

C. H. Teo, T. Soga, and I. S. Parhar.
Brain beta-catenin signalling during stress and depression.
*Neurosignals*, 26(1):31–42, 2018.

R. F. Thompson.
The search for the engram.
*American Psychologist*, 31(3):209, 1976.

S. Tonegawa, M. Pignatelli, D. S. Roy, and T. J. Ryan.
Memory engram storage and retrieval.
*Current Opinion in Neurobiology*, 35:101–109, 2015.

M. Uddo, J. J. Vasterling, K. Brailey, and P. B. Sutker.
Memory and attention in combat-related post-traumatic stress disorder (ptsd).
*Journal of Psychopathology and Behavioral Assessment*, 15(1):43–52, 1993.

A. F. Ulivi, T. P. Castello-Waldow, . Weston, L. Yan, R. Yasuda, A. Chen, and A. Attardo.
Longitudinal two-photon imaging of dorsal hippocampal ca1 in live mice.
*JoVE (Journal of Visualized Experiments)*, (148):e59598, 2019.

R. A. J. van Elburg and A. van Ooyen.
Impact of dendritic size and dendritic topology on burst firing in pyramidal cells.
*PLoS Computational Biology*, 6(5):e1000781, 2010.

A. Van Ooyen, J. Duijnhouwer, M. W. H. Remme, and J. van Pelt.
The effect of dendritic topology on firing patterns in model neurons.
*Network: Computation in Neural Systems*, 13(3):311–325, 2002.

Y. Watanabe, E. Gould, and B. S. McEwen.
Stress induces atrophy of apical dendrites of hippocampal ca3 pyramidal neurons.
*Brain Research*, 588(2):341–345, 1992.

J. R. Whitlock, A. J. Heynen, M. G. Shuler, and M. F. Bear.
Learning induces long-term potentiation in the hippocampus.
*Science*, 313(5790):1093–1097, 2006.

C. S. Woolley, E. Gould, and B. S. McEwen.
Exposure to excess glucocorticoids alters dendritic morphology of adult hippocampal pyramidal neurons.

*Brain Research*, 531(1-2):225–231, 1990.

L. Xu, R. Anwyl, and M. J. Rowan.
Behavioural stress facilitates the induction of long-term depression in the hippocampus.
*Nature*, 387(6632):497, 1997.

T. Xu, X. Yu, A. J. Perlik, W. F. Tobin, J. A. Zweig, K. Tennant, T. Jones, and Y. Zuo.
Rapid formation and selective stabilization of synapses for enduring motor memories.
*Nature*, 462(7275):915, 2009.

G. Yang, F. Pan, and W. Gan.
Stably maintained dendritic spines are associated with lifelong memories.
*Nature*, 462(7275):920, 2009.

T. R. Zhang, A. Larosa, M. Di Raddo, V. Wong, A. S. Wong, and T. P. Wong.
Negative memory engrams in the hippocampus enhance the susceptibility to chronic social defeat stress.
*bioRxiv*, page 379669, 2018.

J. Zhou, F. Zhang, and Y. Zhang.
Corticosterone inhibits generation of long-term potentiation in rat hippocampal slice: involvement of brain-derived neurotrophic factor.
*Brain Research*, 885(2):182–191, 2000.

# Acknowledgements

I could not have completed this thesis without the support of a number of people.

Thank you to my TAC members Prof. Alon Chen, Prof. Tobias Bonhoeffer and Dr. Alessio Attardo for your insightful input and for dedicating your precious time to provide valuable advice and feedback.

Thank you to the GSN for the opportunity to be part of a fantastic group of forward thinkers, for the endless opportunities and for your support and advice whenever I needed it.

Alessio, thank you for always taking the time to discuss my data with me, for teaching me the value of good science and for taking a leap of faith in an engineer! Thank you also for your support and kindness, especially when my experiments were not working - your good humour and positivity made for a wonderful work environment.

Thank you to the A-lab for the laughs, the data-discussions, the hikes and, most of all, for your friendships. I must admit I was apprehensive about moving to a country where I knew not a soul, but I was lucky to land in the best of labs and be surrounded by kind, funny and smart people. You taught me to take life a little less seriously, to eat too much cake and more than anything, to feel like I had a family away from home.

A special thank you to Ale - for your time, effort, patience and support when I needed it most!

To Gameema, thank you for being my backbone and my inspiration no matter where we are in the world.

Thank you to my mom, Soraya Johaar, for crossing continents to support our family every time I had to be away from home.

And finally, to Reyan and little K. Thank you for being the most supportive family, for always encouraging me and believing in me, for cheering me on and for pulling me through in every possible way. Thank you for understanding all the late nights and long weekends in the lab. We're finally reaching the end and I could not have made it without you.

## Eidesstattliche Versicherung/Affidavit

Hiermit versichere ich an Eides statt, dass ich die vorliegende Dissertation 'The Effects of Stress on *in vivo* Hippocampal CA1 Synaptic Dynamics and Hippocampal Learning and Memory' selbstständig angefertigt habe, mich außer der angegebenen keiner weiteren Hilfsmittel bedient und alle Erkenntnisse, die aus dem Schrifttum ganz oder annähernd übernommen sind, als solche kenntlich gemacht und nach ihrer Herkunft unter Bezeichnung der Fundstelle einzeln nachgewiesen habe.

I hereby confirm that the dissertation 'The Effects of Stress on *in vivo* Hippocampal CA1 Synaptic Dynamics and Hippocampal Learning and Memory' is the result of my own work and that I have only used sources or materials listed and specified in the dissertation.

18 July 2019
München, den
Munich, date

Ghabiba Weston
Unterschrift
Signature